National Library of Canada
Bibliothèque nationale du Canada

Canadian Theses Service
Service des thèses canadiennes

Ottawa, Canada
K1A 0N4

NOTICE

The quality of this microform is heavily dependent upon the quality of the original thesis submitted for microfilming. Every effort has been made to ensure the highest quality of reproduction possible.

If pages are missing, contact the university which granted the degree.

Some pages may have indistinct print especially if the original pages were typed with a poor typewriter ribbon or if the university sent us an inferior photocopy.

Reproduction in full or in part of this microform is governed by the Canadian Copyright Act, R.S.C. 1970, c. C-30, and subsequent amendments.

AVIS

La qualité de cette microforme dépend grandement de la qualité de la thèse soumise au microfilmage. Nous avons tout fait pour assurer une qualité supérieure de reproduction.

S'il manque des pages, veuillez communiquer avec l'université qui a conféré le grade.

La qualité d'impression de certaines pages peut laisser à désirer, surtout si les pages originales ont été dactylographiées à l'aide d'un ruban usé ou si l'université nous a fait parvenir une photocopie de qualité inférieure.

La reproduction, même partielle, de cette microforme est soumise à la Loi canadienne sur le droit d'auteur, SRC 1970, c. C-30, et ses amendements subséquents.

NL-339 (r. 88/04) c

Canada

National Library of Canada
Bibliothèque nationale du Canada

Canadian Theses Service
Service des thèses canadiennes

Ottawa, Canada
K1A 0N4

The author has granted an irrevocable non-exclusive licence allowing the National Library of Canada to reproduce, loan, distribute or sell copies of his/her thesis by any means and in any form or format, making this thesis available to interested persons.

L'auteur a accordé une licence irrévocable et non exclusive permettant à la Bibliothèque nationale du Canada de reproduire, prêter, distribuer ou vendre des copies de sa thèse de quelque manière et sous quelque forme que ce soit pour mettre des exemplaires de cette thèse à la disposition des personnes intéressées.

The author retains ownership of the copyright in his/her thesis. Neither the thesis nor substantial extracts from it may be printed or otherwise reproduced without his/her permission.

L'auteur conserve la propriété du droit d'auteur qui protège sa thèse. Ni la thèse ni des extraits substantiels de celle-ci ne doivent être imprimés ou autrement reproduits sans son autorisation.

ISBN 0-315-55546-7

Canada

THE UNIVERSITY OF ALBERTA

SINGLE ZONE AIR INFILTRATION MODELLING

by

IAIN STUART WALKER

A THESIS

SUBMITTED TO THE FACULTY OF GRADUATE STUDIES AND RESEARCH

IN PARTIAL FULFILMENT OF THE REQUIREMENTS FOR THE DEGREE

OF MASTER OF SCIENCE

DEPARTMENT OF MECHANICAL ENGINEERING

EDMONTON, ALBERTA

FALL, 1989

THE UNIVERSITY OF ALBERTA

Release Form

NAME OF AUTHOR: Iain Stuart Walker

TITLE OF THESIS: Single Zone Air Infiltration Modelling

DEGREE: Master Of Science

YEAR THIS DEGREE GRANTED: 1989

Permission is hereby granted to THE UNVERSITY OF ALBERTA LIBRARY to reproduce single copies for private, scholarly or scientific purposes only.

The author reserves other publication rights, and neither the thesis nor extensive extracts from it may be printed or otherwise reproduced without the authors written permission.

Ian S. Walker

10943 - 82 Avenue

Edmonton, Alberta

T6G 0S7

DATE: 3rd October 1989

THE UNIVERSITY OF ALBERTA

FACULTY OF GRADUATE STUDIES AND RESEARCH

The undersigned certify that they have read, and recommend to the Faculty of Graduate Studies and Research, for acceptance, a thesis entitled Single Zone Air Infiltration Modelling

submitted by Iain Stuart Walker

in partial fulfilment of the requirements for the degree of Master of Science in Mechanical Engineering.

N. Wilson

Supervisor

John Reid

John Fedders

Date: 20th September 1989

Abstract

Fan pressurization and furnace flue tests were performed to determine building leakage characteristics. The results of these tests show that the characteristics of building leakage do not change over the tested pressure range (1 to 100 Pa). This indicates that current CGSB and ASTM standards that use pressure above 10 Pa are adequate to determine the characteristics for the lower pressures typical of wind and temperature difference effects.

Two single zone infiltration models, EXACTAIM and AIM-2, have been developed. In EXACTAIM, crack flow theory, fan pressurization results and assumptions about leakage distribution were used to determine exact equations for stack and wind driven infiltration. These equations require numerical solution. AIM-2 has empirical equations that give the same results as EXACTAIM within 5%. The major improvements in these models over other simple models are the treatment of the flue as a separate leak, and a wind shelter coefficient that is a continuous function of wind direction and allows the flue to have different shelter from the rest of the building. In addition, EXACTAIM and AIM-2 have separate equations for houses with basements or crawl spaces.

The predictions of AIM-2 and four other simple single zone models have been compared to infiltration data measured at the Alberta Home Heating Research Facility. The results show that AIM-2 is the best at

predicting infiltration rates because it allows the flue to be a separate leak and have different shelter, and it has the correct variation with windspeed and indoor-outdoor temperature difference. Typical values for the bias and scatter of AIM-2 compared to the measured data are 10%.

The method of combining mechanical and natural ventilation in AIM-2 was found to consistently underpredict the total ventilation rate.

Acknowledgements

Thw author would like to thank Dr. D.J. Wilson for his guidance and support throught tjis project.

Financial support was provided by an ASHRAE Grant-In-Aid. Research grants to Dr. D.J. Wilson from Alberta/Canada Energy Research Fund and NSERC have made this research possible. The author is very grateful for this support.

I would also like to thank Mark Ackerman, Wayne Pittman and Brian Zelt for their technical and moral support, as well as the Department of Mechanical Engineering machine shop staff and technicians for their high quality of workmanship and technical assistance.

Table of Contents

Chapter		Page
1.	Introduction	1
	Why do we Need Building Ventilation Models	1
	A Short History of Ventilation Research	2
	Crack Flow Theory	7
	Simple Ventilation Modelling	8
	Model Verification	8
	Mechanical Ventilation	14
2.	Development of a Pressure - Flow Relation for Building Leakage	15
	Introduction	15
	Flue Leakage	17
	Fan Pressurization Testing	25
	Summary	34
3.	EXACTAIM and AIM-2 : Simple Models for Estimating Infiltration Rates	35
	Introduction	35
	Review of some other Single-Zone Infiltration Models	36
	Development of EXACTAIM	40
	Stack Effect	41
	Some Special Cases of Stack Effect Infiltration	48
	Neutral Level Above Ceiling	48
	Including Flue Leakage in the Ceiling	50
	Assuming Orifice Flow through Leaks and No Separate Flue	50

Estimating Solutions to Stack Flow Equations..... 51
Estimating Neutral Level Location..... 52
Direct Estimation of Stack Factor for AIM-2..... 57
Wind Effect..... 68
Pressure Coefficients..... 72
Effects of Local Shielding on Wind Pressures..... 77
Theoretical Estimates for Wind Effect..... 90
Estimating Wind Factor for AIM-2..... 92
Superposition of Wind and Stack Effects..... 105
Superposition of Mechanical Ventilation..... 115
Summary..... 117
4. Comparison of AIM-2 with other Simple Ventilation Models.. 119
Introduction..... 119
The LBL model of Sherman..... 119
Variable n model..... 122
Warren and Webb's model..... 125
Shaw's Semi-Empirical NRC model..... 127
Summary..... 130
5. Model Evaluation..... 131
Introduction..... 131
Outline of Evaluation Procedure..... 131
Windspeed Dependance..... 134
Sheltered Conditions..... 139
Unsheltered Conditions..... 146
Model Accuracy for Stack Effect..... 151
Effect of Changing Leakage Distribution on Model

Predictions 156
Accounting for Mechanical Ventilation with AIM-2 161
Predicting Hourly Ventilation Rates 167
Summary 173
6. Conclusions and Recommendations 176
Furnace Flue Testing 176
Fan Pressurization Testing 177
Model Development and Verification 177
Recommendations 180
References 182
Appendix A 188

List of Tables

Table	Description	Page
1.1	Construction details of Houses Tested at AHHRF	12
3.1a	Atmospheric Stability Classes (Pasquill(1973))	71
3.1b	Power law exponent, p, as a function of atmospheric stability and terrain (Irwin 1978)	71
3.2	Estimates of Shelter Coefficient S_{wo} for no Flue	78
3.3	Details of Infiltration data sets used to Examine Building Shelter and Superposition Methods	80
5.1	Details of Infiltration data sets used to Validate Simple Ventilation Models	135
5.2	Details of Building Leakage used to evaluate Simple Ventilation Models	137
5.3	Equivalent Shelter Coefficients for simple ventilation models for East and West winds	140
5.4	Model Errors for Binned Averages of Wind Dominated Ventilation for Sheltered Buildings at AHHRF	149
5.5	Model Errors for Binned Averages of Wind Dominated Ventilation for Unsheltered Buildings at AHHRF	150
5.6	Model Errors for Binned Averages of Stack Dominated Ventilation at AHHRF	155
5.7	The Effect of Leakage Distribution Estimates on Model Predictions of Stack Dominated Ventilation for House#4 with an open 7.5 cm diameter orifice in a 15 cm diameter Flue	157
5.8	Summary of AIM-2 Errors in Predicting Hourly Ventilation rates in House #4 at AHHRF with a 7.5 cm diameter orifice in the Flue	168

List of Figures

Figure	Description	Page
1.1	The Alberta Home Heating Research Facility (AHHRF) from Kostiuk and Dale (1985).	10
1.2	Exploded view of House #5 at AHHRF from Wilson and Dale (1985)	11
2.1	Schematic of Flue Testing Apparatus	19
2.2	Pressure-Flowrate Relationship for 15 cm diameter Furnace Flue with Forward Flow	21
2.3	Pressure-Flowrate Relationship for 15cm diameter Furnace Flue with Reversed Flow (Backdraughting)	22
2.4	Schematic of Blower Test Apparatus with the Building Depressurised	28
2.5	Blower Test Results for a Brick Walled House (House #1 at AHHRF), with an Open 15 cm I.D. Flue with a 7.5 cm diameter orifice at the bottom, and with a blocked Flue. Windspeed < 1.0 m/s and $\Delta T < 10^oC$	30
2.6	Blower Test Results for a House with Single Stud Wood Framed Walls (House #2 at AHHRF), with an Open 15 cm I.D. Flue with a 7.5 cm diameter orifice at the bottom. Windspeed = 0.84 m/s and $\Delta T = 10^oC$	31
3.1	Empirical values for Neutral level, β_o, from Equation (3.28) with no Flue Leakage (Y=0), where X is the ceiling-floor difference and R is the ceiling-floor sum	54
3.2	Exact values for Neutral level, β_o, from Equation (3.15) with no Flue Leakage (Y=0), where X is the ceiling-floor difference and R is the ceiling-floor sum	55
3.3	Error in Stack Factor, f_s, using Empirical Equation (3.28) for Neutral Level, β_o, with no Flue Leakage	56
3.4	Empirical values for Neutral level, β_o, from Equation (3.28) with 20% of Leakage in Flue (Y=0.2) and β_f=1.5, where X is the ceiling-floor difference and R is the ceiling-floor sum	58

3.5	Exact values for Neutral level, β_o, from Equation (3.15) with 20% of Leakage in Flue (Y=0.2) and β_f=1.5, where X is the ceiling-floor difference and R is the ceiling-floor sum	59
3.6	Error in Stack Factor, f_s, using Empirical Equation (3.28) for Neutral Level, β_o, with 20% of Leakage in Flue (Y=0.2) and β_f=1.5	60
3.7	Empirical Equation (3.30) for Stack Factor, f_s, with no Flue Leakage (Y=0), where X is the ceiling-floor difference and R is the ceiling-floor sum	63
3.8	Empirical Equation (3.30) for Stack Factor, f_s with 20% of Leakage in the Flue (Y=0.2) and β_f=1.5, where X is the ceiling-floor difference and R is the ceiling-floor sum	64
3.9	Error in using Empirical Equation (3.30) for Stack Factor, f_s, with no Flue Leakage (Y=0), where X is the ceiling-floor difference and R is the ceiling-floor sum	65
3.10	Error in using Empirical Equation (3.30) for Stack Factor, f_s, with 20% of Leakage in the Flue (Y=0.2) and β_f=1.5, where X is the ceiling-floor difference and R is the ceiling-floor sum	66
3.11	Comparison of Empirical Equation (3.30) for Stack Factor, f_s, with 20% of Leakage in the Flue (and β_f=1.5), and f_s estimated using Sherman's Equation (3.33)	67
3.12	Illustration of pressure coefficients taken from Akins (1979)	74
3.13	Variation of measured wind driven ventilation rate with wind angle for House #1 with Flue Blocked where $\Delta T \leq 10$ °C and $3 \leq U \leq 8$ m/s (785 hours)	81
3.14	Variation of measured wind driven ventilation rate with wind angle for House #1 with an open Flue where $\Delta T \leq 10$ °C and $3 \leq U \leq 8$ m/s (498 hours)	82
3.15	Binned measured wind driven ventilation rate with wind angle for House #1 with Flue Blocked where $\Delta T \leq 10$ °C and $3 \leq U \leq 8$ m/s, and Shielding Coefficient Sw (Solid Line) (785 hours)	86

3.16	Binned measured wind driven ventilation rate with wind angle for House #1 with an open Flue where $\Delta T \leq 10°C$ and $3 \leq U \leq 8$ m/s, and Shielding Coefficient Sw (Solid Line) (498 hours)	87
3.17	Binned measured wind driven ventilation rate with wind angle for House #4 with Flue Blocked and more Leakage in South wall than North Wall where $\Delta T \leq 10°C$ and $4 \leq U \leq 8$ m/s, and Shielding Coefficient Sw (Solid Line) (535 hours)	89
3.18	Variation in Calculated Wind Factor from EXACTAIM due to Changing Pressure Coefficients with Wind Angle, with X=0, R=0.5, Y=0.2, βt=1.5, n=2/3. Using Akins data (1979). The solid line connects each calculated value of fw	93
3.19	Variation in Calculated Wind Factor from EXACTAIM for the pressure coefficient data sets of Akins, AIVC, ASHRAE, and Wiren, with R=0.5 and Y=0 and wind perpendicular to upwind building face	95
3.20	Empirical Equation (3.48) for Wind Factor fw in AIM-2 with no Flue Leakage (Y=0) and n=2/3, where X is the ceiling-floor difference and R is the ceiling-floor sum	96
3.21	Empirical Equation (3.48) for Wind Factor fw in AIM-2 with 20% of Leakage in the Flue (Y=0.2), n=2/3 and βt=1.5, where X is the ceiling-floor difference and R is the ceiling-floor sum	97
3.22	Range of Errors associated with the empirical equation (3.48) for fw in AIM-2 with no Flue Leakage (Y=0) and n=2/3	98
3.23	Range of Errors for the empirical equation (3.48) for fw in AIM-2 with 20% of leakage in the Flue (Y=0.2), n=2/3 and βt=1.5	99
3.24	Empirical Equation (3.50) for Wind Factor fw in AIM-2 for a house with a Crawl Space and no Flue Leakage (Y=0), where X is the ceiling-floor difference and R is the ceiling-floor sum	102
3.25	Range of Error for the empirical equation (3.50) for fw in AIM-2 for a house with a Crawl Space and no Flue Leakage (Y=0)	103
3.26	Exact Values of fw calculated by EXACTAIM, using the same assumptions as Sherman: Y=0,	104

n=1/2, Zero external Cp for attic and floor, where the floor is over a crawlspace

3.27 Evaluation of Superposition Methods for house#4 with about 40% of Leakage in the Flue (Using 1047 hours) 110

3.28 Evaluation of Superposition Methods for house#4 with Flue blocked (Using 642 hours) 111

3.29 Evaluation of Superposition Methods for house#1 with about 75% of Leakage in the Flue (Using 977 hours) 114

5.1 Unbinned measured ventilation rates for House#4 with blocked flue, shielded, with $\Delta T \leq 10^{o}C$ and $U \geq 1.5$ m/s (464 hours) 141

5.2 Binned measured ventilation rates for House#4 with blocked flue, shielded, with $\Delta T \leq 10^{o}C$ and $U \geq 1.5$ m/s (464 hours) 142

5.3 Comparison of Ventilation Models with measured data for Shielded Windspeed dependance (East and West Winds) in house #4 with blocked flue and $\Delta T \leq 10^{o}C$ and $U \geq 1.5$ m/s (464 hours) 144

5.4 Comparison of Ventilation Models with measured data for Shielded Windspeed dependance (East and West Winds) in House #5 with an open 15cm diameter flue with $\Delta T \leq 10^{o}C$ and $U \geq 1.5$ m/s (461 hours) 145

5.5 Comparison of Ventilation Models with measured data for Unshielded Windspeed dependance (North and South Winds)in House #4 with blocked flue, and $\Delta T \leq 10^{o}C$ and $U \geq 1.5$ m/s (285 hours) 147

5.6 Comparison of Ventilation Models with measured data for Unshielded Winsdpeed dependance (North and South Winds) in House #5 with an open 15cm diameter flue with $\Delta T \leq 10^{o}C$ and $U \geq 1.5$ m/s (279 hours) 148

5.7 Comparison of Ventilation Models to measured data for ΔT dependance in House #4 with an open 7.5cm diameter orifice in the flue, with $\Delta T \geq 10^{o}C$ and $U \leq 1.5$ m/s. R=0.3, X=0, Y=0.4, and βt=1.5 (102 hours) 152

5.8 Comparison of Ventilation Models to measured data for ΔT dependance in House #5 with flue blocked with $\Delta T \geq 10^{o}C$ and $U \leq 1.5$ m/s (74 hours) 153

5.9 Comparison of Ventilation Models to measured data for ΔT dependance in House #4 with an open 7.5cm diameter orifice in the flue, with ΔT≥10°C and U≤1.5 m/s. R=0, X=0, Y=0.4, and βt=1.5 (102 hours) 158

5.10 Comparison of Ventilation Models to measured data for ΔT dependance in House #4 with an open 7.5cm diameter orifice in the flue, with ΔT≥10°C and U≤1.5 m/s. R=0.2, X=-0.1, Y=0.4, and βt=1.5 (102 hours) 159

5.11 Comparison of Ventilation Models to measured data for ΔT dependance in House #4 with an open 7.5cm diameter orifice in the flue, with ΔT≥10°C and U≤1.5 m/s. R=0.4, X=0.2, Y=0.4, and βt=1.5 (102 hours) 160

5.12 Predicted and measured ventilation rates in House #2 with an open 15 cm diameter flue with mechanical ventilation cycling every 4 hours for wind dominated natural ventilation: U=7.0m/s, ΔT=15.8°C, Qwind/Qstack=1.66 164

5.13 Predicted and measured ventilation rates in House #2 with an open 15 cm diameter flue with mechanical ventilation cycling every 4 hours for stack dominated natural ventilation: U=2.6m/s, ΔT=13.3°C, Qwind/Qstack=0.44 165

5.14 Predicted and measured ventilation rates in House #2 with an open 15 cm diameter flue with mechanical ventilation cycling every 4 hours for similar stack and wind effects: U=2.9m/s, ΔT=9.3°C, Qwind/Qstack=0.88 166

5.15 Predicted and measured natural ventilation rates for wind dominated natural ventilation in House #4 with a 7.5cm diameter orifice in the flue. U=4.1m/s, ΔT=9.4°C, Qwind/Qstack=1.85 170

5.16 Predicted and measured natural ventilation rates for stack dominated natural ventilation in House #4 with a 7.5cm diameter orifice in the flue. U=1.7m/s,ΔT=27.9°C, Qwind/Qstack=0.32 171

5.17 Predicted and measured ventilation rates, both wind and stack effects significant in House #4 with a 7.5cm diameter orifice in the flue. U=3.7m/s,ΔT=16.7°C, Qwind/Qstack=1.0 172

Nomenclature

A	Area
A_o	Equivalent leakage area
A_1	Factor used to determine neutral level
A_c	Crack flow area
A_j	Area of wall j
A_r	Ratio of stack to wind forces in Warren and Webb's model
B_1	Superposition constant for AIM-2
β	Dimensionless height
β_f	Dimensionless flue height
β_o	Dimensionless neutral level height
C	Flow coefficient
C'	Sherman's local shelter coefficient
$C_{building}$	Total building leakage coefficient
C_c	Ceiling leakage
C_f	Floor leakage
C_{flue}	Flue leakage
C_i	Leakage of i^{th} leak
C_p	Pressure coefficient
$C_{pceiling}$	Pressure coefficient for the ceiling
C_{pflue}	Pressure coefficient for the flue
C_{pi}	Pressure coefficient for i^{th} leak
C_{pin}	Indoor pressure coefficient
C_{pwalls}	Average pressure coefficient on the four walls

C_w	Wall leakage
C_1	Superposition constant
D	Pipe diameter
D_1	Flow coefficient for wind driven ventilation
D_2	Flow coefficient for stack driven ventilation
D_{Shaw}	Flow coefficient for Shaw's model
ΔP	Pressure difference
ΔP_{env}	Pressure difference across building envelope
ΔP_{fan}	Pressure difference due to mechanical ventilation fan
ΔP_i	Pressure difference across leak i
$\Delta P_{natural}$	Pressure due to stack and wind effects
ΔP_o	Offset pressure
ΔP_{ref}	Reference pressure for equivalent leakage area
ΔP_s	Stack pressure difference
ΔP_T	Reference pressure for Warren and Webb's model
ΔP_{total}	Combined fan and stack and wind pressures
ΔP_w	Wind pressure difference
ΔT	Indoor-outdoor temperature difference
f_s	Stack factor
$f_{s,LBL}$	LBL stack factor
f_w	Wind factor for house with basement or slab-on-grade
f_{wc}	Wind factor for house with a crawl space
$f_{w,sherman}$	Wind factor from Sherman
F	Factor used to determine neutral level
F'	Factor used to account for wind and stack interaction in Shaw's model

F_B	Stack factor for Warren and Webb's model
F_V	Parameter combining stack and wind factors in Warren and Webb's model
F_W	Wind factor for Warren and Webb's model
g	Acceleration due to gravity
G	Parameter defined to determine stack factor
γ	Superposition exponent
h	Height above grade
h_o	Neutral level height above grade
H	Building ceiling height above grade
H_f	Flue height above grade
H_m	Windspeed measurement height
K	Orifice coefficient
γ	Crack flow flow coefficient
L	Length of pipe for fully developed flow
λ	Average ratio of predicted to measured flowrates
$\dot{M}_{ceiling}$	Mass flow rate through the ceiling
$\dot{M}_{flue}$	Mass flow rate through the flue
$\dot{M}_i$	Mass flow rate through leak i
$\dot{M}_{in}$	Mass flow into building
$\dot{M}_{out}$	Mass flow out of building
$\dot{M}_{stack}$ or $\dot{M}_s$	Stack mass flow rate
$\dot{M}_{wallj}$	Mass flow rate through wall j
$\dot{M}_{wind}$ or $\dot{M}_{wind}$	Wind mass flow rate
n	Flow exponent
N	Parameter defined to determine stack factor

p	Boundary layer wind profile exponent at building
p'	Boundary layer wind profile exponent at measurement site
P	Pressure
P_∞	Free stream reference pressure
$P_{S,LBL}$	LBL defined stack pressure
P_{stack}	Characteristic stack pressure
P_{wind}	Characteristic wind pressure
Q	Volume flowrate
$Q_{balanced}$	Flowrate through balanced mechanical ventilation system
$Q_{ceiling}$	Volume flowrate through ceiling level leaks
Q_{fan}	Flowrate through fan
Q_{floor}	Volume flowrate through floor level leaks
Q_{flue}	Volume flowrate through furnace flue
Q_{lrg}	Largest of stack and wind flowrates
$Q_{natural}$	Flowrate due to stack and wind effects
$Q_{sheltered}$	Infiltration rate for a sheltered building
Q_{sml}	Smallest of stack and wind flowrates
Q_{stack} or Q_s	Stack driven volume flowrate
Q_T	Reference flowrate for Warren and Webb's model
Q_{total}	Combine stack and wind volume flowrate
$Q_{unsheltered}$	Infiltration rate for an unsheltered building
Q_{wall}	Flowrate through the walls
Q_{wind} or Q_w	Wind induced volume flowrate
$\bar{Q}$	Average flowrate
Q'	Fluctuation in flowrate
r	Ratio of indoor air density to outdoor air density

R	Ceiling-floor leakage sum
R^*	Parameter used to determine f_{wc}
ρ	Air density
ρ_{in}	Indoor air density
ρ_i	Air density in leak i
ρ_{out}	Outdoor air density
Re	Reynolds number
S_1	Wind shielding factor for upwind wall
S_2	Wind shielding factor for wall 90° clockwise from upwind wall
S_3	Wind shielding factor for wall 180° clockwise from upwind wall
S_4	Wind shielding factor for wall 270° clockwise from upwind wall
S_w	Total wind shielding factor
S_{wo}	Wind shielding factor for building
S_{wf}	Wind shielding factor for flue
T_{in}	Indoor air temperature
T_{out}	Outdoor air temperature
θ	Wind direction
θ_{local}	Wind direction correction for local terrain changes
θ_{met}	Wind direction at measurement site
θ_o	Angle between normal to upwind wall and North
U	Windspeed
U_{600}	Windspeed at 600 meters above ground
U_{flue}	Windspeed at the flue top

U_H	Windspeed at ceiling height
U_o	Windspeed at measurement height
$U_{sheltered}$	Effective windspeed for a sheltered building
$U_{unsheltered}$	Effective windspeed for an unsheltered building
U'	Sherman's reduced windspeed
$\bar{U}$	Average windspeed
U''	Fluctuation in windspeed
V	Building volume
X	Ceiling-floor leakage difference
X_{crit}	Critical X value
X_s	Shifted X value
X_{scrit}	Critical shifted X value
X^*	Parameter used to determine f_{wc}
Y	Fraction of leakage in the flue
Y^*	Parameter used to determine f_{wc}
z	Height above outside ground reference
z_o	Surface roughness
Z	Parameter used to determine wind factor

Chapter 1

Introduction

1.1 Why do we Need Building Ventilation Models?

As Western Civilization has advanced, people have been spending more and more of their time inside buildings. In order to keep the inhabitants alive these buildings require a supply of fresh, uncontaminated air. If this were the only requirement then we would simply build very leaky buildings. Unfortunately, there is also a requirement that the inhabitants are comfortable indoors, which is, after all, the motive for being inside where one is sheltered from the extremes of the external environment. This necessitates conditioning of the air supply such that it is at a comfortable temperature and humidity.

On one hand there is the demand for fresh air so that the building remains habitable, and on the other is the cost of conditioning that air by heating, cooling, etc. Thus a balance must be struck for the quantity of aif exchanged between inside and outside the building. To determine if this balance is met, the air exchange rate for a building must be known. Although there are methods for directly measuring air change rates these apply only to existing buildings and the results apply only during the time when the measurements were taken. What is required are methods of estimating air exchange rates other than by direct measurement, i.e. by predictive building ventilation models.

These ventilation models can also be used to determine the amount of protection from accidental outdoor releases of toxic substances such

as hydrogen sulphide or chlorine. Or they may be used to study moisture migration in buildings. In addition, methods of increasing or decreasing ventilation rates may be studied without having to actually build and test the structures in question.

1.2 A Short History of Ventilation Research

Of course, the study of ventilation is not a new one. The ancient Romans developed ideas about heating and ventilating buildings, including such things as radiant floor heating systems. A little closer to the present, in 1844, Dr. D.B. Reid published a volume entitled "Illustrations of Ventilation". Reid was a Scottish physician who was concerned about indoor air quality, and its physical and mental effects on the human body. The following quotation shows how seriously Reid believed in the need to study ventilation. From Reid (1844, p.7):

"... the ravages of consumption, and the extended catalogue of evils accompanying diseases of the organs of respiration, point out the vast amount of misery that might be obviated, and of death that might be prevented, were the leading principles and practice of ventilation more generally understood."

Reid goes on to give some illuminating examples of the rejuvenating effects of fresh air; one of which is:

"...; that cases have actually presented themselves where the apparently lifeless corpse, subdued and oppressed far more by the atmosphere with which it was surrounded, than by the disease to which it was supposed to have fallen a victim, has actually been known to revive after removal to the dead-room, a separate apartment, where the play of

a wholesome atmosphere, flowing unrestrictedly upon it, revived the fading flame of life after it was to all appearance gone, ...".

To improve the quality of indoor air, Reid catalogued many methods of ventilation, including ventilation by the natural effects of wind and indoor-outdoor temperature difference, mechanical ventilation by fans (at that time extremely unreliable) and systems of "passive" ventilation (maximizing the ventilation due to natural effects), and also how to regulate these ventilation systems. Reid compiled a surprisingly complete listing of sources of pollution including such things as furniture, exhaust fume recirculation, tobacco smoke and flue backdraughting due to excessive mechanical ventilation which are often considered to be problems of more recent interest. This book also includes methods of gas analysis, standards to determine the purity of air, and recommendations for ventilation standards. For example, Reid (1844) recommends a supply of approximately 10 cubic feet per minute (CFM) of fresh air per person and ASHRAE Standard 62-1981R (1986) recommends 15 CFM. These values are very close considering the vast variation on air requirements depending on many factors including exercise rate and variations from person to person which are hard to quantify.

It is interesting to see that almost 150 years ago a great deal was known about ventilation and how little has changed in the study of ventilation in the intervening years. The changes that have occurred have mainly been in the field of fluid mechanics. In 1907 Sir William Napier Shaw published a book entitled "Air Currents and the Laws of Ventilation", by which time it was known that the relationship between flowrate and pressure had two distinct terms. One term was the contribution of laminar

skin friction, where flowrate is directly proportional to pressure difference, and the other was the contribution of kinetic energy losses where flowrate is proportional to the square root of pressure difference. Shaw was concerned with the ventilation of large rooms with many occupants where the flow through the ventilation ducts dominates the pressure-flow relationship for the ventilated space. Shaw therefore assumed that the kinetic energy term was dominant in ventilation flows, thus the equation Shaw used to describe the relationship between flow and pressure was for orifice flow where:

$$Q = C(\Delta P)^{1/2} \qquad (1.1)$$

where Q = flowrate

C = flow coefficient proportional to area

ΔP = pressure difference across the system

Shaw used an electrical analogy to represent the ventilation system where:

$$\text{flow } (Q) \Rightarrow (\text{current})^{1/2}$$

$$\text{Pressure difference } (\Delta P) \Rightarrow \text{Voltage}$$

$$\text{Flow coefficient } (C) \Rightarrow \left(\frac{1}{\text{Resistance}} \right)^{1/2}$$

This electrical analogy was applied to ducts in series and parallel and for mechanical ventilation, so that complex configurations could be modelled. Shaw also extended this analogy to multi-zone models. In a multi-zone model a building is divided into distinct areas, or zones.

Each zone can communicate air with other zones and the outside of the building. The net flow through the building is found by simultaneously solving the flow equations for flow into and out of each zone. Shaw gave tables of pressures due to temperature difference, stagnation flow on a flat plate, and typical fan pressures to be used as inputs to his model. Shaw's other input to the model was a known flowrate, because he was concerned with providing a sufficient ventilation rate for buildings containing many people, and his model found the driving force and duct size neccessary to provide this flowrate. This is the major difference from the models that will be examined and developed in later chapters of this thesis, where the flowrate is unknown, and is determined by estimations of the driving forces and building leakage. The models in this thesis have been developed for application to residential houses rather than for large buildings with many occupants.

The study of ventilation in homes, rather than large buildings, was not greatly advanced until the work of Dick (1950). Dick looked at the fundamental aspects of the driving forces involved in building ventilation: the stack and wind effects, but still assumed that orifice flow equations described building leakage. The basic ideas behind ventilation modelling have not changed a great deal since his work.

The major theoretical change is:

- instead of assuming orifice flow, actual tests on houses, and increased knowledge of crack flow lead to replacing the pressure flow relationship in (1.1) with

$$Q = C\Delta P^{n} \qquad (1.2)$$

where C and n are experimentally determined flow coefficients.

It is interesting to note that many current infiltration models (For example, Sherman and Grimsrud (1980) and ASHRAE (1985)) do not even make this change, and retain the orifice flow equation used by Shaw in 1907. Other changes are to the parameters that form the input to the model:

1. Better estimates of wind pressure are available from pressure coefficients calculated from wind tunnel data, and estimates of shielding effects.
2. Instead of just the flow resistance of ventilation ducts, the flow characteristics of the entire building envelope or its individual components can be found.
3. The effects of leakage distribution and location can be included.
4. The flow through open windows and doors can be modelled based on experimental results.

The use of computers to find exact solutions to flow equations has allowed the development of simple estimating equations for use in handbooks. In addition, complex models with different pressure-flow relationships for each leak that calculate exact solutions can now be used on computers. These models work in the reverse of Shaw's model, where the flowrate was assumed to be known, and the ducts sized to provide this flow for some assumed pressure difference. Instead, they calculate the flow based on the leakiness of the building elements and the imposed pressure due to wind stack and mechanical ventilation effects.

1.3 Crack Flow Theory

At the entrance to the crack, or after any sharp disturbance in the crack, a boundary layer develops that grows in thickness from the walls. When the flow no longer changes its velocity profile and the variation in pressure is linear with downstream distance then the flow is said to be fully developed. Cracks in buildings do not have sufficient unobstructed length in which the flow can become fully developed. Experimental studies by Honma (1975), Kronvall (1980), Shapiro, Siegel and Kline (1954), Peterson (1982) and others have shown that flow in cracks similar to those found in buildings is rarely fully developed, due to the geometry of typical building leaks.

This leads to the use of equation (1.2) to describe crack flow.

$$Q = C\Delta P^{n} \tag{1.2}$$

where Q = flowrate

ΔP = pressure difference

C = flow coefficient

n = flow exponent, $1/2 \leq n \leq 1$

with $n = 1/2$ for fully developed turbulent flow

$n = 1$ for fully developed laminar flow

Experiments have been performed on furnace flues in a laboratory which verify (1.2) over the range of pressures and flowrates associated with ventilation flows. The application of (1.2) to building ventilation was also verified by examining the results of some of the 3,000 fan pressurization tests performed in 6 test houses of varying construction, leakage area and leakage distribution.

1.4 Simple Ventilation Modelling

For this study two models have been developed. EXACTAIM uses theoretical relationships and wind tunnel pressure coefficients to develop exact equations for predicting ventilation rates. AIM-2 uses simple empirical approximations to the results of EXACTAIM to make it a more useful tool for finding ventilation rates. For both models equations to estimate ventilation rates will be developed, based on reasonable assumptions about leakage distribution and the wind and temperature difference (stack) driven flows. The wind and stack effects will be examined separately then superposed. The superposition will have an extra term accounting for the interaction between stack and wind effect. The application of these models will be based on the pressure-flow relationship (1.2) whose coefficients, C and n, are determined by fan pressurization tests. AIM-2 has been developed to be as simple as possible for application to routine ventilation design calculations, and its predictions will be compared to those of other simple ventilation models. A variable n model based on the work of Yuill (1985) that uses some of the simplifying relationships developed by Sherman (1980) has also been developed for this study.

1.5 Model Verification

Since 1980 six adjacent unoccupied single-zone test houses at the Alberta Home Heating Research Facility (AHHRF hereafter) have been operated as a research facility to measure building energy use,

including tracer gas measurements of infiltration rates. A sketch of the test facility showing the row of six test houses is shown in Figure 1.1 (from Kostiuk and Dale (1985)). Data taken in Houses one, two, four and five are used in this thesis. A sketch of House #5 is shown as an example in Figure 1.2 (from Wilson and Dale (1985)). The other houses differ in their construction details as given in Table 1.1. All data is collected by an Hewlett Packard Model 85 Microcomputer based data acquisition system eight times an hour for each house, and recorded as hourly averages. Miran 103 gas analyzers are used to monitor SF_6 tracer gas concentrations in a constant concentration tracer gas injection system to measure ventilation rates, thermocouples are used to measure indoor and outdoor temperatures, and wind speed and direction are measured on site on a 10m high meteorological tower. The test facility and tracer gas measurement techniques are described in more detail by Wilson and Pittman (1983). A data base of over 25,000 hours has been compiled in each house for various leakage distributions, including open windows, furnace flues of various sizes, and mechanical ventilation. The predictions of the ventilation models developed here will be tested by comparison to these measured air infiltration rates. Appropriate data sets will also be used to examine wind shelter and superposition techniques for combining wind and stack driven ventilation.

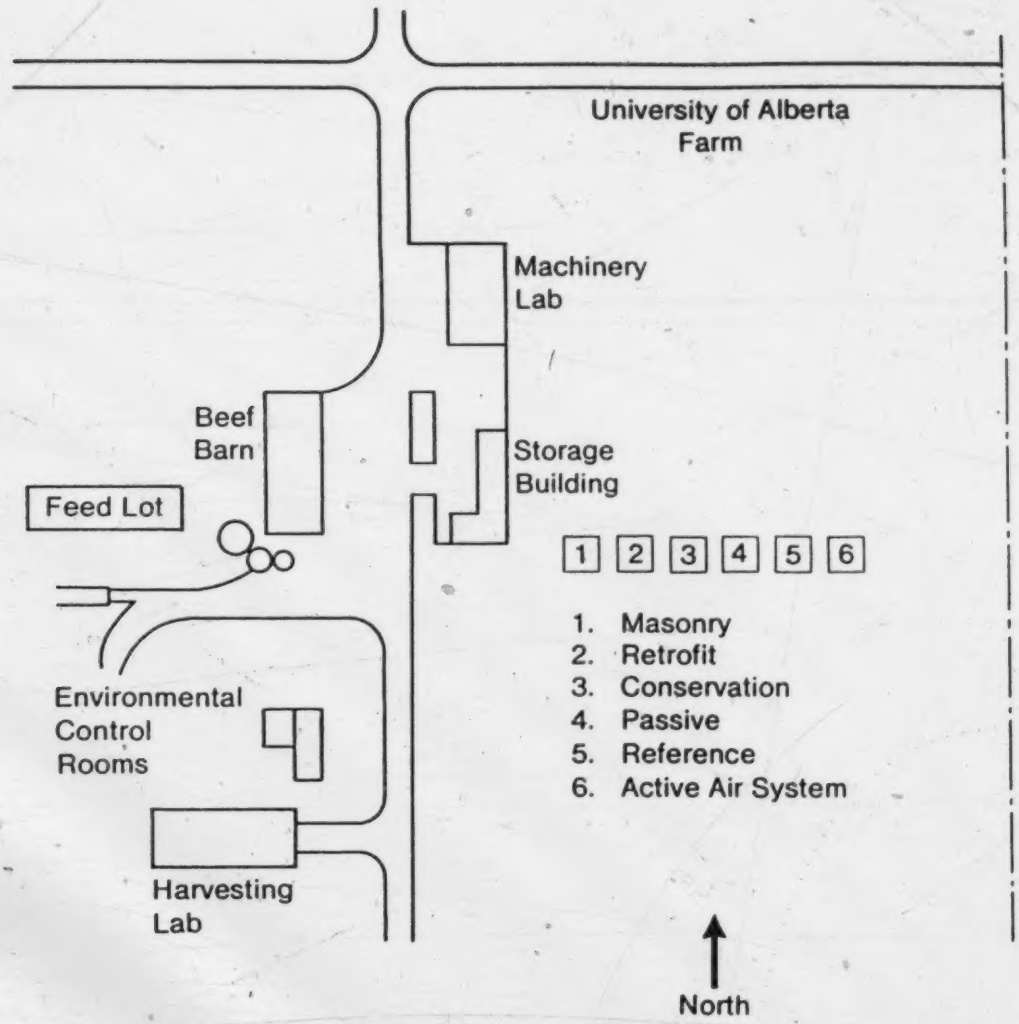

Figure 1.1: The Alberta Home Heating Research Facility (AHHRF) from Kostiuk and Dale (1985).

(no copyright).

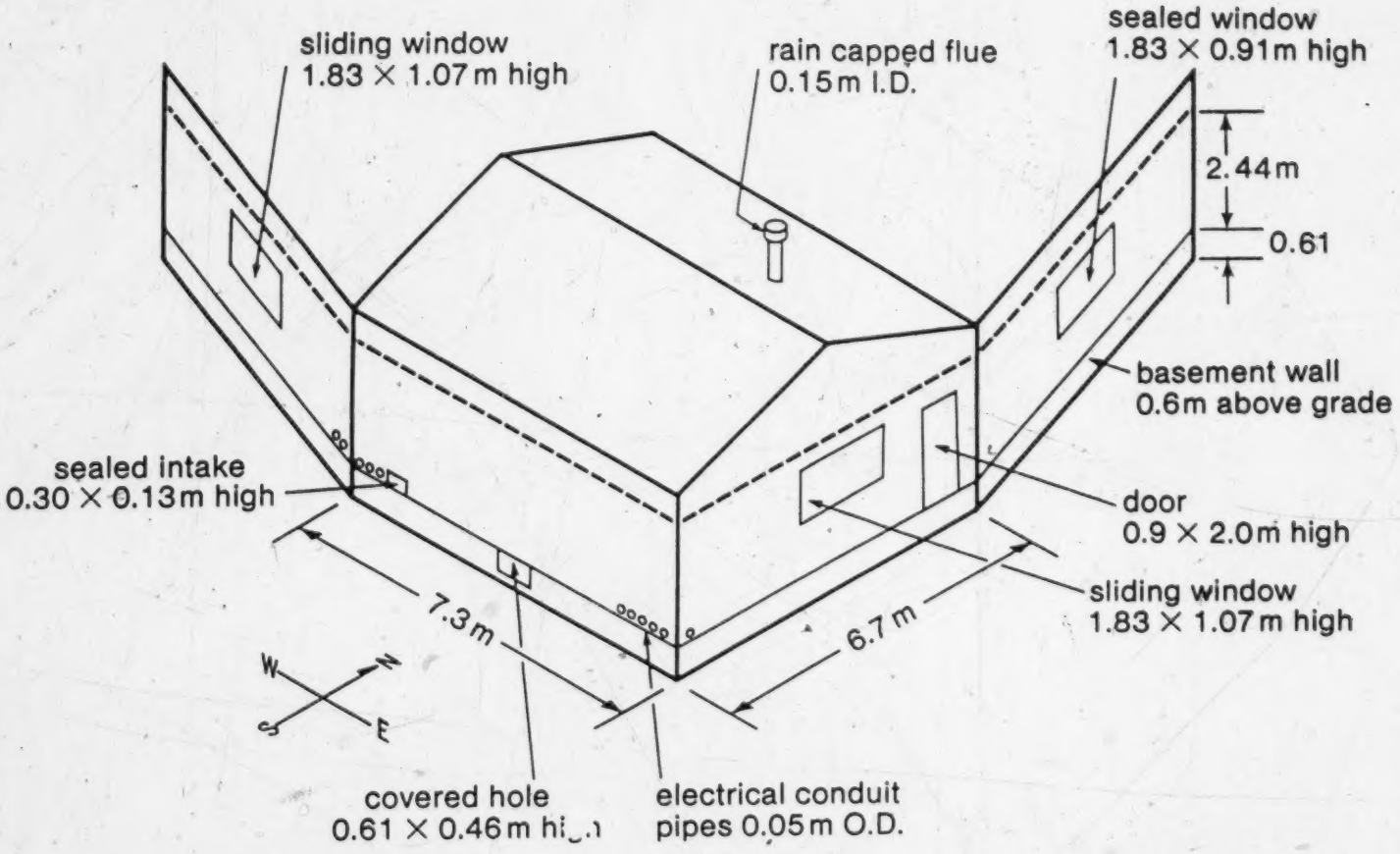

Figure 1.2: Exploded view of House #5 at AHHRF from Wilson and Dale (1985)(no copyright).

Table 1.1 Construction Details of Houses Tested at AHHRF

All houses have gable roofs on elevated roof trusses and full concrete basements.

House #1

Floor Area:	6250 x 6860 mm
Wall Height:	2440 mm
Basement Height:	2440 mm, 1830 mm Below Grade
Walls:	76 mm Burned Clay Brick 64 mm foamed-in-place polyurethane insulation 100 mm Concrete Block
Windows:	North : 1000 x 1950 mm double glazedsealed South : 2 - 1220 x 1220 mm double glazed sealed East : 1000 x 1950 mm double glazed opening West : 1000 x 1950 mm double glazed opening
Ceiling:	0.152 mm polyethylene Vapour Barrier 13 mm Gypsum Wallboard
Door:	910 x 2030 mm solid core fir

House #2

Floor Area:	6250 x 6860 mm
Wall Height:	2440 mm
Basement Height:	2440 mm, 1830 mm Below Grade
Walls:	9.5 mm Prestained Rough Tex Plywood 50 mm x 100 mm studs with fiberglass batt insulation 0.152 mm polyethylene Vapour Barrier 13 mm Painted Gypsum Wallboard
Windows:	North : 1000 x 1950 mm double glazed sealed South : None East : 1000 x 1950 mm double glazed opening West : 1000 x 1950 mm double glazed opening
Ceiling:	9.5 mm plywood sheathing 0.152 mm polyethylene Vapour Barrier 13 mm Gypsum Wallboard
Door:	910 x 2030 mm solid core fir

Table 1.1 continued: Construction Details of Houses Tested at AHHRF

House #4

Floor Area:	6250 x 6860 mm
Wall Height:	2440 mm
Basement Height:	2440 mm, 1830 mm Below Grade
Walls:	9.5 mm Prestained Rough Tex Plywood 50 mm Rigid Insulation 50 mm x 100 mm studs with fiberglass batt insulation 0.228 mm polyethylene Vapour Barrier 13 mm Painted Gypsum Wallboard
Windows:	North : None South : 2 - 2870 x 910 mm double glazed sealed East : 1090 x 1065 mm double glazed opening West : None
Ceiling:	9.5 mm plywood sheathing 0.228 mm polyethylene Vapour Barrier 13 mm Gypsum Wallboard
Door:	910 x 2030 mm insulated metal

House #5

Floor Area:	6250 x 6860 mm
Wall Height:	2440 mm
Basement Height:	2440 mm, 1830 mm Below Grade
Walls:	9.5 mm Prestained Rough Tex Plywood 50 mm x 100 mm studs with fiberglass batt insulation 0.152 mm polyethylene Vapour Barrier 13 mm Painted Gypsum Wallboard
Windows:	North : 990 x 1950 mm double glazed sealed South : None East : 1000 x 1950 mm double glazed opening West : 1000 x 1950 mm double glazed opening
Ceiling:	9.5 mm plywood sheathing 0.152 mm polyethylene Vapour Barrier 13 mm Gypsum Wallboard
Door:	910 x 2030 mm insulated metal

1.6 Mechanical Ventilation

The majority of houses constructed in recent years have fans to ventilate the rooms that have the greatest pollutant levels, such as kitchens and bathrooms. The effect of these fans on the ventilation rate of houses is currently a topic of debate. For example, Kiel and Wilson (1987) showed that the existing method recommended for combining natural infiltration with fan ventilation in the ASHRAE Fundamentals Handbook (1989) underestimates the combined ventilation flow by up to 50%. Current methods of superposing mechanical and natural (due to wind and stack effects) will be examined and compared to the results of experiments performed in House #2 at AHHRF. The mechanical ventilation system in House #2 has been developed to have a large pressure drop of about 350 Pa across an orifice used to measure the flowrate, so that the flow rate is independant of the natural ventilation rate occurring due wind and stack pressures (typically <10 Pa) on the building.

Chapter 2

Development of a Pressure - Flow Relation for Building Leakage

2.1 Introduction

The objective of a ventilation model is to predict the quantity of air exchanged through the building envelope (which is the external surface of the building that experiences some pressure differential due natural or mechanical ventilation effects). In this chapter previous studies of crack flow will be reviewed, and the results of experiments performed for this study will be examined, to determine an appropriate relationship between pressure difference and flowrate. This relationship is to be used in ventilation models to predict flowrates from a known pressure distribution. The particular experiments performed for this study examined flow through furnace flues under controlled laboratory conditions and field tests of flow through entire building envelopes.

2.2 Crack Flow

The pressure-flow relationships for fully developed laminar (Poiseille) flow and turbulent (orifice) flow give the limiting cases for crack flow where:

$$Q = \kappa \Delta P \qquad \text{laminar} \qquad (2.1)$$

$$Q = \kappa \Delta P^{1/2} \qquad \text{turbulent} \qquad (2.2)$$

Q = Flowrate

ΔP = Pressure difference across crack

κ = A constant flow coefficient

These relationships are simple and well known and the equation for fully turbulent orifice flow has been used often in ventilation modelling (beginning with Shaw (1907)). For crack geometries typical of building leaks, however, studies by Hopkins and Hansford (1974), Shapiro, Siegel and Kline (1954), Kreith and Eisenstadt (1957), Honma (1975), Kronvall (1980) and many others have shown that the flow in these cracks is never fully developed and a more general power law relationship appropriate, as in equation (1.2), where:

$$Q = C\Delta P^n \tag{1.2}$$

and $$\frac{1}{2} \leq n \leq 1$$

and C is a flow coefficient.

Furthermore, Kronvall showed that equation (1.2) applies not only to single cracks, but also to cracks arranged in series and parallel. This is significant, because the leaks in building envelopes are a combination of series and parallel flow paths.

For the simple crack geometries tested by Kreith and Eisenstadt they found that for a given crack length and diameter, n depends on Q and ΔP. At low flow rates (and pressures) the flow becomes more laminar and n approaches 1, while at high flow rates (and pressures) the flow becomes more turbulent and n approaches 1/2. If more complex, and therefore more realistic, geometries are tested Kronvall's and Honma's experiments showed that (despite Honma's claim to the opposite) n is constant over a very wide range of flowrates and pressures (Honma performed tests from 1 to 50 Pa), encompassing the typical values

experienced by a building envelope. In addition, envelope pressurization leakage testing discussed later in this chapter confirms that C and n do not vary with flowrate and pressure difference for the test houses at the Alberta Home Heating Research Facility.

Dimensional analysis by Kiel, Wilson and Sherman (1985) has shown that C and n are not independent and are related by:

$$C \propto A_c^{(n+0.5)} \tag{2.3}$$

where A_c is the flow area of the crack.

If the leakage of a building does not change, then A_c is fixed and single values of C and n describe characteristics of flow through the building envelope. The specific nature of the cracks in the building determines unique values of C and n for the building.

2.2 Flue Leakage

Except for open doors and windows, the furnace flue is usually the largest single leakage site in a building envelope. It is also the easiest to define in terms of size, shape and location. Thus an exact pressure-flow relationship for a flue will be useful in reducing errors in air infiltration modelling. In order to determine an exact relationship between flue flow rate and pressure difference across a flue, laboratory tests were performed on a furnace flue typical of Canadian housing. The test flue consisted of 5 meters of 15 cm I.D. double walled pipe (Class B vent). There is a raincap at one end of the pipe and a sharp edged inlet at the other. Tests were also

performed with the sharp edged inlet replaced by a 7.5 cm diameter orifice. The test houses at AHHRF currently have an orifice of this size at the bottom of the furnace flue. This is used to reduce the effective area of the flue, and it is also used as an orifice meter to monitor flowrates through the flue. The laboratory tests were performed under known, controlled conditions of temperature and pressure to eliminate their effects on the measurements. The flue was tested horizontally to eliminate any contribution to the flow due to bouyancy caused by temperature differences in the laboratory.

A settling chamber consisting of a one meter cube partially filled with filter material was placed at each end of the flue and the pressure difference between these chambers was the driving pressure along the flue. An ASME standard orifice flow meter with flange taps was placed upstream of the flue to measure the flowrate. Several orifice diameters were used so that errors due to low Reynolds number effects were reduced.

Air was drawn through the flue using a centrifugal fan on the outlet so that fan turbulence would not affect the results. A schematic of the flue testing apparatus is shown in Figure 2.1. The pressures were measured using Validyne magnetic reluctance metal diaphram pressure transducers and a time averaging voltmeter. The pressure transducers were calibrated using a water column pressure source and a micromanometer. The uncertainty associated with the pressure measurement is about 0.25 Pa.

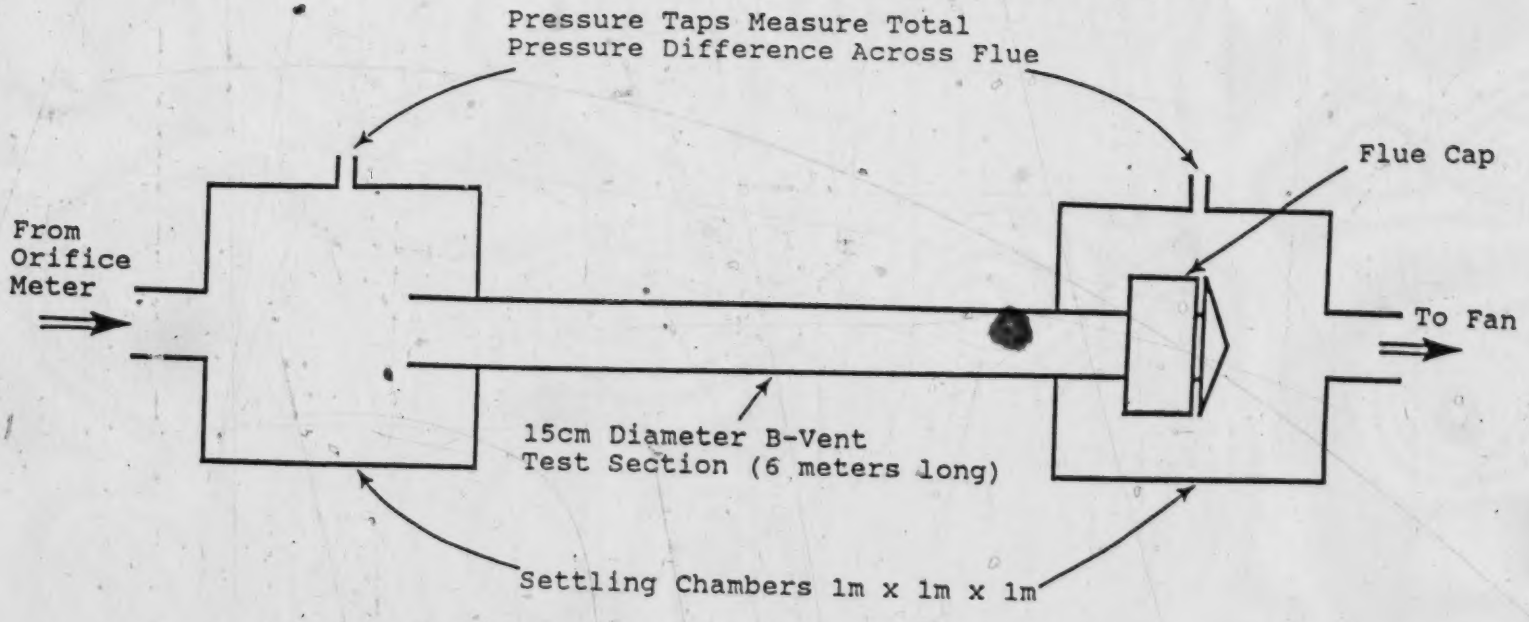

Figure 2.1: Schematic of Flue Testing Apparatus

In order to obtain reasonable results below 1 Pa it is necessary to make very careful calibrations, and to correct for the offset pressures measured at zero flow. An averaging time of 100 seconds was found to remove any unsteady contribution and produce repeatable results.

The flue was tested for both regular operation and backdraughting i.e. forward and reversed flow. The results are shown graphically in Figure 2.2 and Figure 2.3. Both data sets show that single values of C and n describe the flow over a wide range of pressures and flowrates. A least squares fit to the data gives values of C and n where:

$C = 0.0137, \quad n = 0.54$ forward flow

$C = 0.0118, \quad n = 0.54$ reversed flow

The exponent, n, (i.e. the slope) is the same in both cases, but the leakage coefficient C, is 13% less for backdraughting (reversed flow) due to the change in flow geometry through the raincap. There is no observable transition between laminar and turbulent flow ($n = 1.0$ and $n = 1/2$ respectively). This transition may have been expected because the Reynolds number has a range from approximately 600 at a flow rate of 0.001 m^3/s to over 30,000 at 0.05 m^3/s. This change in exponent is not seen because the flow is never fully developed for the whole flue.

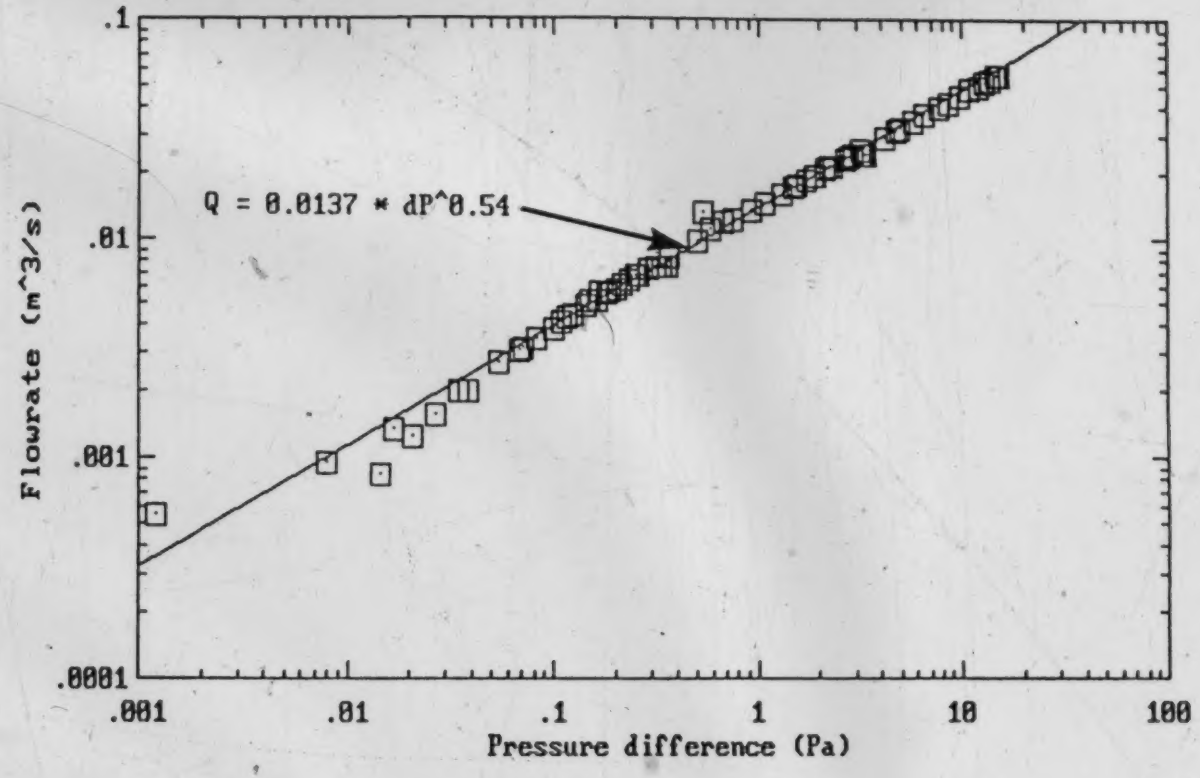

Figure 2.2: Pressure-Flowrate Relationship for 15 cm diameter Furnace Flue with Forward Flow

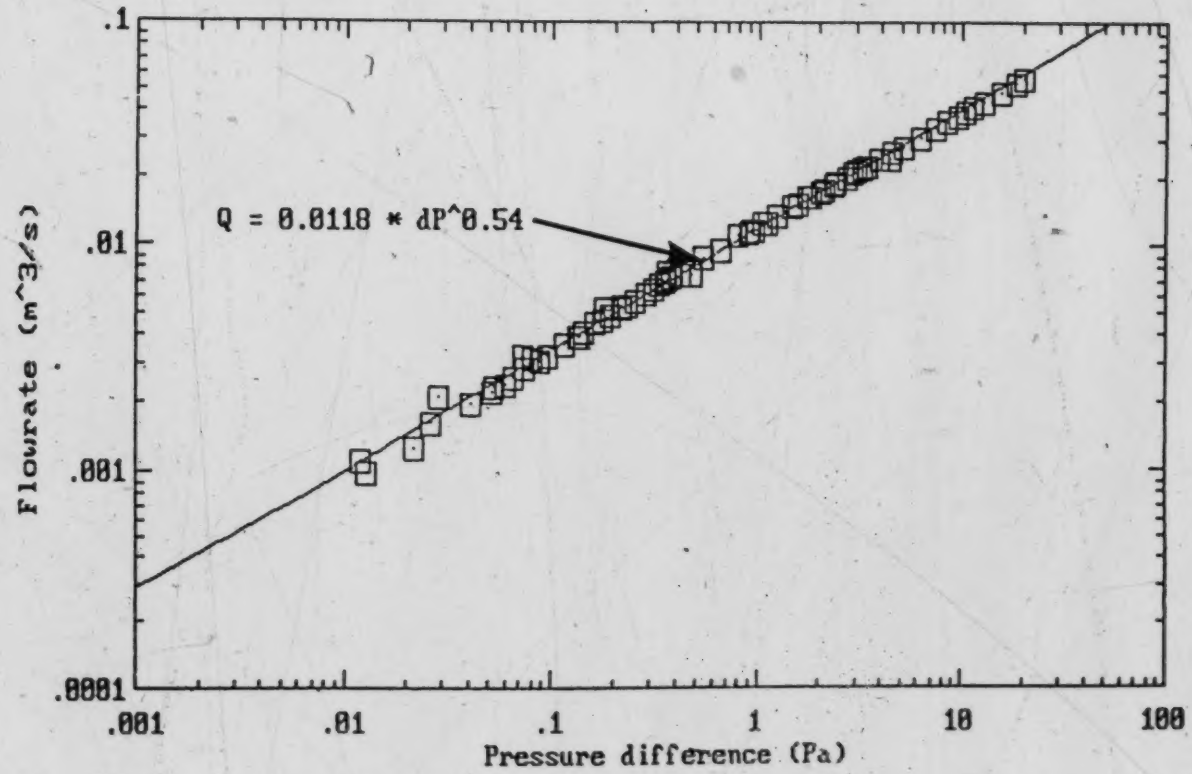

Figure 2.3: Pressure-Flowrate Relationship for 15cm diameter Furnace Flue with Reversed Flow (Backdraughting)

From Schlicting (1979):

$$L \approx 0.03\ D\ Re \quad \text{- length for fully developed laminar flow} \qquad (2.4)$$

where L - length of pipe

D - diameter

Re - Reynolds number

For Re ≈ 600 the length of pipe required is 18 pipe diameters, or 2.7 metres, for fully developed laminar flow. Therefore approximately one half of the flue length could contain fully developed laminar flow. Similarly at higher Reynolds numbers (Re ≈ 30,000) the flow in the flue is not all fully developed turbulent flow.

At flowrates less than 0.002 m^3/s there appears to be a change in slope where the slope is increasing with decreasing flowrate, indicating that the friction factor loss term is significant and not constant with flowrate i.e. there is some laminar flow friction factor contribution. This situation occurs with flow in either direction. It should be noted that this occurs at a pressure difference of less than 0.1 Pa (which is extremely difficult to measure) and may be due to experimental error. For practical purposes this change is insignificant because building leakage sites always see pressure differences greater than 1 Pa.

The same tests performed on the flue with the 7.5 cm diameter orifice in place give:

C = 0.0045, n = 0.50 forward flow

C = 0.0041, n = 0.50 reversed flow

The comments applied to the tests without the orifice also apply to the tests with the orifice in place.

Because the flow exponent, n, is close to 1/2 for all of the tests it is reasonable to compare flue flow to orifice flow and determine an orifice coefficient for a flue.

$$\text{For Orifice Flow:} \quad Q = KA \left(\frac{2\Delta P}{\rho} \right)^{1/2} \tag{2.5}$$

where A = Area of orifice

K = orifice coefficient

ρ = air density

Equating (2.5) to the results of the laboratory flue tests with no orifice, and using typical values for C, n and ρ:

$$K \simeq 0.60\ \Delta P^{0.04} \tag{2.6}$$

As expected, K is a weak function of ΔP because the flow resistance of the flue, which determines the pressure to flowrate relationship, is dominated by entry, exit and fluid acceleration losses rather than friction factor effects.

For ΔP's ranging from 1 to 50 Pa , K varies from 0.60 to 0.7. It is reasonable to assume that this orifice coefficient may be applied to other flue sizes so that for any flue diameter a simple equation for estimating flue flow is given by equation (2.7).

$$Q_{flue} = K \frac{\pi D^2}{4} \left(\frac{2\Delta P}{\rho} \right)^{1/2} \tag{2.7}$$

For the flue with the inlet orifice K = 0.75 and there is no dependance on ΔP because n = 0.5.

2.3 Fan Pressurization Testing

Fan pressurization testing is a method of finding the leakage characteristics of a building. The test is performed by using a large fan to pressurize or depressurize the building. The fan is usually located in an open window or doorway and for this reason this method of testing is often called a "blower door test". Several flowrates through the fan along with indoor-outdoor pressure differences are measured, these data are then fitted to an equation of the form $Q = C\Delta P^n$.

Standard methods for fan pressurization exist in Canada (CGSB (1986)) and the U.S.A. (ASTM (1981)). Both standards have recommended values for the pressure differences at which to take measurements. These pressure differences cover a range of 15 to 50 Pa for CGSB tests and 12.5 to 75 Pa for ASTM tests. Most of the time the actual pressures caused by wind and stack effects will be less than 10 Pa. It is a fair question to ask if test results from high pressures may be extrapolated to the lower pressures that a building envelope usually experiences, because at lower flowrates the flow characteristics of the leaks may become more laminar. This would imply that a different C and n apply at the low pressures a building experiences due to natural conditions than at the elevated pressures of a fan pressurization test. The reason for not testing at lower pressures is that the pressures due to wind and stack effects are of the same magnitude as those that the blower system is attempting to superpose on the house, and fluctuations in the natural pressures on the house create scatter in the test data

that cannot be removed by measuring offset pressures with the blower not in operation.

Fan pressurization tests were conducted at the Alberta Home Heating Research Facility (AHHRF) located south of Edmonton on open agricultural terrain. The facility consists of six test houses, each constructed in a different way in order to examine different heating and ventilating strategies. The houses are unoccupied and the fan pressurization test system is automated which has allowed over 5,000 fan pressurization tests to be performed between 1983 and 1988. Two types of tests have been performed: a test every hour, and tests only at windspeeds less than 1.5 m/s. Windspeed, wind direction, and ambient temperature data are taken from meteorological towers at the test site.

Indoor-outdoor temperature difference varies slowly and the pressures arising from this factor can be removed by measuring an offset pressure at each data point. However, windspeed and direction have rapid fluctuations which result in rapid fluctuations in the pressures exerted on the building. These fluctuations make it difficult to estimate the pressure across the building envelope for the operator of a blower system. In addition, most pressure transducers are inappropriate for measuring pressures below 10 Pa. For example, an inclined manometer cannot resolve these low pressures with sufficient accuracy.

In order to examine these problems a sophisticated fan pressurization test system has been developed over the past 5 years to

perform over 5,000 tests. For this study the system was adapted to measure offset pressures for each data point with the damper shown in Figure 2.4 closed, and to measure the data points required for the ASTM and CGSB standards. In addition, the system has been changed so that tests are only performed if the windspeed is less than 1.5 m/s. The system is controlled by a Hewlett-Packard HP85 microcomputer. To accurately measure low pressures a Validyne magnetic reluctance metal diaphram pressure transducer is calibrated using a water column pressure source and a micropoint manometer with a resolution of 0.25 Pa. The pressure transducer measures up to 250 Pa ± 0.5 Pa. The flowrates are measured using a laminar element flowmeter which has been calibrated against an ASME standard orifice meter. The error associated with the flow measurement is 3% of the measured value. The flowrates are corrected for pressure and temperature variation, and the effects of fan loading on the laminar element flowmeter at high fan speeds and low flowrates (which occur in a "tight" house).

Pressure and flowrate measurements are taken over 15 seconds and averaged for each data point. The indoor-outdoor pressure difference is measured using a pressure averaging manifold that has a tap on each wall of the building that removes some of the wind pressure effects. Offset pressures due to stack and wind effects with the fan not in operation are measured at every data point. A damper is closed over the fan opening for each offset reading as the fan opening can change the pressure distribution of the building significantly. A schematic of the apparatus is shown in Figure 2.4.

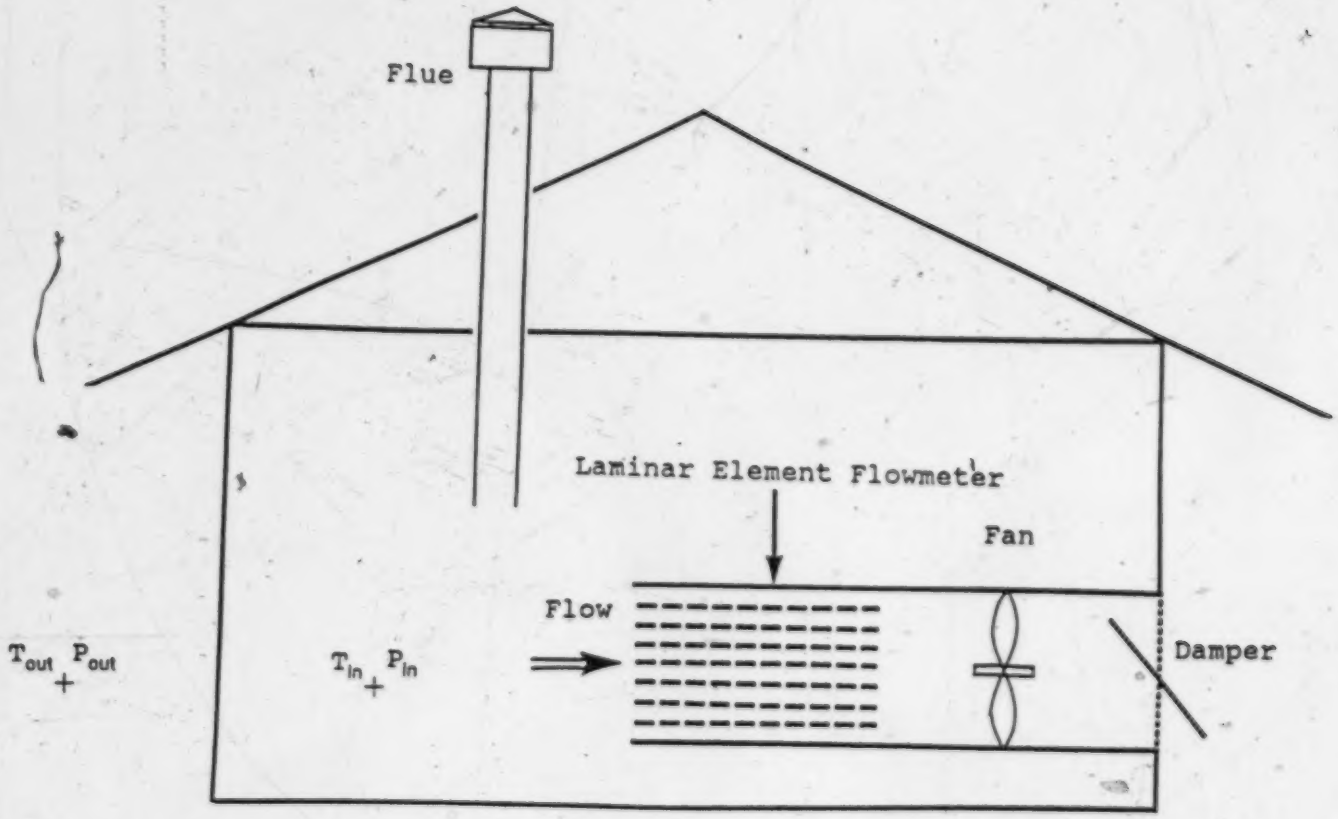

Figure 2.4: Schematic of Blower Test Apparatus with the Building Depressurised

Figure 2.5 shows the results of a typical test in a house with very little envelope leakage with and without an open 15 cm diameter furnace flue with a 7.5 cm diameter orifice at the bottom (House #1 at AHHRF). Because the leaks in this house are all small without the flue, and there are few of them, the value of C = 0.0028 is lower and n = 0.73 is higher than for a typical house (C is less than for a furnace flue.). The open furnace flue increases the total leakage, such that C = 0.085. (Note that one cannot simply add the values of C for a house with the flue closed and for a flue to obtain the C for a house with the flue open). The value of n = 0.56 is lower than with the flue closed since the flue flow exponent is 1/2, and performing a test with the flue open will bring the value of the flow exponent for the whole building closer to 0.5.

Figure 2.6 shows the results of a test performed in one of the test houses of similar construction to most Alberta houses (wood frame, single stud walls. House #2 at AHHRF with an open 15 cm diameter furnace flue with a 7.5 cm diameter orifice at the bottom). The value of C = 0.012 is smaller than for an average home since the test houses are not very large, but the value of n = 0.66 is typical of tests performed elsewhere.

To obtain a physical feeling for C and n, C can be thought of as the quantity of leakage across the building envelope and n as a characteristic describing the type of leaks. For buildings of similar leakage types (the same proportion of large holes and small cracks) but

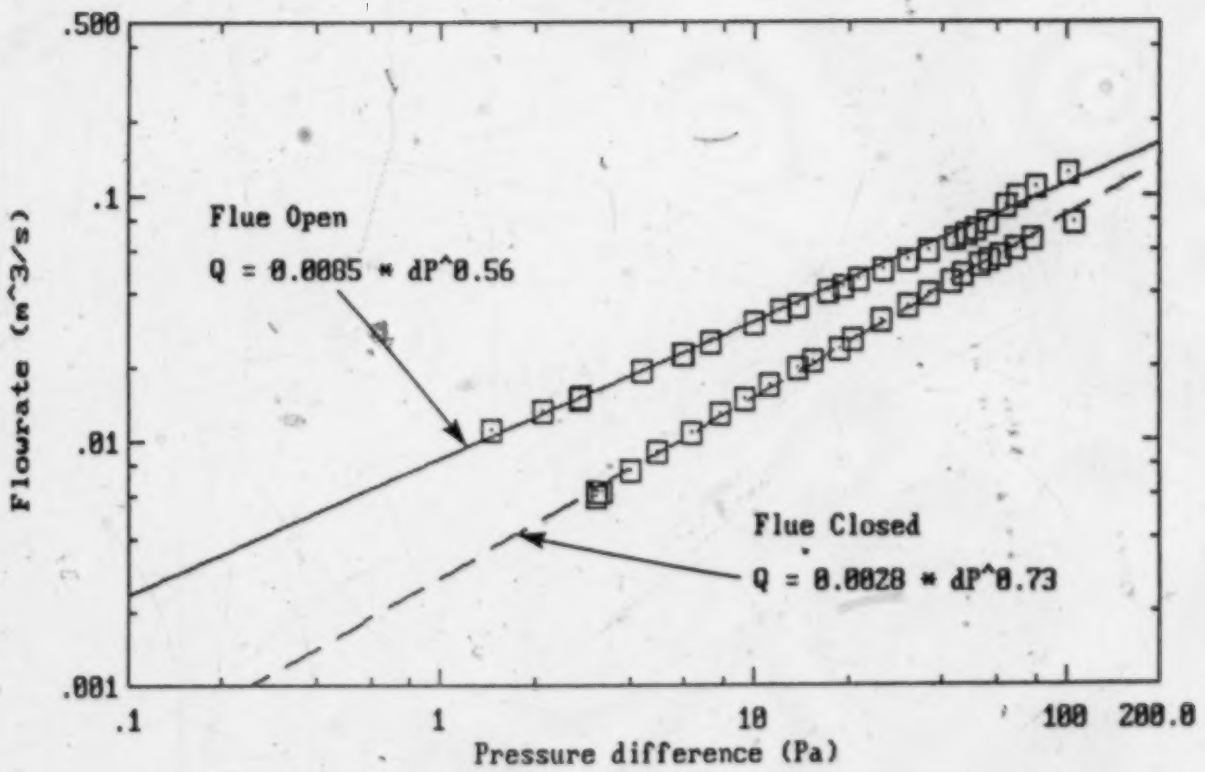

Figure 2.5: Blower Test Results for a Brick Walled House (House #1 at AHHRF), with an Open 15 cm I.D. Flue with a 7.5 cm diameter orifice at the bottom, and with a blocked Flue. Windspeed < 1.0 m/s and ΔT < 10°C

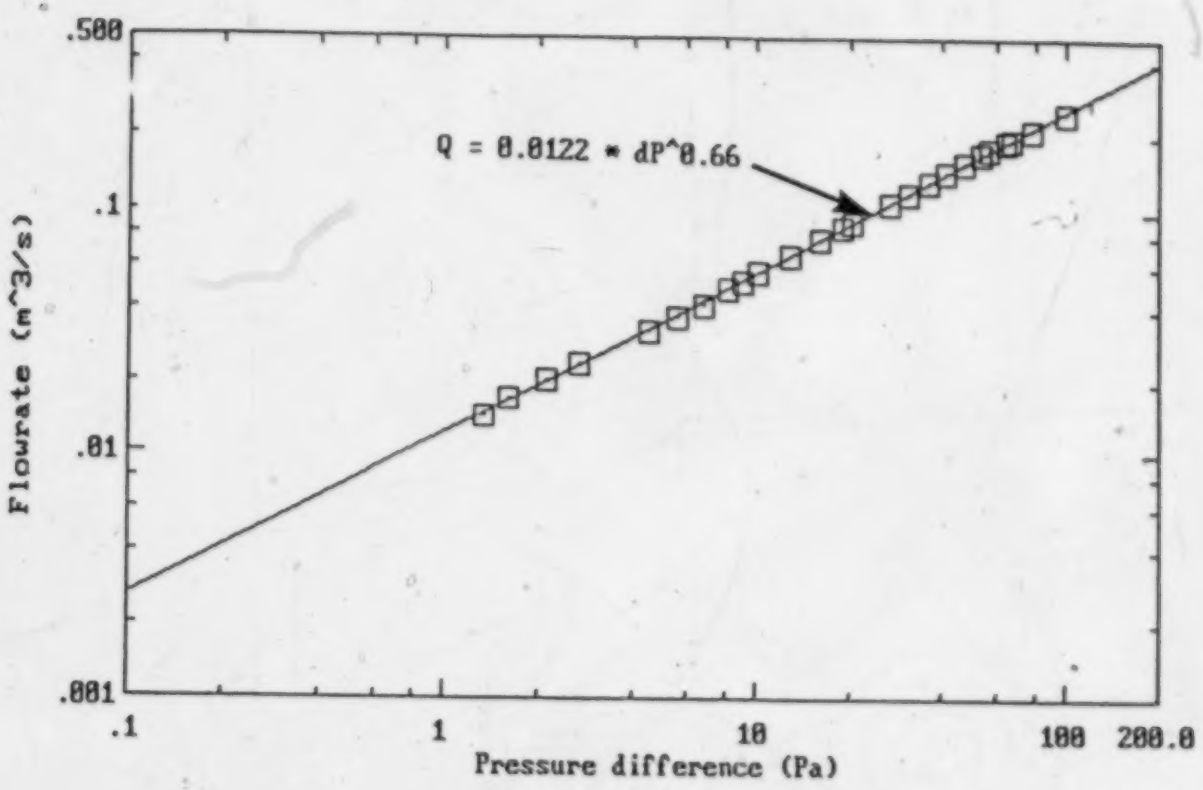

Figure 2.6: Blower Test Results for a House with Single Stud Wood Framed Walls (House #2 at AHHRF), with an Open 15 cm I.D. Flue with a 7.5 cm diameter orifice at the bottom. Windspeed = 0.84 m/s and $\Delta T = 10°C$

different sizes, the value of n will remain the same, and only C will change.

The type of leaks depend on building construction, so for houses of similar construction a single, typical value of n may be specified. Examining the results of tests performed at AHHRF and the published values of Beach (1979), Dumont et. al. (1981), Sulatisky (1984), Turner et. al. (1982), Lipschutz et. al. (1981), Offerman et. al. (1982), Warren and Webb (1980) and Liddament (for the Air Infiltration and Ventilation Centre (AIVC)) (1986), n is typically 2/3. W. Jones of Ontario Hydro proposed in a letter in 1987 that the results of Shapiro, Siegel and Klirfe (1954) for undeveloped laminar flow in circular tubes imply an exponent of $n = 2/3$ for this flow regime. Although tempting, this does not prove that flow in cracks in building envelopes is undeveloped laminar flow. It remains an intriguing coincidence, however, and must be worthy of future research.

The results of fan pressurization testing at AHHRF are repeatable only at lower windspeeds as the amount of scatter in the data incereases with windspeed. At windspeeds greater than 1.5 m/s the scatter in the data at low pressures is too great to apply a least squares procedure to find C and n. At windspeeds greater than 1.5 m/s pressure data below 10 Pa should not be used. The data taken at higher indoor-outdoor pressure differences, as for the ASTM and CGSB standards, can be used to find C and n up to windspeeds of about 4 m/s. With less sophisticated test procedures the low windspeed limit should be further increased to yield valid results. In order to

estimate the uncertainty in the values of C and n obtained from a least squares fit a t test, from Miller and Freund (1985), has been performed on some low windspeed test data (windspeeds less than 1.5 m/s). For a typical low windspeed test and a 95% confidence interval the uncertainty is ± 2% for C and ± 1% for n.

A significant observation to be made from the results of these tests, as shown in Figures 2.5 and 2.6 is that the realationship between flowrate and pressure difference does not change over the range of values tested which include typical pressure differences driving ventilation flows. There is no observable trend towards more laminar flow at low flowrates and pressures (i.e. n approaches 1) or more turbulent flow at higher values (i.e. n approaches 0.5). This shows that the C and n derived from blower test results in the 10 to 50 Pa range are true constants describing the building leakage. These results also imply that tests at higher pressures of the CGSB and ASTM standards can be used to determine the leakage characteristics of a building for the pressure range that a building actually experiences.

Blower tests may either pressurize or depressurize the building. The CGSB study calls for depressurization only and the ASTM study allows for either method to be used. AHHRF test results indicate that in most cases both pressurization and depressurization yield values of C and n that differ by less than 1%. However, in House #4 at AHHRF, n is about 5% less and C is about 20% less from a depressurization test than from a pressurization test. This is probably due to valving action possibly due to a loose vapour barrier or some other cracks which change shape due to airflow direction. This difference may also

be the source of some of the errors in ventilation model predictions for ventilation in House #4. The best way to obtain a single value for C and n for use in infiltration models is to average the flowrates of the pressurization and depressurization curves and fit another curve to these average flowrates. An approximation would be to average the C and n from pressurization and depressurization tests.

2.4 Summary

• Crack flow theory shows that flow in cracks is rarely fully developed, so the relationship between pressure, ΔP, and flowrate, Q, is best described by an equation of the form:

$$Q = C\Delta P^n \qquad (1.2)$$

where: $0.5 \leq n \leq 1$

• Laboratory experiments have shown that there is no laminar to turbulent transition for flow in a furnace flue from 0.01 to 50 Pa. Therefore C and n are independant of Q and ΔP for a furnace flue.

• Fan pressurisation, or blower, tests have shown that C and n for the entire building envelope are also independant of Q and ΔP. Thus C and n from a blower test are true constants describing the building envelope leakage.

• Both the furnace flue and the blower door experiments have shown that (1.2) is applicable to building envelope leaks.

Chapter 3

EXACTAIM and AIM-2 : Simple Models for Estimating Infiltration Rates

3.1 Introduction

Both AIM-2 and EXACTAIM are single zone models developed for this study. EXACTAIM uses the solution to the exact theoretical relationships to determine the ventilation rate. The ventilation rate is determined separately for wind and stack effects. The two effects are superposed by pressure addition with an empirical correction term allowing for their interaction. For EXACTAIM, the effects of wind shelter have been quantified to allow wind shelter to be a continuous function of wind angle.

The Alberta Infiltration Model, version 2, or AIM-2, has been developed by using empirical equations to estimate ventilation rates that approximate exact theoretical relationships (derived for EXACTAIM) requiring numerical solution. In modern housing the furnace flue is the single largest leak. The leakage characteristics of the flue are studied in chapter 2, and are well defined. To improve infiltration predictions both models have been derived with the furnace flue included as a totally separate leak. This is the distinguishing feature that makes these different from other models. The equations derived for including flue leakage separately can be applied to any large leak in the building envelope, which is useful for examining passive ventilation strategies. A method to account for the addition of mechanical ventilation has also been included.

3.2 Review of some other Single-Zone Infiltration Models

One of the simplest and most popular methods of estimating air exchange rates has been to fit empirical equations to measured data (usually a tracer gas technique is used) . The problem with empirical models that are fitted to a measured air exchange rates is that they may work well for the specific houses and weather conditions tested, but cannot be applied with a sufficient degree of accuracy to houses outside the test group or in other weather conditions.

An example of the problems arising from empirical fits to a limited quantity of data can be seen in Shaw's model (1985). Shaw's model uses an equation of the form $Q = C\Delta P^n$ to find wind and stack flowrates, which is physically realistic. However, the constants in Shaw's model were found from empirical fits to measured data. Warren and Webb (1980) also used empirical coefficients in theoretically based (i.e. dimensionally correct) wind and stack terms. Shaw developed the following equations for wind induced infiltration.

$$Q_{wind} = 0.4\ C \left(\frac{A}{V} \right) U^{2n} \qquad \text{Exposed building} \qquad (3.1)$$

$$Q_{wind} = 0.7\ C \left(\frac{A}{V} \right) U^{n} \qquad \text{Sheltered building} \qquad (3.2)$$

where C and n are flow coefficients from fan pressurization tests.

A = area of building envelope

V = building volume

U = Windspeed 20 m above grade

Some simple calculations show that with n = 0.65 for U < 2.36 m/s the air exchange rate of a sheltered building is greater than for an exposed building, which cannot be true. For any value of n between 0.5 and 1.0 there is a critical windspeed, above which the exposed building has a greater infiltration rate than the sheltered building. Below this critical windspeed the sheltered building has a greater infiltration rate. This is clearly inconsistent and the case of a sheltered building having the larger Q_{wind} cannot be correct.

Another avenue for predictive ventilation models that can be applied to many different buildings is that begun by Sherman (1980), and continued by Sherman and Grimsrud (1980). Sherman separated the two natural driving forces due to wind and indoor-outdoor temperature difference and used the idea of distributed leakage and leakage area from fan pressurization tests to create a model applicable to a wide variety of weather conditions and buildings. Sherman estimated some model inputs empirically e.g. wind shelter factors were given in a table with corresponding descriptions of the surrounding terrain. Sherman developed estimating relationships that depend on leakage distribution and pressure coefficients, and Sherman modelled the building leaks as orifices (n = 0.5) to determine flowrates. An attempt was then made by Yuill (1985) to extend this analysis for use with the more general crack flow equation $Q = C\Delta P^n$.

The theory here in EXACTAIM, and the fitted equations in AIM-2 further develops the ideas of Sherman and Yuill but with significant changes. The major differences are listed below:

1. The attic space above the ceiling was assumed in Sherman's model (and Yuill's extension) to have zero pressure coefficient. This means that the pressure in the attic is the same as the pressure measured in the atmosphere remote from the building. The attic pressure coefficient in EXACTAIM and AIM-2 is assumed to be the weighted average of the pressure coefficients on the eave vents and the roof surface vents. The eave vents are assumed to have the same pressure coefficients as the wall they are adjacent to. For the empirical estimation of Q_{wind} the eaves on each wall have the same flow area weighting and the roof vents have a flow area weighting equal to the sum of the eaves. The roof surface vents are assumed to have the average of the windward and leeward roof pressure coefficients.

2. The floor leakage in Sherman's model (and in Yuill's extension) was located above a crawl space which was assumed to have zero pressure coefficient. This model will develop two different solutions, one of which is for houses with crawl spaces, and one which is developed for a typical Canadian house with a full basement or slab-on-grade. For a house with a crawl space the wind pressure inside the crawl space is approximated by the average pressure on the four walls. For full basement or slab-on-grade construction, the "floor" leakage is the crack around the floor plate resting on the foundation, and cracks, holes, and other leaks in the concrete foundation above grade. For the estimation of stack

and wind factors, these floor level leaks are assumed to be uniformly distributed around the perimeter of the house at grade level, and to be exposed to the same pressure coefficients as each of the walls on which they are located.

3. There is no furnace in Sherman's or Yuill's model. In these models the furnace flue (or fireplace) leakage is simply added to the ceiling leakage and sees the zero pressure coefficient of the attic. In EXACTAIM and AIM-2 the furnace flue is incorporated as a separate leakage site, at a normalized flue height, β_f, above the floor. The ceiling is at $\beta = 1.0$ and the ground floor is at $\beta = 0$. It is assumed to be filled with indoor air at room temperature, and is exposed at its top to the pressure determined by wind flow around the rain cap. The effect of hot air in the furnace flue was not considered.

4. Sherman's model assumes orifice flow with $n = 0.5$ in $Q = C\Delta P^n$ for each leak. Both Yuill's extension, EXACTAIM and AIM-2 use a single value of n in the range 0.5 to 1.0. The same value of n is assumed to apply to every leakage site (floor, walls, ceiling and flue).

5. Both Sherman and Yuill assume that wind and stack flows combine as a sum of squares (ie. in quadrature). EXACTAIM and AIM-2 include an empirical interaction term which accounts for the wind induced shift of the neutral pressure level. In addition, each term is not squared but is taken to the 1/n power, the sum of the terms is then taken to the

n power (this has the form of pressure addition). A true exact solution would combine the wind and stack effects at each leak to account for the interaction.

The theory developed here also includes two significant effects not included by Sherman, Yuill, Shaw, or Warren and Webb.

6. The effect of the different densities of infiltrating and exfiltrating air is accounted for in EXACTAIM and AIM-2 so that a mass balance, rather than a flow balance as used by Sherman and Yuill, is used to equate inflow and outflow. For simplicity this factor is not included in the empirical equations for wind and stack factor in AIM-2.
7. This chapter also examines the variation of shielding effect with wind angle. The shielding factor accounts for changes in wind speed due to local obstacles other than the test building.

3.3 Development of EXACTAIM

The air infiltration models developed in this chapter have been formulated to predict infiltration for "typical" Canadian housing. The major difference from other models is the inclusion of a full basement and a furnace flue, which change the assumptions about leakage distribution as outlined previously.

Air is driven through the leaks by the difference in pressure across each leak. This pressure difference is caused by wind (Wind

Effect), indoor-outdoor temperature difference (Stack Effect) and by mechanical ventilation. These 3 effects will be evaluated separately, then superposed.

Strictly speaking, the infiltration rate is defined as the volume flow at which air enters a building and the exfiltration rate is the volume flow at which air is leaving the building. In terms of mass flow these two flowrates will be identical only if the indoor and outdoor densities are the same. To avoid confusion the analysis here will retain the strict definitions of infiltration and exfiltration.

3.4 Stack Effect

The change in hydrostatic pressure in an incompressible fluid with depth is given by equation (3.3)

$$\frac{dP}{dz} = -\rho g \tag{3.3}$$

where P is static pressure

z is height above reference (outside ground level)

ρ is density of fluid body.

g is acceleration due to gravity

The inside and outside of a building will generally have air at different densities, therefore the pressure gradient with height will be different. This results in a differential pressure across the building envelope that varies with height. This differential pressure may be written as in equation (3.4).

$$\frac{d\Delta P}{dz} = -(\rho_{out} - \rho_{in})g \tag{3.4}$$

where ρ_{out} is density of outside air

ρ_{in} is density of inside air

and $\Delta P = P_{out} - P_{in}$, the pressure differential that drives the airflow.

Assuming that air behaves as an ideal gas allows the restating of equation (3.4) in terms of an indoor-outdoor temperature difference. This is much more convenient because all weather data will have temperatures, but generally densities are not known. An additional assumption here is that both the inside and outside air is well mixed and has no vertical temperature gradient.

$$\frac{d\Delta P}{dz} = -g\rho_{out}\frac{\Delta T}{T_{in}} \tag{3.5}$$

where $\Delta T = T_{in} - T_{out}$

and T_{in} = inside temperature

T_{out} = outside temperature

Equation (3.5) may be integrated to find the pressure difference, ΔP, across the building envelope as a function of height.

$$\Delta P(z) = \Delta P_o - g\,\rho_{out}\frac{\Delta T}{T_{in}}\,z \tag{3.6}$$

ΔP_o is the pressure offset at $z = 0$. This corresponds to an internal pressure shift so that mass flow in = mass flow out. i.e. The mass of air inside the building remains constant with time.

The following variables can be defined

Stack Pressure:

$$P_s = \rho_{out}\,g\,H\,\frac{\Delta T}{T_{in}} \tag{3.7}$$

where H is the ceiling height of the conditioned space measured from ground level. For a split level house there is a different value of H for different parts of the house. To account for this in a simple manner it is suggested that the ceiling heights in the different sections may be averaged (weighted by the floor area of each section) to find an appropriate value of H for use in these equations.

Dimensionless Height:

$$\beta = \frac{h}{H} \tag{3.8}$$

where h is some height above grade.

Dimensionless Flue Height:

$$\beta_f = \frac{H_f}{H} \tag{3.9}$$

where H_f is height of flue top above grade

Dimensionless height of the neutral level, where $\Delta P = 0$.

$$\beta_o = \frac{h_o}{H} \tag{3.10}$$

where β_o is a spatially averaged neutral level for the whole building, and h_o is the height above grade of the neutral level. When considering stack effect alone β_o is a constant height on all walls.

From equation (3.6) it can be seen that ΔP_o can be written in terms of the neutral level height.

$$\Delta P_o = \beta_o P_s \tag{3.11}$$

Then, equation (3.4) may be written in terms of P_s, β_o and β.

$$\Delta P(h) = P_s(\beta_o - \beta) \tag{3.12}$$

The pressure across each leak in the building envelope is determined by equation (3.12).

To find the flowrate from the pressure in equation (3.12), the leakage characteristics of the building envelope must be determined. These leakage characteristics are found by the fan pressurization technique. There are both Canadian (CGSB (1986)) and American (ASTM (1982)) standards for fan pressurization methods. Chapter 2 discusses both of these methods and the method used at AHHRF. Over 5,000 fan pressurization tests have been performed on the houses at AHHRF. The tests cover a wide range of windspeeds and indoor-outdoor temperature differences, and the tests performed at low windspeeds (less than 1.5 m/s) have been found to produce the best results. Analysis of these low windspeed tests indicate that the building leakage is well described by a function of the form:

$$Q = C\Delta P^{n} \qquad (1.2)$$

where Q = Flowrate

ΔP = Pressure differential across the building envelope

and C and n are the leakage coefficient and exponent.

In EXACTAIM (and AIM-2) it is assumed that the exponent n is the same for all the building leaks. The pressurization tests confimed that C and n do not change over the range of pressures (1 to 50 Pa) experienced by a building due to stack and wind effects. This allows C for the whole building to be equal to the sum of the individual C's for each leak.

$$C_{building} = C_c + C_f + C_w + C_{flue} = C \qquad (3.13)$$

where:

C_c = leakage in the ceiling at height $\beta = 1$

C_f = leakage in the floor at height $\beta = 0$

C_w = leaks in the walls at height $0 \leq \beta \leq 1$

C_{flue} = leakage of the furnace flue at $\beta = \beta_f$

Equations (3.12) and (1.2) may now be used to find the flowrate through each leak. It is important to keep track of the direction of flow through each leak to find β_o by equating the mass flows in and out of the building. It is assumed that $T_{in} > T_{out}$ in determining the sign of P_s, which determines the direction of flow. In Canada this assumption is valid except in exceptional cases. Usually T_{in} is approximately 20°C, but in summer when windows or doors are left open T_{in} is approximately equal to T_{out} and without air conditioning (which is beyond the scope of this simple model), T_{in} is never less than T_{out}. In hot climates (e.g. the southern U.S.) where air conditioning is common then for much of the time T_{in} is less than T_{out}. This simply reverses the direction of flow through the leaks for the stack effect and does not change the analysis performed here. i.e. the net infiltration rate for a given temperature difference will be the same if $T_{in} > T_{out}$ or $T_{out} > T_{in}$.

It is convenient to define some non-dimensional parameters that describe the leakage distribution. These parameters express the leakage as a fraction of the total leakage of the building.

Let:

$$R = \frac{C_c + C_f}{C}$$ the "ceiling-floor sum"

$$X = \frac{C_c - C_f}{C}$$ the "ceiling-floor difference"

$$Y = \frac{C_{flue}}{C}$$

The wall leakage, C_w, can be expressued in terms of R and Y:

$$\frac{C_w}{C} = 1 - R - Y$$

R and X are similar to those defined by Sherman and Grimsrud except that the leakage of the flue is not included in the leakage of the ceiling, C_c. For a given value of R there is a limit on the range of values of X, where $X \leq \pm R$. This will be seen in the figures in this chapter where some curves will stop when $X = \pm R$. Also, when $R = 0$ then $X = 0$, and the curves reduce to a single point shown by a cross.

Assuming that air inside a building is at a constant temperature (i.e. Any cold air entering the building at T_{out} is heated to T_{in}), then the mass of air inside the building is constant, and the mass flowrate into the building at ρ_{out} must equal the mass flow out at ρ_{in}. This assumption leads to an equation which expresses the relationship between the dimensionless neutral level (β_o), the leakage distribution parameters (R, X, Y and β_f), and n. It is convenient to define a variable r which is the ratio between indoor and outdoor densities:

$$r = \frac{\rho_{in}}{\rho_{out}}$$

The ventilation rate due to stack effect, M_s, is found by first solving equation (3.14) to find β_o, then using equation β_o in (3.16) to find the stack factor. The stack factor is then used in (3.15) to find the stack effect ventilation rate.

Equation (3.14) uniquely determines β_o and is derived in Appendix A as equation A.11. This equation is found by finding the flow through the floor, ceiling, walls, and flue in terms of R, X, Y, β_f, C, P_s, and β_o. The flows in and out of the building are summed separately, then equated. Equation (3.14) is a result of equating the flows in and out of the building.

$$X = \frac{R\left[\beta_o^n - r(1-\beta_o)^n\right] + \frac{2(1-R-Y)}{n+1}\left[\beta_o^{n+1} - r(1-\beta_o)^{n+1}\right] - 2Yr(\beta_f-\beta_o)^n}{\left[\beta_o^n + r(1-\beta_o)^n\right]}$$

(3.14)

Equation (3.14) does not give β_o explicitly. In order to find β_o equation (3.14) may be solved numerically as Yuill (1985) recommends for his model with no separate flue. In the present study a Newton-Raphson technique was used to find β_o from equation (3.14). This was found to work well except when β_o was very close to the floor or the ceiling (within about 1%) where β_o becomes almost independent of X and the numerical solution is not always stable, and requires special over relaxation techniques to converge.

The net infiltration rate is found by averaging the inflows and outflows. This averaging was first suggested by Sherman and Grimsrud (1980) and reduces the effect of errors in calculating β_o. For example, if β_o is slightly overestimated, then the inflow will be slightly greater than the outflow (For $T_{in} > T_{out}$), but the average of the two will not change by as much as the error in either inflow or outflow. Appendix A shows how equations (3.15) and (3.16) were derived (Equations A.16 and A.15 respectively). These equations are found by averaging the flow rates into and out of the building, and substituting equation (3.14) wherever X appears in the equation.

$$\dot{M}_s = \rho_{out}\, r\, C\, f_s P_s^n \tag{3.15}$$

where the stack factor, f_s, is

$$f_s = \frac{\left[\beta_o^n(1-\beta_o)^n \frac{1+nR-Y}{n+1}\right] + Y(\beta_f-\beta_o)^n\beta_o^n}{\left[\beta_o^n + r(1-\beta_o)^n\right]} \tag{3.16}$$

The stack factor contains all the effects of the leakage distribution, but is independant of the weather and indoor temperature.

3.5 Some Special Cases of Stack Effect Infiltration

3.5.1 Neutral Level Above Ceiling

For a tight house with a large flue it is possible that the neutral level may be above the ceiling. i.e. $\beta_o > 1$. This changes the direction of flow through the ceiling and part of the walls. In this case all of the leaks except the flue flow in and all the outflow

is through the flue. Equations (3.17) and (3.18) have been derived in Appendix A for this situation (Equations A.21 and A24 respectively) in the same way as equations (3.14) and (3.15).

$$X = \frac{R\left[\beta_o^n+(\beta_o-1)^n\right]+2\frac{(1-R-Y)}{n+1}\left[\beta_o^{n+1}-(\beta_o-1)^{n+1}\right]-2rY(\beta_f-\beta_o)^n}{\left[\beta_o^n-(\beta_o-1)^n\right]} \tag{3.17}$$

$$\dot{M}_s = \rho_{out} rYCP_s^n \ (\beta_f-\beta_o)^n \tag{3.18}$$

This may be written in the same form as equations (3.15) and (3.16)

$$\dot{M}_s = \rho_{out} rC\ f_s P_s^n \tag{3.19}$$

where

$$f_s = Y(\beta_f - \beta_o)^n \tag{3.20}$$

Note that the average of the inflows and the outflows in this situation reduces to just the flow out through the flue in equations (3.18), (3.19) and (3.20), and (3.19) is the same as (3.18) but with a different stack factor.

3.5.2 Including Flue Leakage in the Ceiling

In other simple infiltration models the flue leakage is placed in the ceiling. To see what effect this assumption has, the leakage of the flue is now included in X and R, and Y = 0. If the density difference between inflowing and outflowing air is also neglected then r = 1, and equation (3.21) (for β_o) can be found from equation (3.14), and equation (3.22) (for f_s) can be found from equation (3.16). The mass flow can be found by using (3.22) in (3.15).

$$X = \frac{R\left[\beta_o^n - (1-\beta_o)^n\right] + \frac{2(1-R)}{n+1}\left[\beta_o^{n+1} - (1-\beta_o)^{n+1}\right]}{\left[\beta_o^n + (1-\beta_o)^n\right]} \qquad (3.21)$$

$$f_s = \frac{\beta_o^n (1-\beta_o)^n \left[\frac{1+nR}{n+1}\right]}{\left[\beta_o^n + (1-\beta_o)^n\right]} \qquad (3.22)$$

Because the flue is now treated as part of the ceiling the neutral level can never be above the ceiling. Equations (3.21) and (3.22) are the same as those derived by Yuill (1985).

3.5.3 Assuming Orifice Flow through Leaks, and No Separate Flue

If it is further assumed that simple orifice flow equations describe the flow through the building envelope, then in equations (3.21) and (3.22), n = 1/2. This results in equations of the following form:

$$X = \frac{R\left[\beta_o^{1/2} - (1-\beta_o)^{1/2}\right] + \frac{4(1-R)}{3}\left[\beta_o^{3/2} - (1-\beta_o)^{3/2}\right]}{\left[\beta_o^{1/2} + (1-\beta_o)^{1/2}\right]} \tag{3.23}$$

$$f_s = \frac{\beta_o^{1/2}(1-\beta_o)^{1/2}\left[\frac{2+R}{3}\right]}{\left[\beta_o^{1/2} + (1-\beta_o)^{1/2}\right]} \tag{3.24}$$

These equations are the same as those of Sherman (1980) if Sherman's definition of stack pressure, $P_{S,LBL}$ is used.

$$P_{S,LBL} = g\,H\,\frac{\Delta T}{T_{in}} - \frac{P_s}{\rho_{out}} \tag{3.25}$$

3.6 Estimating Solutions to Stack Flow Equations

It is not convenient or possible to use iterative numerical analysis to solve the non-linear algebraic mass balance equations for stack flow. This is especially true for routine design problems where an equation suitable for a hand calculator is more appropriate. The objective of this thesis is not only to test fundamental theories for finding infiltration rates, but also to develop relationships which may be used in practice. In most cases, there is neither the time or inclination to solve the equations numerically on a computer. AIM-2 was developed to meet practical needs by fitting closed form equations to the results of EXACTAIM. The approximating functions were chosen to have the proper shape of function, and to have the correct asymptotic values at the extremes. The error of the estimating functions is defined as: Empirical fit - Exact Value, such that a

positive error is an overprediction. The approximating functions have the correct value for simple situations where the equations for EXACTAIM have exact solutions (Where all the leaks are in one place, or all in the ceiling and the floor). Also, single digit coefficients were chosen for ease of use. The following relationships have been found as estimates for finding stack flow. For simplicity, in AIM-2, the density difference between in and out flows is assumed to be negligible so that r = 1 in equations (3.14) and (3.15).

3.6.1 Estimating Neutral Level Location

The location of the neutral level is the essential variable to find the stack induced air exchange rate, and knowledge of neutral level location is useful in other ways. When designing or retrofitting passive ventilation systems the ventilation holes ideally should be placed as far from the neutral level as possible. This ensures that the ventilators have the greatest possible flowrate for a given size of passive ventilator. Unavoidable leaks like the cracks around doors and windows, and exhaust fan dampers should be placed near the neutral level to minimise their effect. First, it must be determined if the neutral level is above the ceiling. If β_o is set equal to 1 in equation (3.14), then a critical value of X, X_{crit}, may be determined. If $X > X_{crit}$ then the neutral level is above the ceiling and a different estimating equation must be used, because the direction of flow through the ceiling and part of the walls has changed.

$$X_{crit} = R + \frac{2(1-R-Y)}{n+1} - 2Y\,(\beta_f - 1)^n \qquad (3.26)$$

The following empirical equations can be used to determine the dimensionless neutral level, β_o, to within 5%. The equations below are explicit approximations to numerical solution of (3.14).

For $X < X_{crit}$

$$\beta_o = \frac{1}{2} + \frac{1}{2} \tanh \left(\frac{\mathrm{sgn}(X_s)\ F}{\left(\left(\frac{X_{scrit}}{X_s} \right)^2 - 1 \right)^{1/2}} \right) \qquad (3.27)$$

where sgn (X_s) is the sign of X_s, and

$$X_s = X + (2n + 1)Y(\beta_f - 1)^n$$

$$X_{scrit} = X_{crit} + (2n + 1)Y(\beta_f - 1)^n$$

$$F = \left[1 + 4\left[(n-1)R \right]^2 \right]$$

For $X > X_{crit}$

$$\beta_o = A_1(X - X_{crit})Y(\beta_f - 1) \qquad (3.28)$$

where

$$A_1 = 1 + \frac{10(1-Y)^3(2n-1)}{(2\beta_f - 1)}$$

Figure 3.1 shows the variation in estimated values of β_o with the leakage distribution parameters R and X using the empirical estimate (equation (3.27)). Figure 3.2 shows the variation in β_o calculated by solving the exact solution equation (3.14), for the case where there is no flue and for a typical value of n = 2/3. This "typical" value of n was chosen based on blower tests performed at AHHRF, laboratory furnace flue testing, and published summaries of blower test results

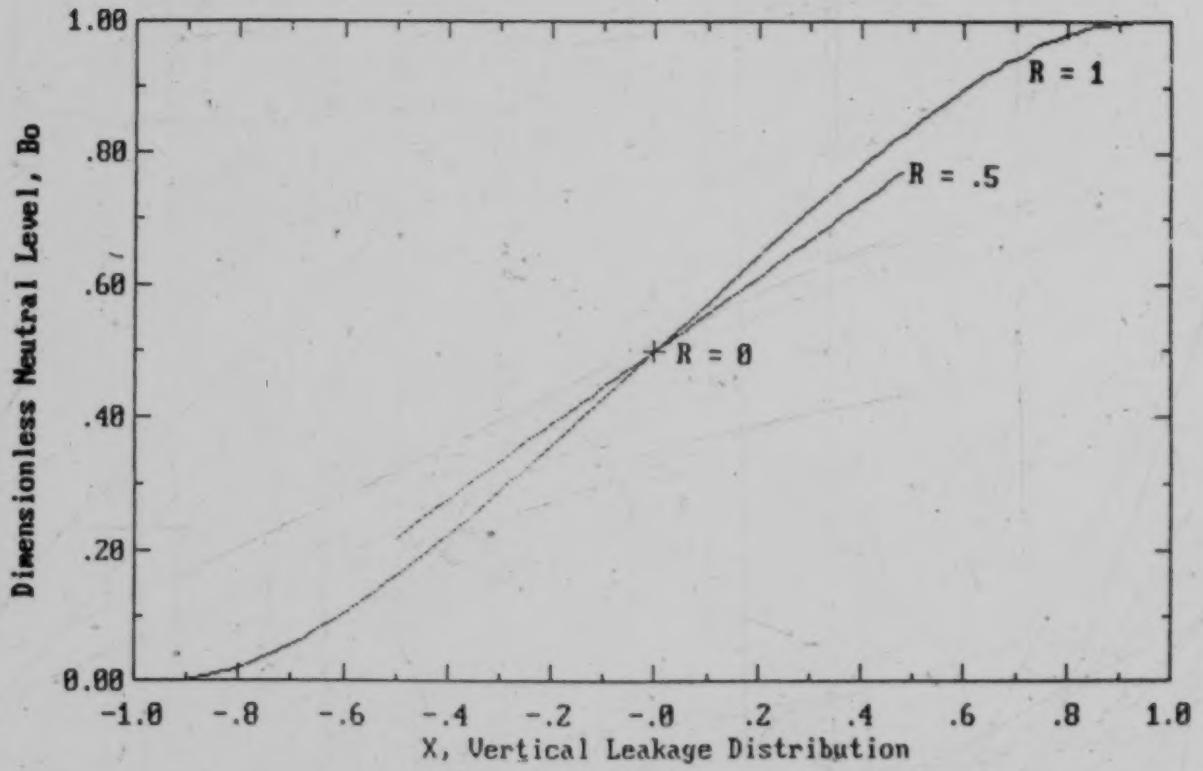

Figure 3.1: Empirical values for Neutral level, β_o, from Equation (3.28) with no Flue Leakage (Y=0), where X is the ceiling-floor difference and R is the ceiling-floor sum

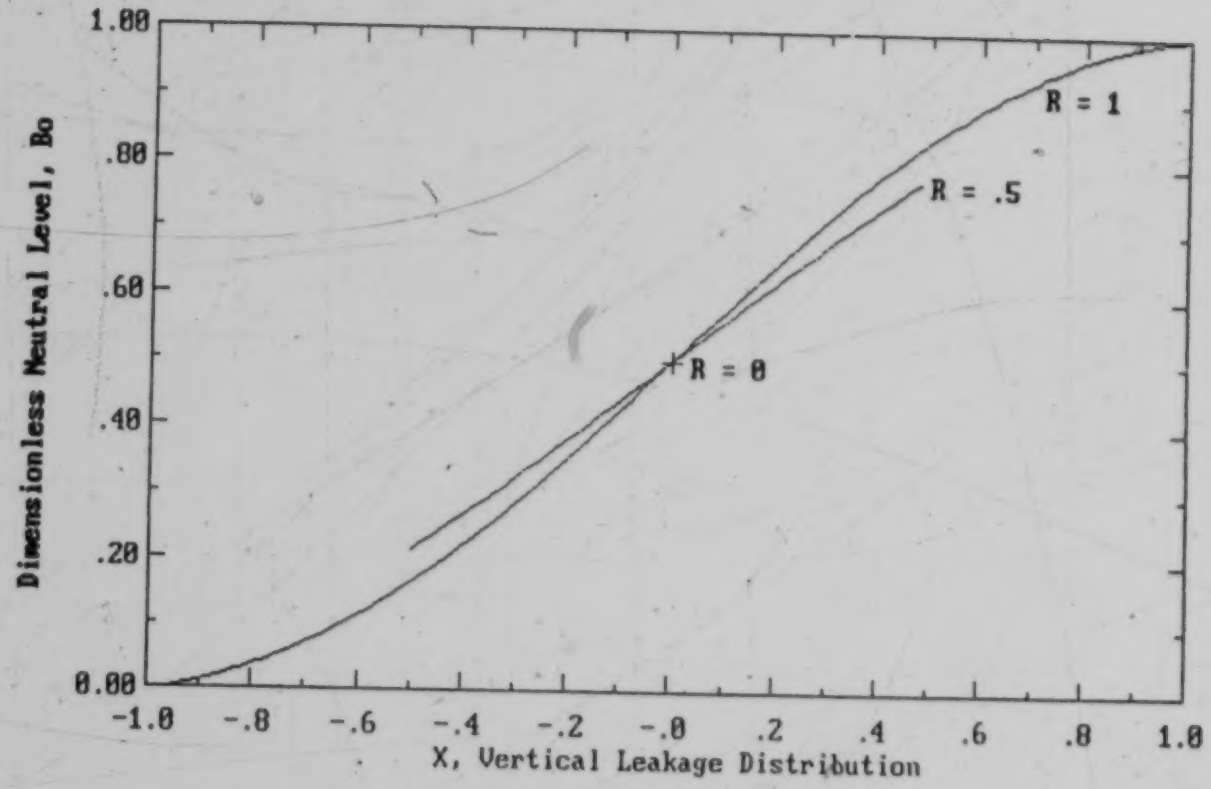

Figure 3.2: Exact values for Neutral level, β_o, from Equation (3.14) with no Flue Leakage (Y=0), where X is the ceiling-floor difference and R is the ceiling-floor sum

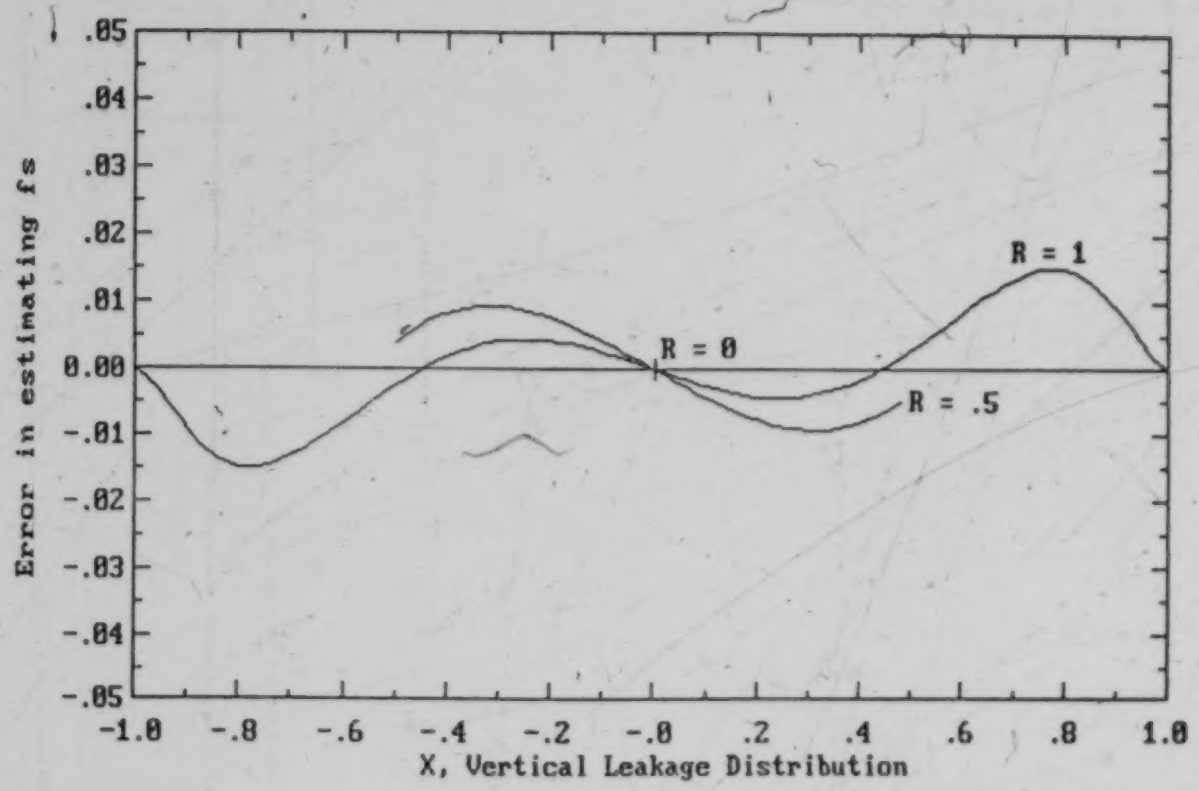

Figure 3.3: Error in Stack Factor, f_s, using Empirical Equation (3.28) for Neutral Level, β_n, with no Flue Leakage

(Kiel, Wilson and Sherman (1985), and Sherman, Wilson and Kiel (1984)). Figure 3.3 shows how the error in estimating f_s in EXACTAIM varies with R and X if the empirical fit for β_o is used. The maximum error of .015 occurs when R = 1.

The fraction of the total leakage in the furnace flue is usually less than 20%, so using values of Y = 0 and Y = 0.2 encompasses the range of flue leakage likely to be found in a residential building. Some airtight, energy conserving houses may have more than 20% of the leakage in the flue. Figures 3.4 to 3.6 are the same as Figures 3.1 to 3.3 but with 20% of the leakage in the flue and $\beta_f = 1.5$. The maximum error is now .04 and also occurs at R = 1. A value of $\beta_f = 1.5$ lies in the middle of the reasonable range for residential buildings where: $1 \leq \beta_f \leq 2$.

Once β_o is determined it is substituted into equation (3.16) or (3.17) to find the appropriate stack factor, which determines the air exchange rate in EXACTAIM according to equation (3.15).

3.6.2 Direct Estimation of Stack Factor for AIM-2

To simplify the calculation procedure for stack flow, an empirical approximation for obtaining stack factor directly was developed to create the simplified Alberta Infiltration Model, AIM-2, and is given by (3.29).

$$f_s = \left(\frac{1+nR}{n+1}\right)\left(\frac{1}{2} - \frac{1}{2} N^{5/4}\right)^{n+1} + G \qquad (3.29)$$

where

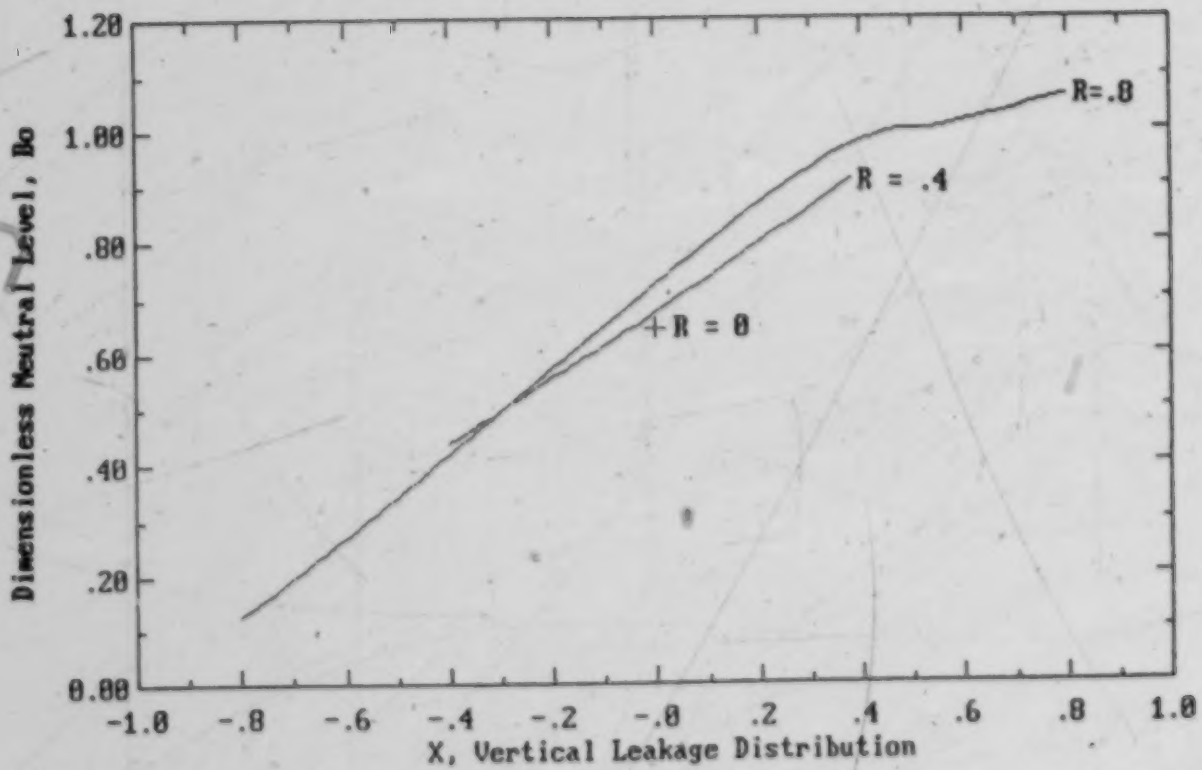

Figure 3.4: Empirical values for Neutral level, β_o, from Equation (3.28) with 20% of Leakage in Flue (Y=0.2) and β_t=1.5, where X is the ceiling-floor difference and R is the ceiling-floor sum

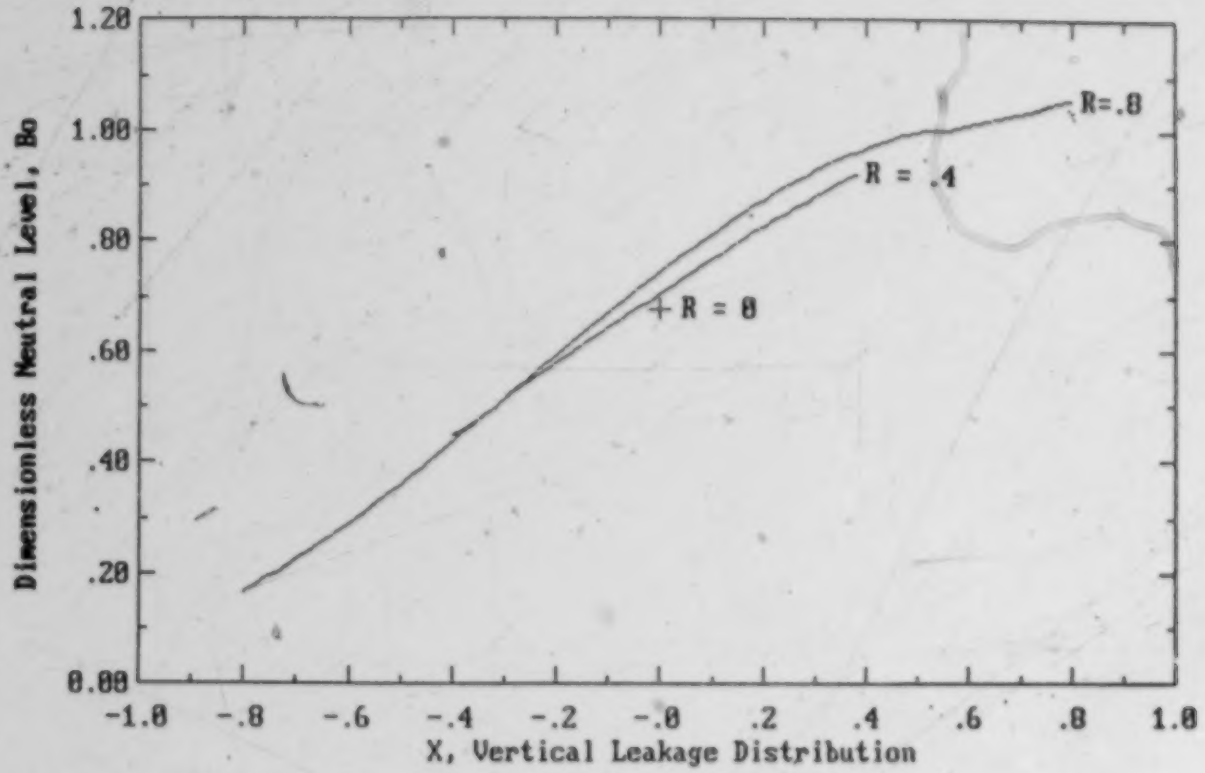

Figure 3.5: Exact values for Neutral level, β_o, from Equation (3.15) with 20% of Leakage in Flue (Y=0.2) and β_f=1.5, where X is the ceiling-floor difference and R is the ceiling-floor sum

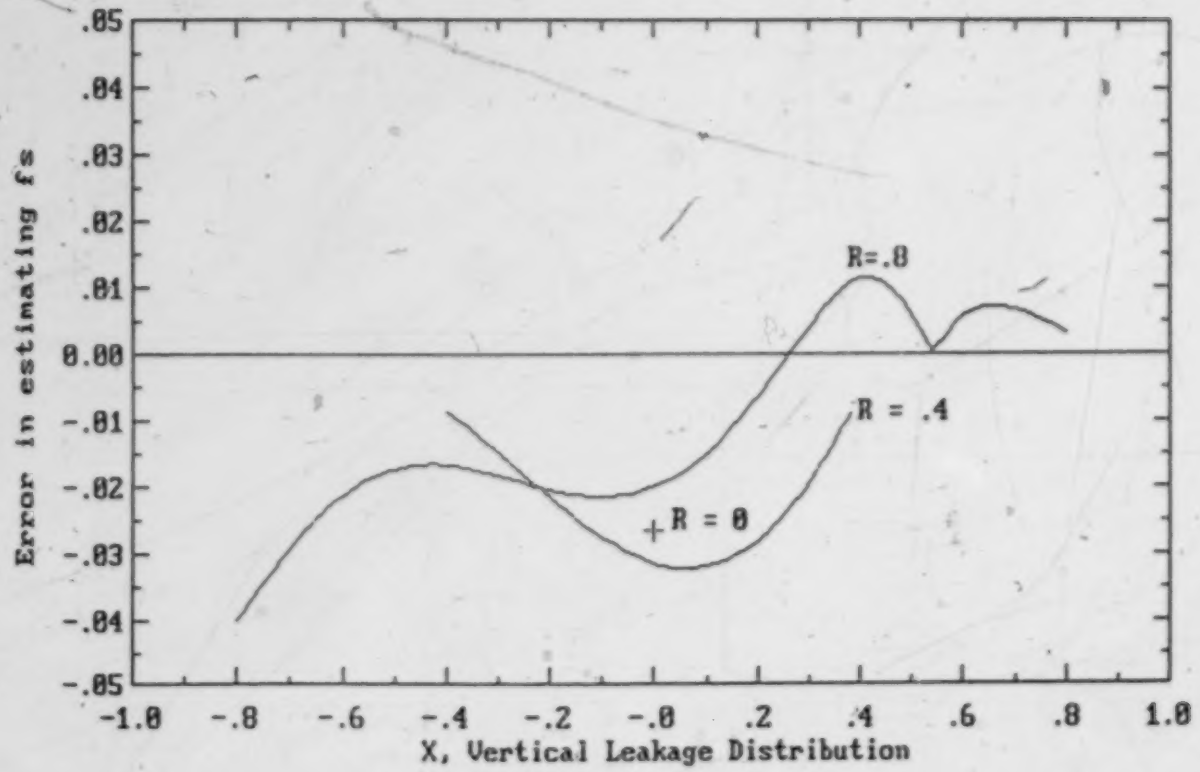

Figure 3.6: Error in Stack Factor, f_s', using Empirical Equation (3.28) for Neutral Level, β_o, with 20% of Leakage in Flue (Y=0.2) and β_f=1.5

$$N = \frac{(X + (2n+1)Y)^2}{2-R} \quad \text{for} \quad \frac{(X + (2n+1)Y)^2}{2-R} \leq 1$$

or

$$N = 1.0 \quad \text{for} \quad \frac{(X+(2n+1)Y)^2}{2-R} > 1$$

and

$$G = nY(\beta_f - 1)^{\frac{3n-1}{3}} \left[1 - \frac{3(X_{crit} - X)^2 R^{1-n}}{2(\beta_f+1)}\right]$$

where, as for β_o:

$$X_{crit} = R + \frac{2(1-R-Y)}{n+1} - 2Y(\beta_f - 1)^n \qquad (3.30)$$

X_{crit} is the critical value of X at which the neutral level passes through the ceiling in the exact solution.

For Y = 0, equation (3.31) applies

$$f_s = \left[\frac{1+nR}{n+1}\right]\left[\frac{1}{2} - \frac{1}{2}\left[\frac{X^2}{2-R}\right]^{5/4}\right]^{n+1} \qquad (3.31)$$

For the case where Y = 0 and n = 1/2 (Sherman's assumption) equation (3.31) reduces to equation (3.32)

$$f_s = \left[\frac{2+R}{3}\right]\left[\frac{1}{2} - \frac{1}{2}\left[\frac{X^2}{2-R}\right]^{5/4}\right]^{3/2} \qquad (3.32)$$

This can be shown to differ from Sherman's empirical equation by a constant due to his different definition of P_{stack}, by not squaring the (2 - R) term, and by using the power 5/4, instead of 1. From Sherman (1980):

$$f_{s,LBL} = \left[\frac{2+R}{3}\right]\left[\frac{1}{2} - \frac{1}{2}\left[\frac{X}{2-R}\right]^2\right]^{3/2} \qquad (3.33)$$

Figures 3.7 and 3.8 show the variation stack factor with R and X for Y = 0 and Y = 0.2 respectively. The stack factor was calculated using equation (3.30) and also by numerical solution of the exact equations (3.14) and 3.16). Figure 3.7 shows that for a given value of R, the stack factor, f_s, is symmetric in X and has its maximum at X = 0. When all the leaks are at either roof or floor height the stack factor becomes zero, because all the leaks have the same pressure across them, so there is no net flow. The stack factor increases with R because as more of the leakage is separated by the ceiling to floor distance and so is further from the neutral level and has a greater pressure across it. Note that by definition the absolute value of X may never be greater than R, hence the lines in these figures become shorter as R decreases.

In figure 3.8, including a flue has made the variation of f_s with X non-symmetric. It no longer holds that increasing R will always increase X and the maximum f_s is not at X = 0. Finding a suitable approximation for f_s is now much more complicated, as reflected in the approximating equation (3.30) when a flue is to be included.

The errors in using the empirical equations (3.30) and (3.31) for f_s with and without a flue are shown in figures 3.9 and 3.10. With no flue the greatest error is an underprediction of approximately .025. With a flue the greatest error is an overprediction by the same amount.

Failure to treat the flue as a separate leakage site may be a significant source of error in other models, as shown in figure 3.11. This compares f_s with n = 0.5 and a flue, equation (3.30), to Sherman's

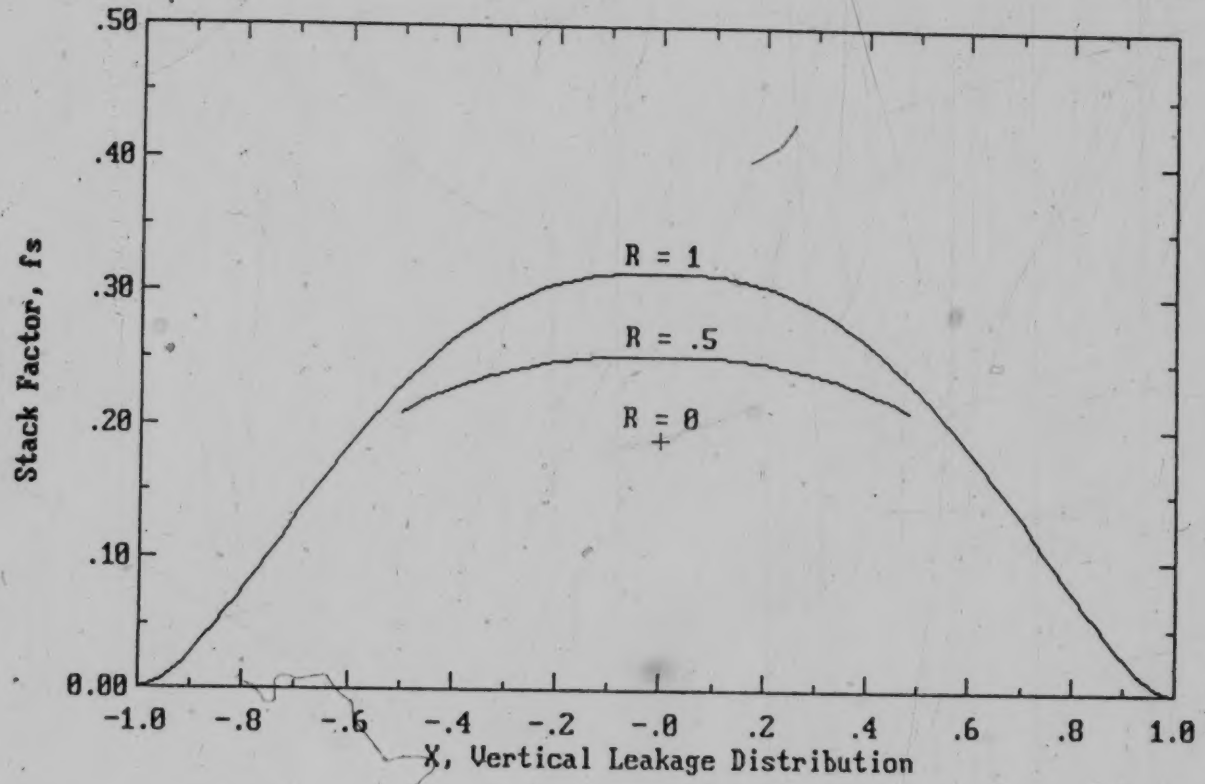

Figure 3.7: Empirical Equation (3.30) for Stack Factor, f_s, with no Flue Leakage (Y=0), where X is the ceiling-floor difference and R is the ceiling-floor sum

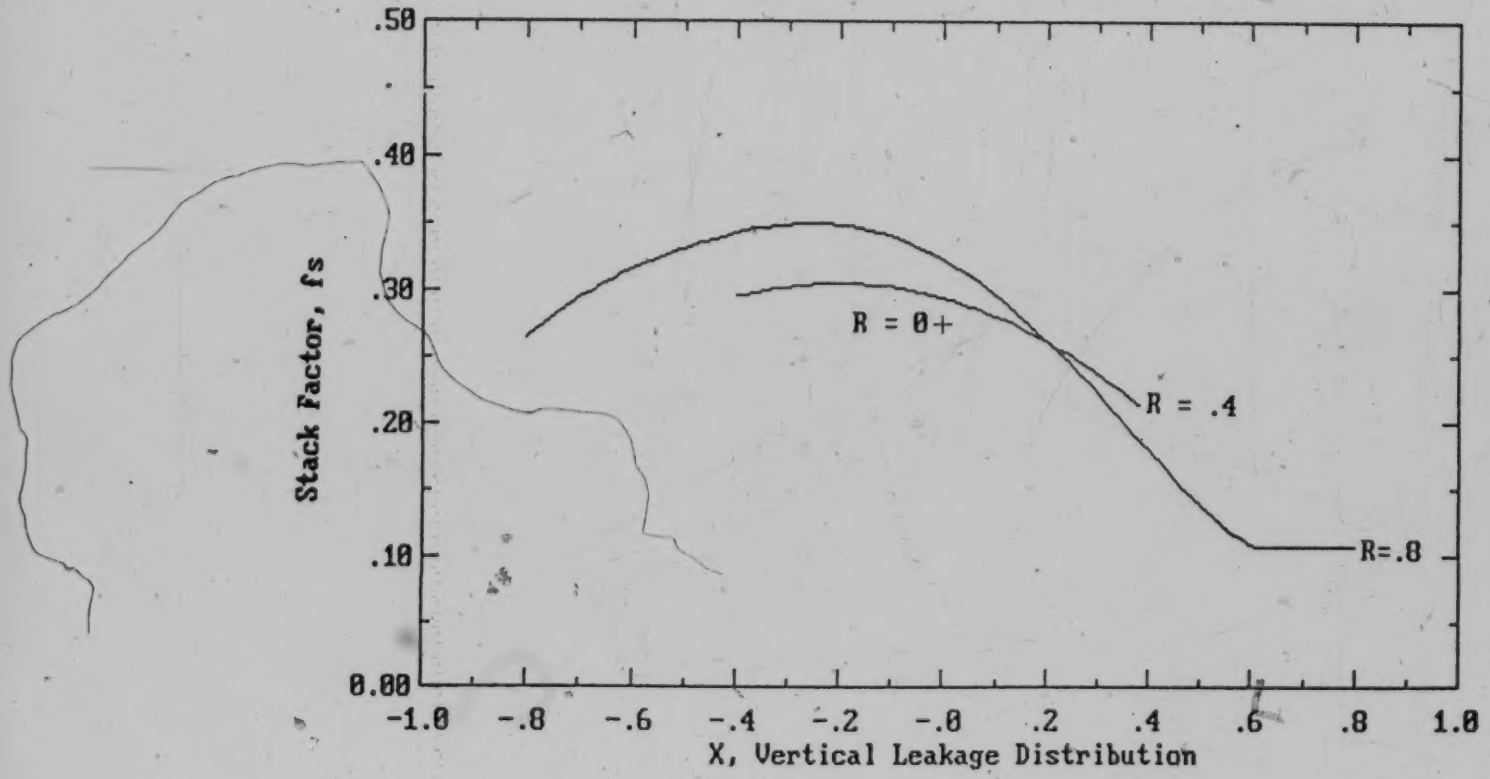

Figure 3.8: Empirical Equation (3.30) for Stack Factor, f_s, with 20% of Leakage in the Flue (Y=0.2) and β_f=1.5, where X is the ceiling-floor difference and R is the ceiling-floor sum

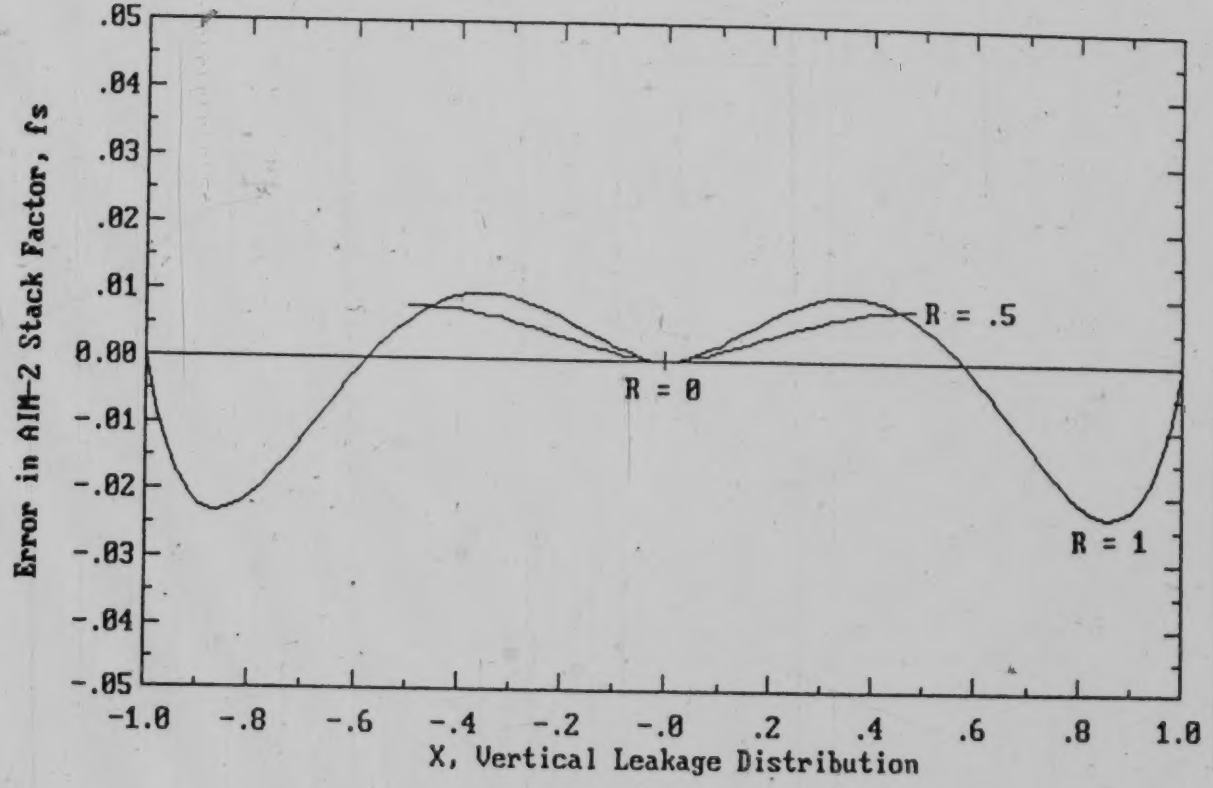

Figure 3.9: Error in using Empirical Equation (3.30) for Stack Factor, f_s, with no Flue Leakage (Y=0), where X is the ceiling-floor difference and R is the ceiling-floor sum

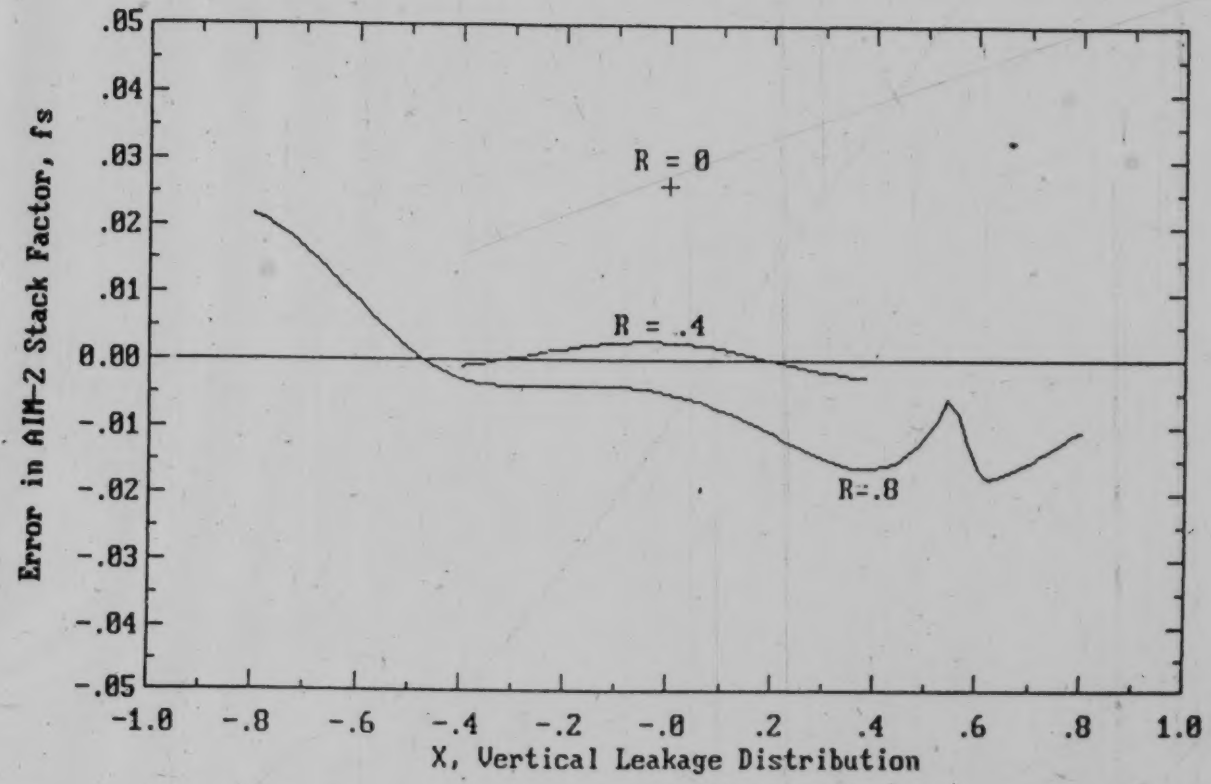

Figure 3.10: Error in using Empirical Equation (3.30) for Stack Factor, f_s, with 20% of Leakage in the Flue (Y=0.2) and β_t=1.5, where X is the ceiling-floor difference and R is the ceiling-floor sum

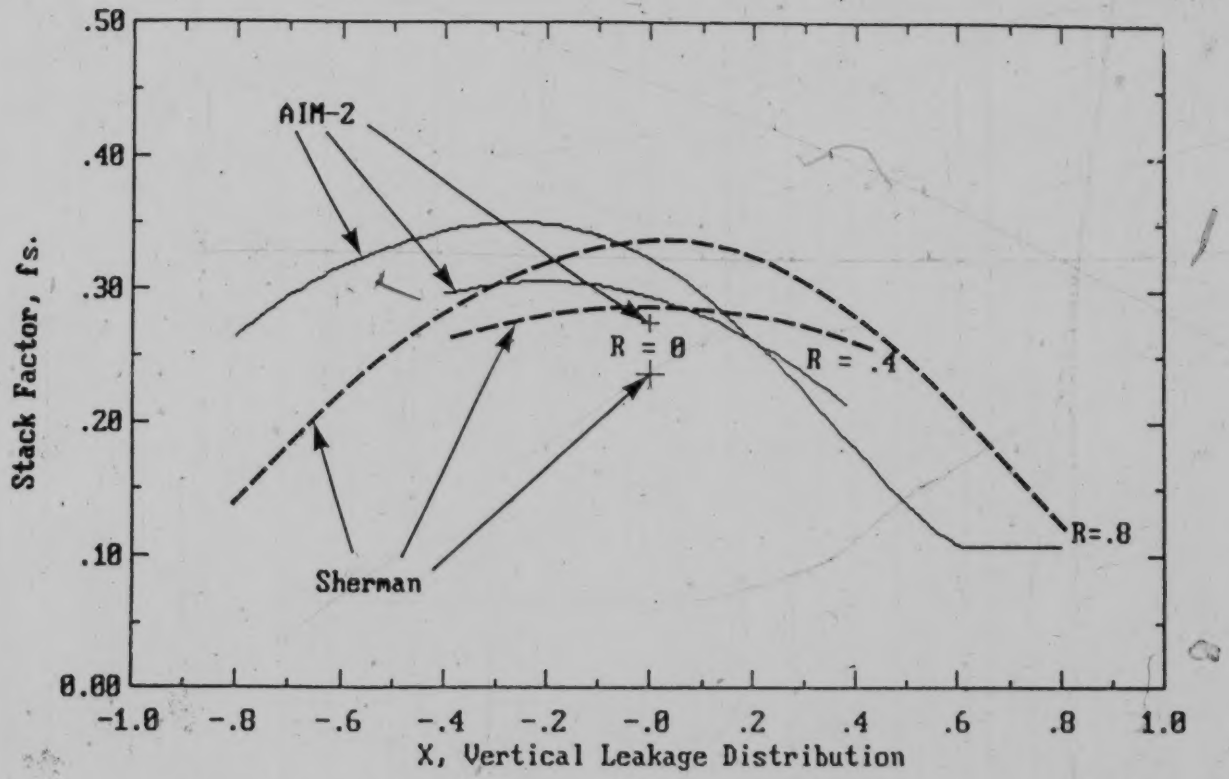

Figure 3.11: Comparison of Empirical Equation (3.30) for Stack Factor, f_s, with 20% of Leakage in the Flue (and β_f=1.5), and f_s estimated using Sherman's Equation (3.33)

equation (3.33) for f_s with the flue leakage in the ceiling. The error in using (3.33) flues is large (greater than .05) for most values of R and X. The largest error is an underprediction of 0.1, about 40%.

3.7 Wind Effect

The pressure caused by the wind on a building is due to the acceleration of the airflow around the structure, and deceleration at stagnation conditions. By applying Bernoulli's equation for incompressible flow to a streamline approaching the building, equation (3.34) may be written

$$P = P_\infty + \frac{1}{2} \rho_{out} U^2 \qquad (3.34)$$

where: P_∞ is the free steam reference pressure, which is the pressure at ceiling height far upwind of the building away from its influence

U is the free stream wind velocity at the reference height

P is the stagnation pressure on the building exterior, where the wind velocity is zero.

P and P_∞ are measured at the same reference height.

The flow does not simply stagnate on the building, and a pressure coefficient must be used to find the actual pressure on each part of the structure exposed to the wind.

The pressure coefficient, C_p is:

$$C_p = \frac{P - P_\infty}{\frac{1}{2} \rho_{out} U_H^2} \qquad (3.35)$$

where U_H is the windspeed at the reference height, H.

The reference height will be taken to be the building ceiling height. This is convenient because most references for wind pressures on structures use the windspeed at eave height to determine C_p. It is assumed that the eave and the ceiling are at the same height. Generally meteorological data is not measured at the eave height of a specific building, but at some other reference height. To find the windspeed at eave height a power law boundary layer profile for the atmosphere is assumed such that:

$$U_H = U_o \left(\frac{H}{H_m} \right)^p \tag{3.36}$$

where U_o - wind speed at measured height

H_m - measurement height

p an exponent that depends on terrain, windspeed and atmospheric stability at the building location.

It is possible that the windspeed may be measured at a location far from the building site where the terrain, windspeed and atmospheric stability are different. This means that p will be different at the measurement site. To correct for these changes, it is assumed that the windspeed at the top of the atmospheric boundary layer will be the same at both locations. A reasonable estimate for atmospheric boundary layer thickness is 600 meters from the review of available data by Counihan (1975), such that:

$$U_o = U_{600} \left(\frac{H_m}{600} \right)^{p'} \tag{3.37}$$

where U_{600} is the windspeed at a height of 600 m.

p' is the constant describing the boundary layer wind profile at the measurement site.

There are obvious limits, in that the meteorological station and the test location should experience the same local weather system. Now equation (3.36) may be rewritten.

$$U_H = U_{600}\left(\frac{H}{600}\right)^{p} \qquad (3.38)$$

Combining equations (3.37) and (3.38) yields (3.39) which is a general equation for correcting the windspeed from a meteorological station to the reference windspeed for this model.

$$U_H = U_o \frac{\left(\frac{H}{600}\right)^{p}}{\left(\frac{H_m}{600}\right)^{p'}} \qquad (3.39)$$

Table 3.1a gives atmospheric stability categories in terms of wind speed, and time of day adapted from Pasquill and Smith (1983). These stability categories are used to find values of the exponents p and p' in Table 3.1b from Irwin (1978). There are two sets of exponents, one for rural areas with a surface roughness z_o = 0.1 metres, and one for urban areas with a surface roughness z_o = 1.0 metre.

For simplicity in EXACTAIM and the simplified AIM-2 it is assumed that the building will be in a built up urban area with a neutrally stable atmosphere, and the measurement site is usually in rural terrain (for airport meteorological data), then

Table 3.1a Atmospheric Stability Classes (Pasquill(1983))

Windspeed (m/s)	DAY		NIGHT	
	summer	winter	summer	winter
<2	A	B	E	F
2-3	B	C	E	F
3-5	B	C	D	E
>5	C	D	D	D

Table 3.1b Power law exponent, p, as a function of atmospheric stability and terrain (Irwin(1978))

Stability Class	Rural z_o= 0.1m	Urban z_o= 1.0m
A	0.08	0.17
B	0.09	0.17
C	0.11	0.20
D	0.16	0.27
E	0.32	0.38
F	0.54	0.61

$p = 0.16$

$p' = 0.27$

It should be noted that the above relationships are based on average wind velocities and do not take into account the effect of atmospheric turbulence. Assuming $n = 1/2$, then flowrate is linearly proportional to the windspeed, and Appendix A shows how 20% turbulence intensity in the atmosphere produces only a 2% fluctuation in flowrate. Thus, it is reasonable to neglect the effects of atmospheric turbulence on infiltration.

3.8 Pressure Coefficients

The C_p's for this model were taken from established data sets. Most pressure coefficient data are available from wind tunnel testing of scale models. For many years pressure coefficients on buildings were determined for the purpose of estimating wind loads where only peak values are of the most interest. Estimating infiltration rates requires that the average pressure coefficients be found. For this reason much pressure coefficient data is not suitable for use in an infiltration model, and it is only in more recent years that relevant data sets have been compiled. In general the wind tunnel studies were performed on solid walls with no flow though them. A real house is leaky and it is conceivable that flow through the leaks may affect the pressure coefficients. Vickery, Baddour and Karakatsanis (1983) found that the flows through the building envelope did not affect the external flow field significantly (and hence the pressure coefficients) at wall porosities of up to 25%. These wall porosities are much

greater than would occur in a typical Canadian house and so the measured pressure coefficients need no correction.

Pressure coefficient data may be referenced to either the windspeed at eave height or the local windspeed at the pressure measurement height. In the latter case a detailed knowledge of the boundary layer velocity profile used in the wind tunnel tests is required in order to find the pressure coefficients referenced to a single velocity, which is the form required for simple infiltration models. Because this infiltration model spreads the leaks evenly over a wall, a further requirement of the pressure coefficient data is that it must be averaged over the entire wall. The effect of wind angle (with respect to the normal on the upwind wall) will also be included in the infiltration model, so data sets containing pressure coefficients from a single angle, whilst valid for comparing to other data sets, will not be used.

After a literature review four data sets were chosen for comparison: ASHRAE Chapter 14 (1989) (derived from the unpublished data of B. Vickery, and the published data sets of Swami and Chandra (1987) and Holmes (1986)), Akins, Peterka and Cermak (1979), Liddament (for AIVC) (1986) and Wiren (1984). One of these (Akins) was chosen to develop empirical estimates of infiltration rates. The pressure coefficients of Akins are illustrated in Figure 3.12 for winds perpendicular to the upwind wall (in this case Wall#1). These four data sets also cover a range of building side ratios from the square (1:1 ratio) of Akins to the rectangular (1:2 ratio) of ASHRAE. Also, the AIVC data set contains pressure coefficients for varying roof

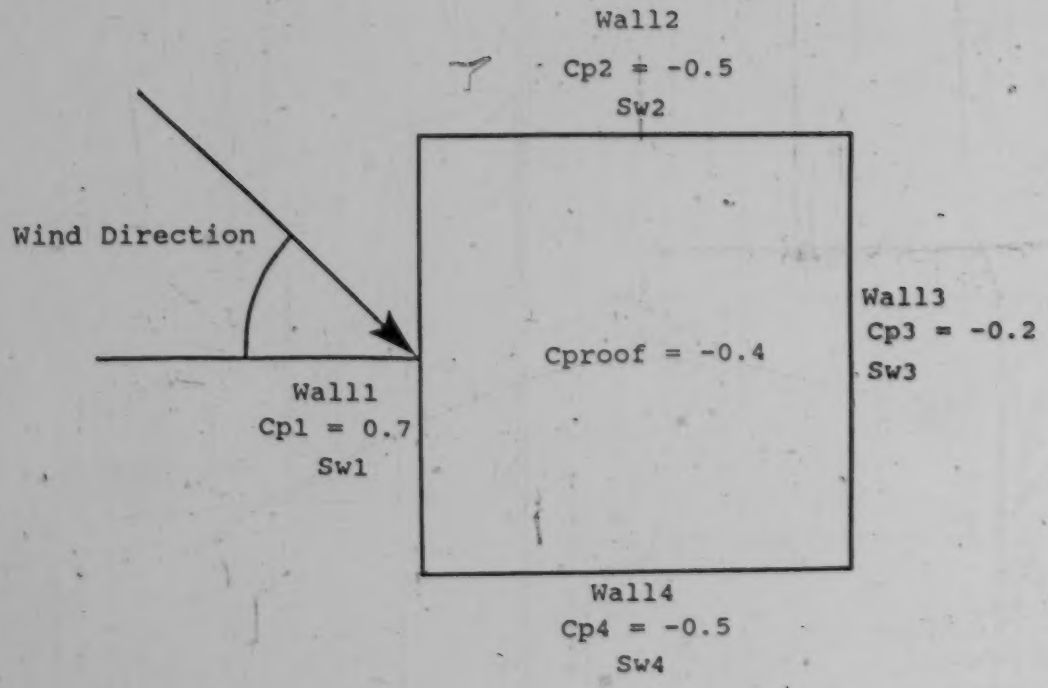

Figure 3.12: Illustration of pressure coefficients taken from Akins (1979)

slopes. The data shows that roof slope has a large effect on roof Cp's, with roof Cp's varying from -0.8 to +0.3 for a square building. A broad range of data sets in Swami and Chandra (1987) show for flat roofs to roofs with a slope of 60°, that roof slope changes the Cp's for the walls over approximately a 30% range. The roof slope interacts with the geometry of the whole building to change the Cp's in such a complex manner that no simple correlation can be found to allow for the change in Cp's with roof slope. Swami and Chandra found that roof slope has no predictable effect on Cp's. For EXACTAIM and AIM-2 the effect of roof slope will be neglected as it is beyond the scope of this work to perform the detailed analysis and measurements required to quantify it's effect. In EXACTAIM and AIM-2, the Cp for the roof (-0.4) is taken from Akins data for a flat roofed building. This value of Cp is typical of the roof Cp's given in the AIVC data set.

In all available data sets the models tested were regular shapes (either square or rectangular). A brief look at modern housing shows a distinct trend towards more complex house shapes such as split levels and L-shapes. Also, many houses have porches or attached garages. Such complicated shapes will have different pressure distributions than rectangular boxes, and therefore different wind induced infiltration rates. These complications are beyond the scope of the present model. As outlined by Swami and Chandra (1987), one can only guess at an approximate pressure distribution for these buildings . Unfortunately, very little data have been taken at full scale in real houses, due to the difficulty in instrumenting an entire house with pressure taps, and the unsteadyness of wind direction. The information that is available,

Handa and Gusten (1982) and Gusten (1984), is limited by the lack of data taken. Pressures were measured on only 2 occasions for 2 different wind angles. To adequately examine full scale effects a dedicated test facility is required. Other difficulties for full scale testing involve the effects of wind shelter and finding P_∞ remote from the building effects.

The pressure coefficient for the top of the furnace flue is highly variable and depends on the type of flue cap, and the specific roof and flue geometry. A typical value for flue pressure coefficient is -0.5 for a round flue with a raincap, from Haysom and Swinton (1987), and this is the value used in EXACTAIM and AIM-2.

For a building with leakage sites there is also an internal pressure coefficient that acts to balance the inflows and the outflows for mass conservation. Studies have been performed by Holmes (1979) which show that the resonant frequencies of building cavities are high compared with the dominant frequencies occurring in the variation of atmospheric wind, so that any resonant effects may be ignored. Stathopoulos, Surrey and Davenport (1979) found that the internal pressure shows spatial variation only if very close to a dominant opening (e.g. a door) so the assumption of a single internal pressure for the model is a good one.

3.8 Effects of Local Shielding on Wind Pressures

Local shielding accounts for the effect that obstructions close to the building have on the pressure distribution on the building. Most residential areas have trees, bushes, fences, garages and other houses close to the building under study (within 3 house heights), which alters the wind flow pattern around the building. This, in turn, changes the pressure distribution.

Some detailed wind tunnel studies of local shielding have been made, notably Wiren (1984), and Lee, Hussian, and Soliman (1979). Only regular patterns of regular sized obstructions were used in these studies because for more complicated configurations a systematic analysis of the results of the wind tunnel tests would be difficult. In reality the obstructions around a building are of many sizes. It is beyond the scope of the theoretical models to attempt to quantify local shielding effects except in the most rudimentary fashion, as outlined in Table 3.2. Sherman (1980) produced a similar table to account for shielding effects. The values in Table 3.2 differ from those of Sherman because they do not contain any spacially averaged pressure coefficients, and are applied directly to the windspeed.

The shielding coefficient is simply a number to multiply the windspeed by in order to account for shielding effects. It is non-dimensional and ranges from 0.3, for total shielding, to 1.0 for no shielding. The wind tunnel C_p data used in developing this model is all for the unshielded case with no nearby obstructions in the wind tunnel, but with upwind roughness far from the model to generate wind variation with height.

Table 3.2 Estimates of Shelter Coefficient S_{wo} for No Flue

Shelter Coefficient	Description
1.00	No obstructions or local shielding
0.90	Light local shielding with few obstructions within two house heights
0.70	Heavy shielding, many large obstructions within two house heights
0.50	Very heavy shielding, many large obstructions within one house height
0.30	Complete shielding

Note that exact shielding effects are practically impossible to determine, unless an exact scale model is used in a wind tunnel to determine these effects. Because wind shelter is very difficult to estimate accurately and has a significant effect on infiltration rates, estimates of wind shelter are one of the largest sources of uncertainty in a simple infiltration model.

Analysis of infiltration data taken at AHHRF shows that wind dominated infiltration rate may vary by a factor of two or more, depending on the local shielding. Table 3.3 gives details of the infiltration data sets from AHHRF used to examine building shelter. Figures 3.13 and 3.14 show the variations (with wind angle) of wind driven ventilation rates for a house with a closed flue and an open flue respectively. The data has been sorted for temperature differences less than 10 °C and for relatively high windspeeds of 3 to 8 m/s. The ventilation rates are normalised by dividing by U^{2n} to remove the variation due to windspeed, and by dividing by the average ventilation rate for winds from the South (θ = 180 +/- 15°) . This is done because the building has no shelter from winds from the South and the shielding factor for southerly winds will be unity. Thus there is a relationship between the shielding factor, S_w, and the normalised air exchange rate, Q_{normal} as follows:

$$Q_{normal} = S_w^{2n}$$

This data was taken in house #1 at AHHRF, it is in a row of 6 test houses, is exposed to the south, has a few farm buildings to the north and is shielded by a neighbouring test house to the East and by a

Table 3.3 Details of Infiltration data sets used to Examine Building Shelter and Superposition Methods

Data File Name	House	Data Set	Dates YYMMDDHH	# hours in figure	Figure#
UNIT1C	1	Flue Blocked Summer n = 0.73	86050101-86082908	785	3.13 3.15
UNIT1O	1	7.5cm dia. orifice in 15 cm Flue n = 0.56	87050101-87090101	498	3.14 3.16
UNIT4C	4	Flue Blocked Summer n = 0.71	86050101-86082908	535	3.17
SUPBIN1	4	7.5cm dia. orifice in 15 cm Flue South Winds Only	86092508-87011614 87011913-87012501	512	3.27
SUPBIN3	4	Low Winds Only n = 0.66	87012901-87023124 87100101-88013124	535	3.27
UBIN2	4	Flue Blocked South Winds n = 0.71	86042415-86082908	202	3.28
TBIN9	4	Flue Blocked Low Wind n = 0.71	86042415-86082908	440	3.28
UBIN11	1	15 cm dia. Flue. South Winds n = 0.55	84101111-85081315	103	3.29
TBIN12	1	15 cm dia. Flue. Low Wind n = 0.55	84101111-85081315	874	3.29

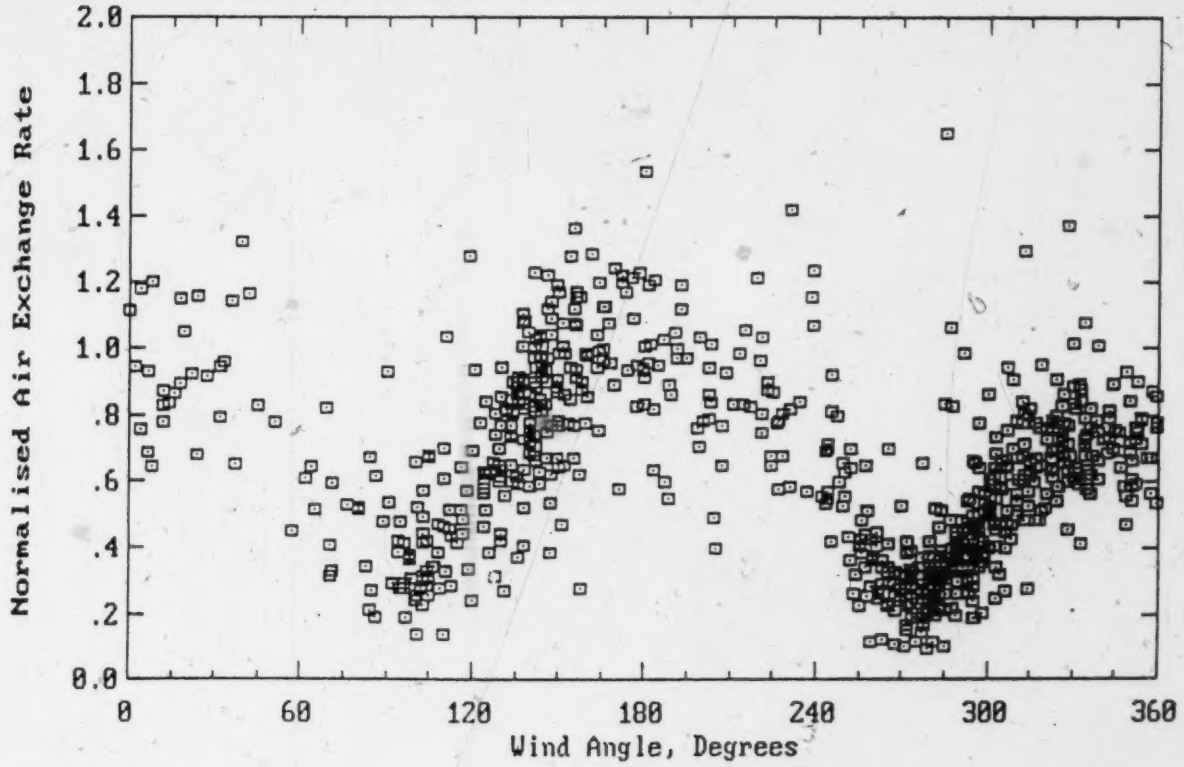

Figure 3.13: Variation of measured wind driven ventilation rate with wind angle for House #1 with Flue Blocked where $\Delta T \leq 10$ °C and $3 \leq U \leq 8$ m/s (785 hours)

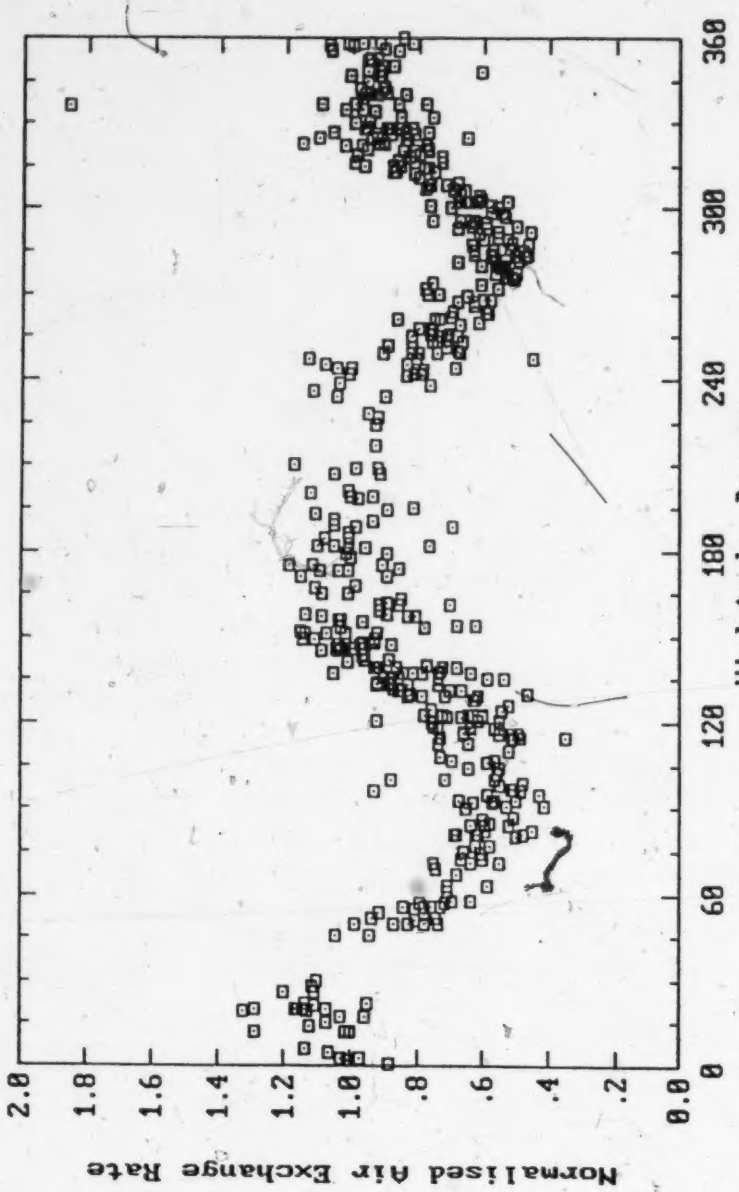

Figure 3.14: Variation of measured wind driven ventilation rate with wind angle for House #1 with an open flue where $\Delta T \leq 10$ °C and $3 < U \leq 8$ m/s (498 hours)

windbreak of the same dimensions as a house wall to the West. House #1 is of double brick wall construction, with foamed in place insulation and has a 15 cm I.D flue with a 7.5 cm diameter orifice at the bottom. From blower test performed in the house, n = 0.56 with the flue open, and n= 0.73 with the flue closed. These blower test results are shown in figure 2.5. In Figure 3.13 the local sheltering effect of the row of test houses is clearly seen with air exchange rates for East and West wind a factor of 2.5 less than for North and South winds. The variation in S_w is a factor of 2. In Figure 3.14, with the flue open, the variation in air exchange rate is reduced with a variation in S_w of a factor of 1.5. This is because the flue top protrudes above the roof line and is not sheltered from the wind by the other test houses. Thus, the shielding factor used to determine the infiltration rate must be a function of both the shelter experienced by the building and by the flue top. To allow for the variation in shielding for a flue the shielding factor, S_w, will be defined as follows:

$$S_w = (1-Y)S_{wo} + 1.5YS_{wf} \qquad (3.40)$$

where S_{wo} = wind shielding factor for building

S_{wf} = wind shielding factor for flue

S_w multiplies the windspeed that is used to find the ventilation rate for the whole house, and equation (3.40) is a semi-empirical estimate of shelter effects, and the effects of leakage distribution. The factor 1.5 accounts in a very simple way for the acceleration of airflow over the roof of the building. It does not imply that the wind

velocity at the flue top is 50% greater, but is simply a correction factor applied to the windspeed to obtain the correct measured ventilation rate. Note that it is possible for S_w to be greater than one for an unsheltered house with a large flue.

Warren and Webb (1980) found a similar variation in shielding effects for a house in the middle of a line of connected row houses. Note that a row house is not completely shielded from wind effects, because the front and back walls, roof, and flue still experience pressures due to the wind.

Clearly, shielding is a function of wind direction. A simple empirical equation has been found which makes S_w a continuous function of wind angle. Equation (3.40) is first used to estimate S_w for winds normal to each side of the building, and these values are inserted in equation (3.41) to find S_w as a function of wind angle.

$$S_w = \frac{1}{2}\left[(S_1 + S_3)\cos^2\theta + (S_1 - S_3)\cos\theta + (S_2 + S_4)\sin^2\theta + (S_2 - S_4)\sin\theta\right] \qquad (3.41)$$

where S_1 through S_4 are S_w values for winds normal to sides 1 through 4 of the building, numbered clockwise from side 1, see Figure 3.12, and θ is the wind angle measured clockwise (looking down) from the normal of side one.

Note that the wind angle measured at the meteorological site is not necessarily identical to θ. The two angles are only the same if the normal to side 1 points north, and there are no terrain-induced local direction changes. In general

$$\theta = \theta_{met} - \theta_o + \theta_{local} \qquad (3.42)$$

where θ_{met} is the wind angle at the measurement site θ_o is the angle between the normal to wall 1 and north, and θ_{local} accounts for local changes due to valleys etc.

Equation (3.42) is used to determine the angle θ in equation (3.41). Equation (3.41) reduces to give the shielding for winds normal to sides 1, 2, 3 and 4 for wind angles of 0°, 90°, 180° and 270° respectively, as it should. If the shielding is to be averaged over all wind angles, then equation (3.41) reduces to equation (3.43),

$$S_w = (S_1 + S_2 + S_3 + S_4)/4 \qquad (3.43)$$

the numerical average of the four shielding factors. This shows that equation (3.41) does not bias the shielding factors.

Figures 3.15 and 3.16 show how equation (3.41) compares to measured data for the same data as figures 3.13 and 3.14. Here the data has been averaged in bins 30 degrees wide because the trends in figures 3.13 and 3.14 are somewhat obscured by scatter in the data. The error bars indicate +/- one standard deviation from the mean for the data in each bin. The shielding values for S_1, S_2, S_3 and S_4 for the theoretical lines in figures 3.15 and 3.16 were calculated from the measured data by averaging the normalised data in the bins at θ = 0°, θ = 90°, θ = 180°, and θ = 270°, (North, East, South and West directions).

The functional form of (3.41) is consistent in that it simply reduces to the appropriate shielding factor for each of the four directions when the appropriate wind angle is chosen, and the rest of

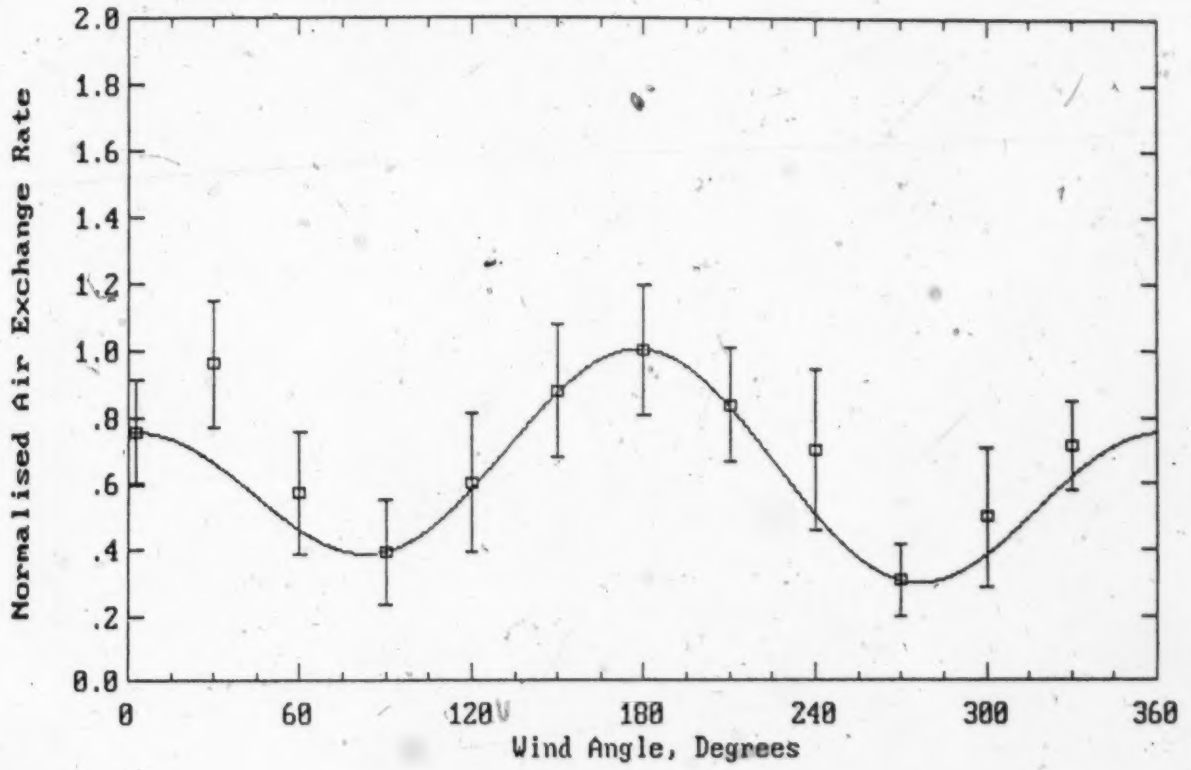

Figure 3.15: Binned measured wind driven ventilation rate with wind angle for House #1 with Flue Blocked where $\Delta T \leq 10$ °C and $3 \leq U \leq 8$ m/s, and Shielding Coefficient Sw (Solid Line) (785 hours)

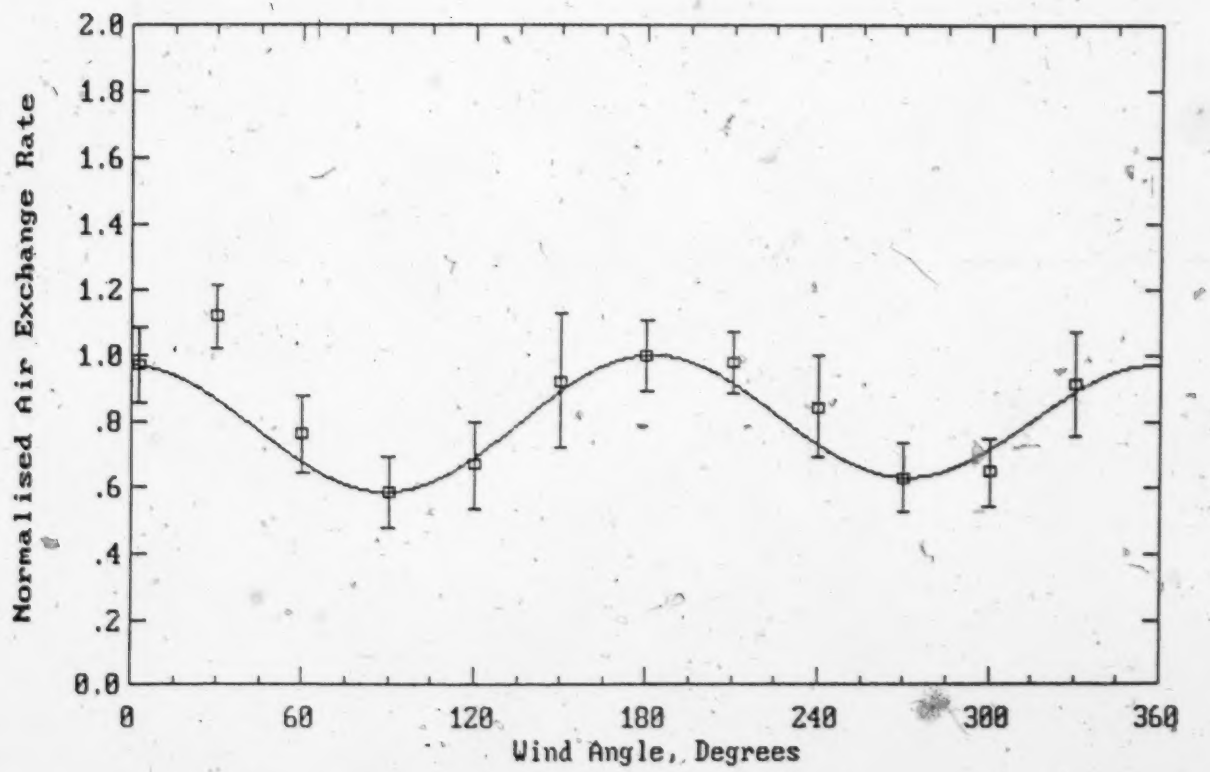

Figure 3.16: Binned measured wind driven ventilation rate with wind angle for House #1 with an open Flue where $\Delta T \leq 10°C$ and $3 \leq U \leq 8$ m/s, and Shielding Coefficient Sw (Solid Line) (498 hours)

the curve is smooth and continuous. Looking at Figures 3.15 and 3.16 it is easy to be seduced into thinking that equation (3.41) is a good fit to the data because it follows the trends in the data very well. On closer observation it can be seen that (3.41) gives only a rough estimate of the average local shelter effect. Looking at a narrow range of wind angle, i.e. one data bin, the deviation from the average S_w is typically +/- 0.1, which is fairly large for a number that varies between zero and unity. The source of this deviation lies in the use of hourly averaged wind direction. Since wind direction may vary considerably over an hour and cause different infiltration rates, using an average value creates a great deal of scatter in the data. For this reason equation (3.41) gives adequate predictions of shelter coefficient for the purposes of infiltration modelling. The effectiveness of these equations for shielding is also highly dependent on how well the estimates of shielding factors are made. Table 3.2 contains some typical values that may be used for estimating local shelter effects.

A further complication for estimating building wind shelter is that the variation of air exchange rate with wind angle also depends on the distribution of leaks among the four walls. For Figures 3.13, 3.14, 3.15 and 3.16 house #1 had approximately the same amount of leakage in each wall. Figure 3.17 shows the variation in air exchange rate and calculated S_w for house #4 at AHHRF with more leakage in the south wall than the north wall. This makes the apparent S_w for north winds about half that for south winds despite both directions having the same wind exposure. The effect of leakage distribution may be

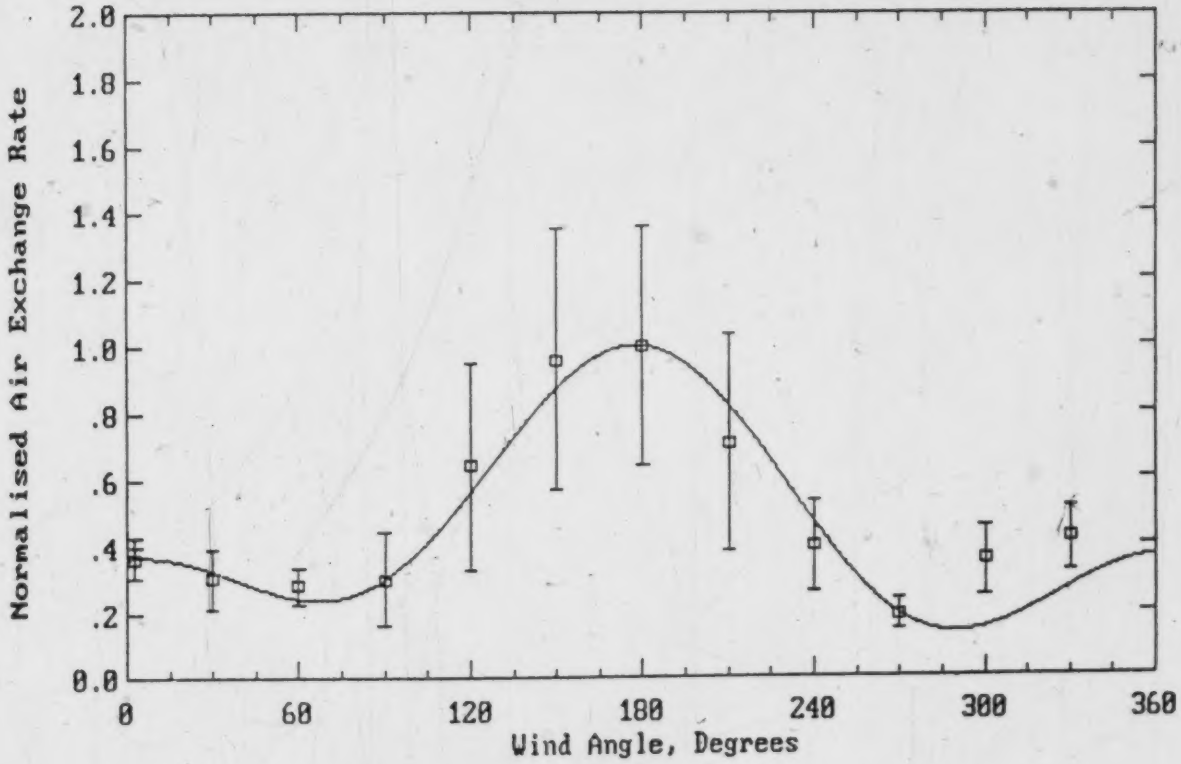

Figure 3.17: Binned measured wind driven ventilation rate with wind angle for House #4 with Flue Blocked and more Leakage in South wall than North Wall where $\Delta T \leq 10°C$ and $4 \leq U \leq 8$ m/s, and Shielding Coefficient Sw (Solid Line) (535 hours)

factored out by calculating the average S_w for north and south winds combined and the average S_w for east and west winds combined because these test houses have the same exposure from north and south and from east and west. To avoid weighting by the number of data points in each bin, it is the average values of S_w that are combined. The ratio of north and south to east and west shelter is the same, i.e. a factor of 2, for the house with evenly distributed wall leakage and for the house with more leakage in one wall. This indicates that S_w is a true indicater of building exposure.

3.9 Theoretical Estimates for Wind Effect

As with stack effect the leakage distribution is split into four main areas: walls, floor, ceiling and furnace flue. For wind driven infiltration each wall must be treated separately as each experiences a different pressure. For each leak a crack flow equation can be applied. For the i^{th} leak

$$\dot{M}_i = \rho_i C_i (\Delta P_i)^n \qquad (3.44)$$

where M_i = mass flow rate

ρ_i = density of flow

C_i = leakage of i^{th} leak

ΔP_i = pressure difference across i^{th} leak

n = flow exponent, assumed to be the same for each leak.

The flow density, ρ_i, is not initially known and depends on the direction of flow, i.e. the sign of ΔP_i. Writing equation (3.44) in terms of pressure coefficients yields equation (3.45)

$$\dot{M}_i = \rho_i C_i \left(\frac{1}{2} \rho_{out} S_w U_H^2 \right)^n (C_{pi} - C_{pin})^n \qquad (3.45)$$

where C_{pi} is the wall averaged external pressure coefficient and C_{pin} is the internal pressure coefficient and is the same for each leak. Here C_{pin} is analogous to β_o for stack effect. C_{pin} is determined by the conservation of mass in equation (3.46).

$$\Sigma \dot{M}_i = 0 = \Sigma \rho_i C_i \left(\frac{1}{2} \rho_{out} S_w U_H \right)^n (C_{pi} - C_{pin})^n \qquad (3.46)$$

For EXACTAIM, equation (3.46) can be solved numerically to find C_{pin}. The ventilation rate is given by either the incoming mass flow or the outgoing mass flow. Errors are minimised by averaging the two. Whether the flow is in or out depends on the sign of $(C_{pi} - C_{pin})$, where a positive sign yields inflow and a negative sign yields outflow. The ventilation rate due to wind action , $\dot{M}_{wind}$, may be expressed with similar terms as the stack effect as

$$\dot{M}_{wind} = \rho_{out} C f_w \Delta P_w^n \qquad (3.47)$$

where f_w = wind factor depending on averaged Cp's and leakage distribution.

$$\Delta P_w = \frac{1}{2} \rho_{out} (S_w U_H)^2$$

Appendix A shows how an exact solution for f_w may be found for EXACTAIM by: finding the flow through each leak, separating the inflows from the outflows, equating the inflows and outflows, then averaging the inflows and outflows to minimise any error. f_w contains all the information about leakage distribution and pressure coefficients.

Note that an explicit exact solution cannot be written for wind effect since the direction of flow through each leak cannot be predicted. Unfortunately C_{pin} must be found by tedious iteration in order to determine f_w. Simple approximating functions which yield f_w directly have been developed using the assumptions outlined at the beginning of this chapter.

3.10 Estimating Wind Factor for AIM-2

Theoretical estimates for f_w in EXACTAIM are based on the pressure coefficients of Akins (1979). Only pressure coefficients with wind normal to the upwind wall are used. This assumes that f_w does not change significantly with wind direction as the pressure coefficients change. Using the rest of Akins data for various wind directions to calculate f_w, figure 3.18 shows that the variation in f_w with wind angle for a typical leakage distribution is small: $f_w \approx 0.25 \pm 10\%$. This shows that although the flow through each wall changes significantly with wind angle, the average flow for the whole building does not. The shelter coefficient S_w includes all wind angle effects. For a house with a basement or slab-on-grade construction the floor leaks are distributed along the bottom edge of each wall and have the same pressure coefficient as the wall above them, and an approximating function for f_w in AIM-2 is given by:

$$f_w = 0.19\ (2-n)\left[1 - \left(\frac{X+R}{2}\right)^{1.5-Y}\right] - \frac{Y}{4}\left[Z - 2YZ^4\right] \quad (3.48)$$

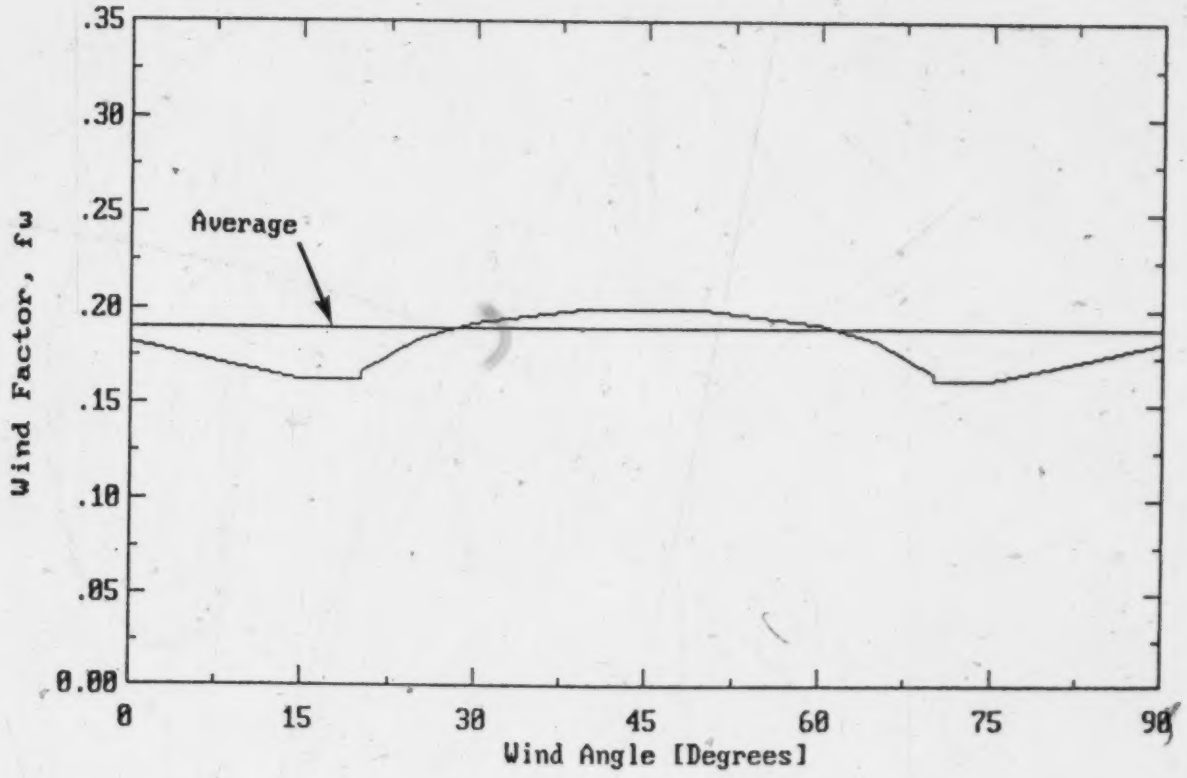

Figure 3.18: Variation in Calculated Wind Factor from EXACTAIM due to Changing Pressure Coefficients with Wind Angle, with X=0, R=0.5, Y=0.2, β_f=1.5, n=2/3. Using Akins data (1979). The solid line connects each calculated value of f_w

where $Z = \frac{X+R+2Y}{2}$

The above relationship was developed to produce the same value of f_w as EXACTAIM, and to have the correct asymptotic limits for easily verified cases: $Y = 0$, $X = \pm 1$ etc. Also, the coefficients were limited to two digits for ease of use. The relationship developed for f_w depends on the Cp data set chosen, and equation (3.48) was found using Akins Cp's. For $R = 1/2$, $Y = 0$ and $n = 2/3$, four C_p data sets (Akins, ASHRAE, AIVC and Wiren) are compared in Figure 3.19. They are functionally similar and the main difference is one of magnitude, with Wiren's giving about 20% larger and ASHRAE about 20% smaller values of f_w than those generated using Akins pressure coefficients. The functional form of equation (3.48) is relatively independant of the pressure coefficients used and the different Cp data sets just alter the lead constant. One of the reasons for selecting Akins pressure coefficients for use in developing this model is that both the Cp values and the f_w values they generate are close to the average of other data sets.

Wind factors calculated using equation (3.48) are shown in Figures 3.20 and 3.21 for $n = 2/3$ and $Y = 0$ (no flue) and $Y = 0.2$ respectively. Figure 3.20 shows that (3.48) has the correct limits i.e. when all the leaks are at one location there is no net infiltration i.e. at $X = \pm 1$. Note that f_w always decreases as the leaks are moved from floor level to ceiling level (increasing X) because the pressure difference between the ceiling and the attic is less than the average pressure difference across the walls. In Figures 3.22 and 3.23 the shaded area illustrates

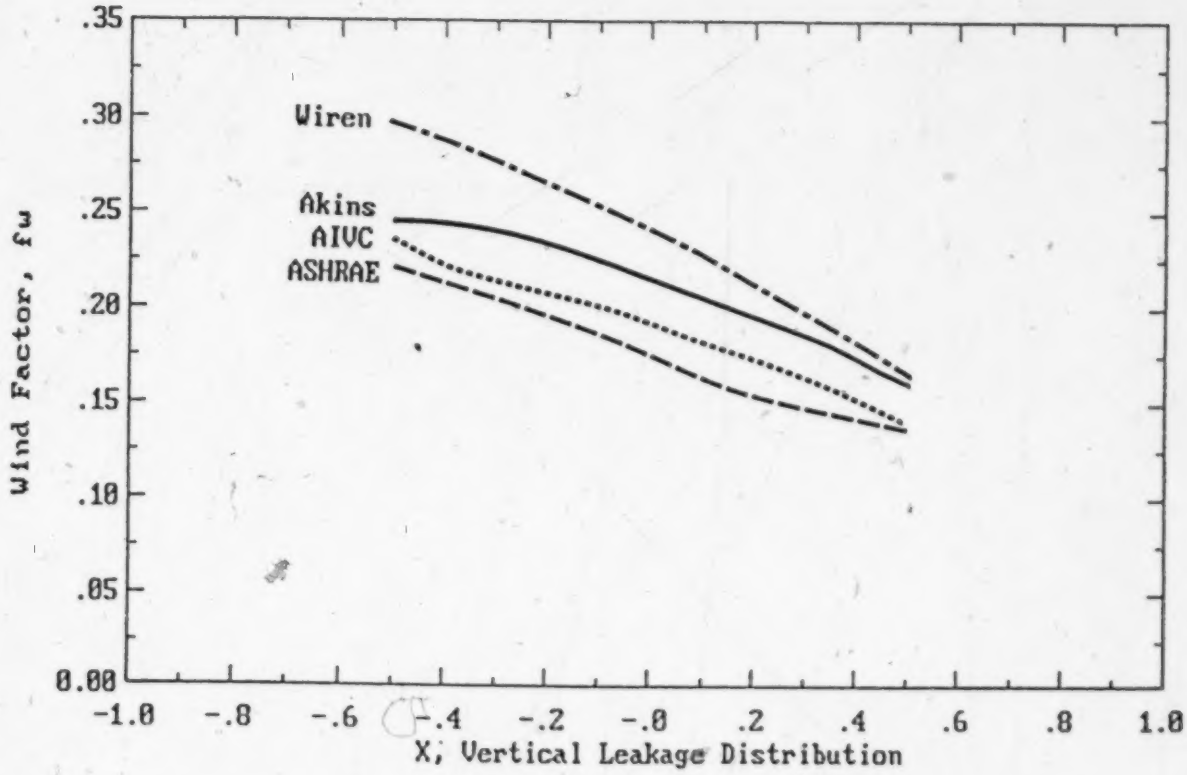

Figure 3.19: Variation in Calculated Wind Factor from EXACTAIM for the pressure coefficient data sets of Akins, AIVC, ASHRAE, and Wiren, with R=0.5 and Y=0 and wind perpendicular to upwind building face

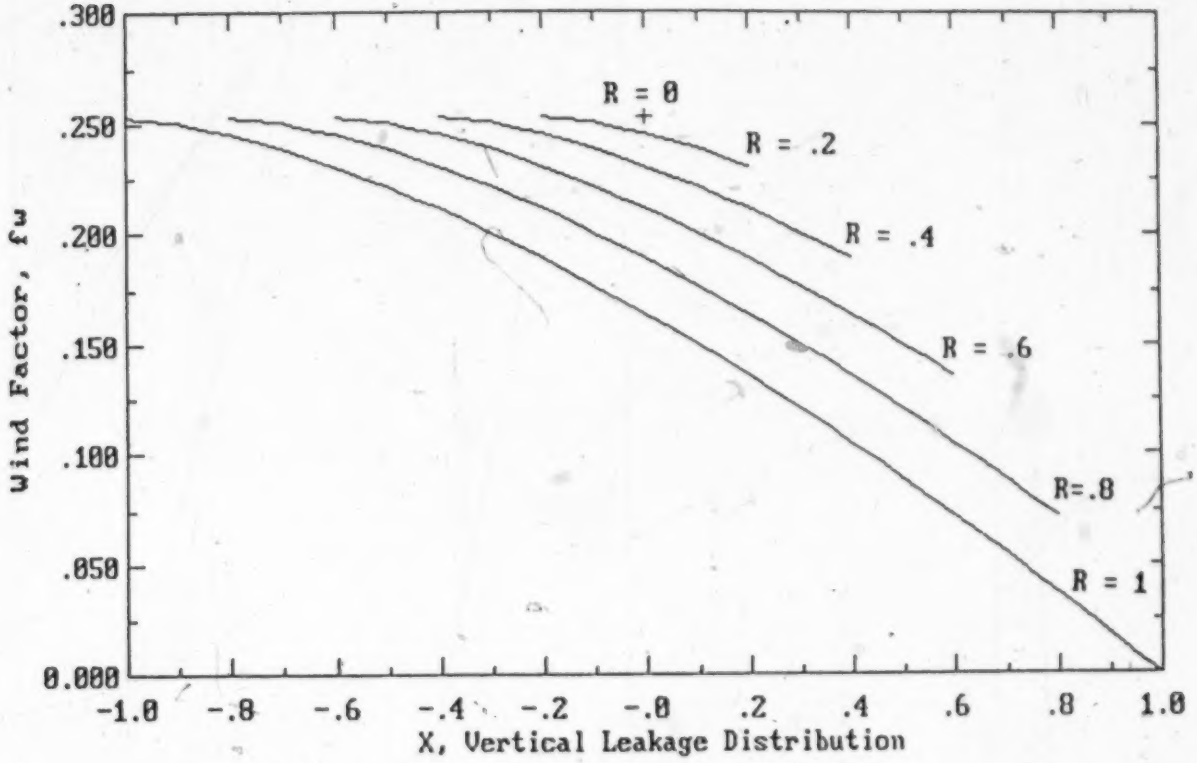

Figure 3.20: Empirical Equation (3.48) for Wind Factor f_w in AIM-2 with no Flue Leakage (Y=0) and n=2/3, where X is the ceiling-floor difference and R is the ceiling-floor sum

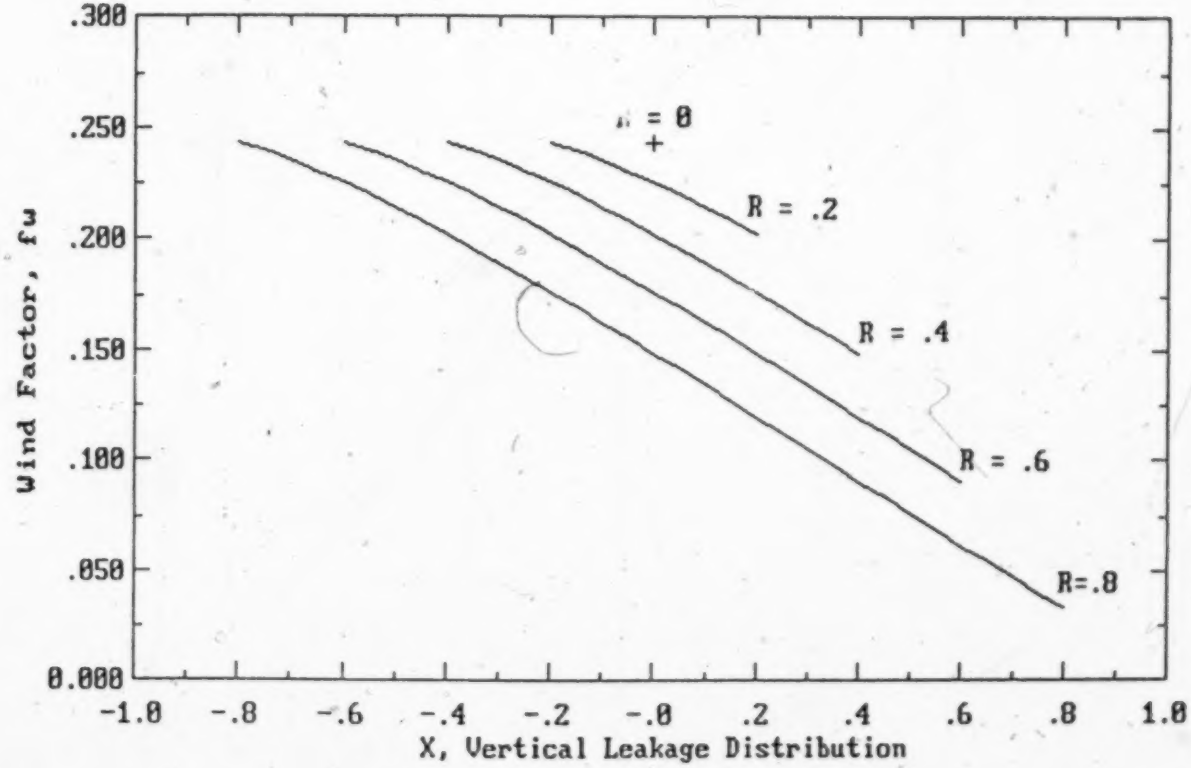

Figure 3.21: Empirical Equation (3.48) for Wind Factor f_w in AIM-2 with 20% of Leakage in the Flue (Y=0.2), n=2/3 and β_t=1.5, where X is the ceiling-floor difference and R is the ceiling-floor sum

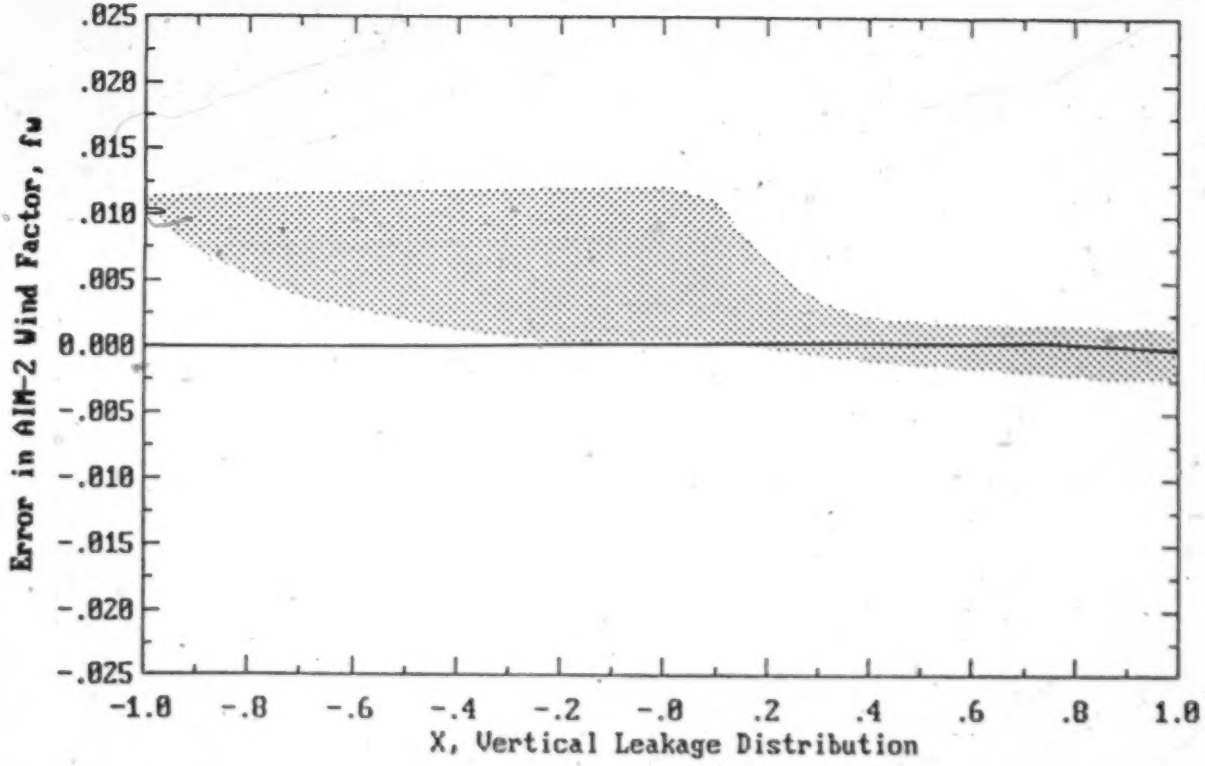

Figure 3.22: Range of Errors associated with the empirical equation (3.48) for f_w in AIM-2 with no Flue Leakage (Y=0) and n=2/3

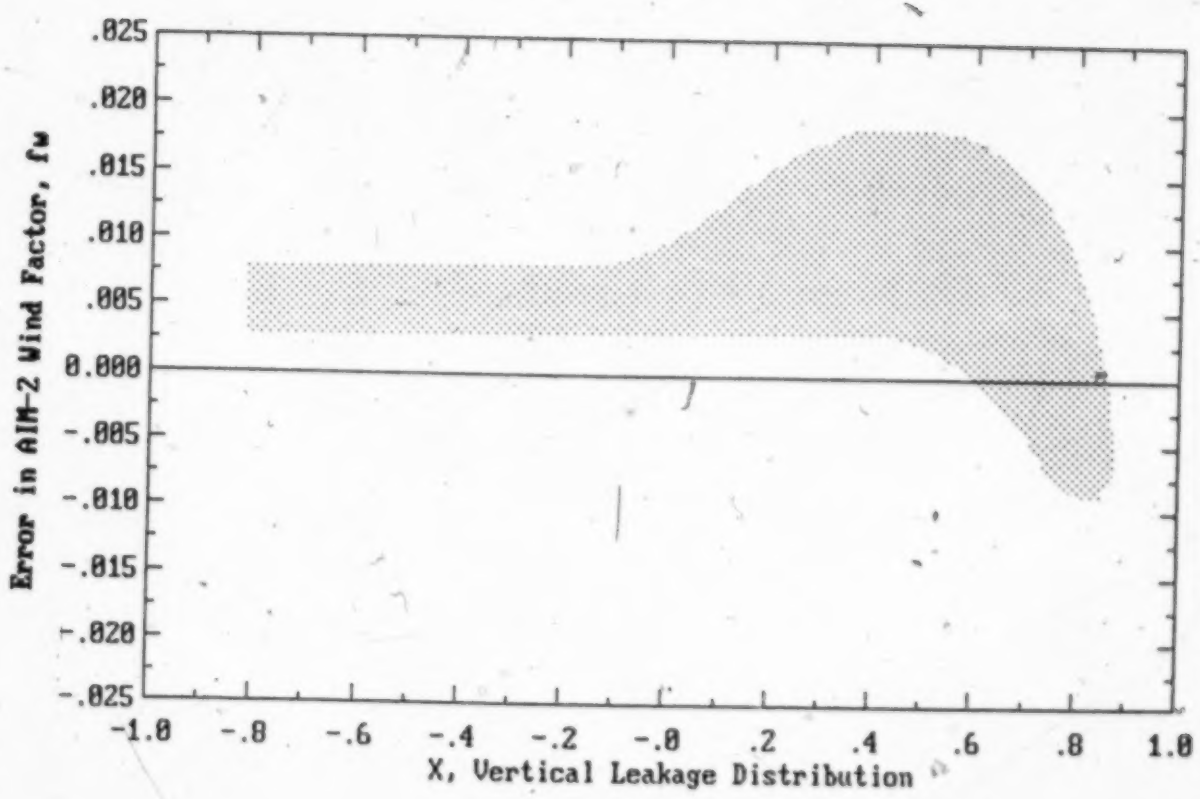

Figure 3.23: Range of Errors for the empirical equation (3.48) for f_w in AIM-2 with 20% of leakage in the Flue (Y=0.2), n=2/3 and β_t=1.5

the range of errors associated with using the estimate of f_w compared to the exact value of f_w resulting from the iterative solution of equation (3.46) (as used for EXACTAIM), showing that (3.48) gives errors less than .015, about 5%, in f_w at Y = 0 and less than .02, about 8%, in f_w at Y = .2 for any value of X and R. Equation (3.48) appears to consistently overpredict. The overprediction is about 5% and is the result of roundoff error when only using two digits for the constants in the equation. Also, this overprediction is insignificant when compared to the variation in f_w between data sets. More detailed studies have shown that (3.48) works well over a range of $0.5 \leq n \leq 0.8$ and $0 \leq Y \leq 0.5$. It is not recommended that (3.48) be used if Y is greater than 0.6 since there will be large errors compared with the exact solution.

It is interesting to compare (3.48) to the wind factor developed by Sherman (1980). For the case of no local shielding, which implies the use of the maximum value of Sherman's "generalized shielding coefficient", f_w is approximated by:

$$f_{w,sherman} = 0.324(1-R)^{1/3} \qquad (3.49)$$

With all the leaks in the walls, X = 0, R = 0, Y = 0 and assuming the same value of n = 1/2 as Sherman, (3.48) predicts $f_w = 0.285$, which is 12% less than Sherman's value in (3.49). In addition (3.48) has a strong X dependence and (3.49) has none. This is due to the different assumptions about floor and ceiling pressures.

For a house with a crawl space, the pressure inside the crawl space may be approximated by the average of the four walls. Using this

assumption to find wind factor yields a different empirical approximation, suitable for use with such house.

$$f_{wc} = 0.19(2-n)\, X^* R^* Y^* \qquad (3.50)$$

where

$$R^* = 1 - R\left(\frac{n}{2} + 0.2\right)$$

$$Y^* = \left(1 - \frac{Y}{4}\right)$$

$$X^* = 1 - \left(\left(\frac{X-X_s}{2-R}\right)^2\right)^{0.75}$$

where $X_s = \left(\frac{(1-R)}{5}\right) - 1.5Y$

and there is a critical value of X , X_{crit} above which f_w does not change with X where:

$$X_{crit} = 1-2Y$$

If $X > X_{crit}$ then use $X = X_{crit}$

For the case where all the leaks are in the walls, R = 0, and f_{wc} = 0.276, which is 15% below Sherman's estimate and 3% less than for a house with no crawl space.

The estimated wind factor for a house with a crawl space with no flue (Y = 0) and n = 2/3 is shown in Figure 3.24. The range of error is compared with the exact iterative solution shown in Figure 3.25. In this case the wind factor is not monotonic in X, and the range of error is less than .01 in f_{wc}. In Figure 3.26 the exact solutions for f_{wc} are shown with n = 1/2, using Sherman's assumptions of $Cp_{attic} = 0$

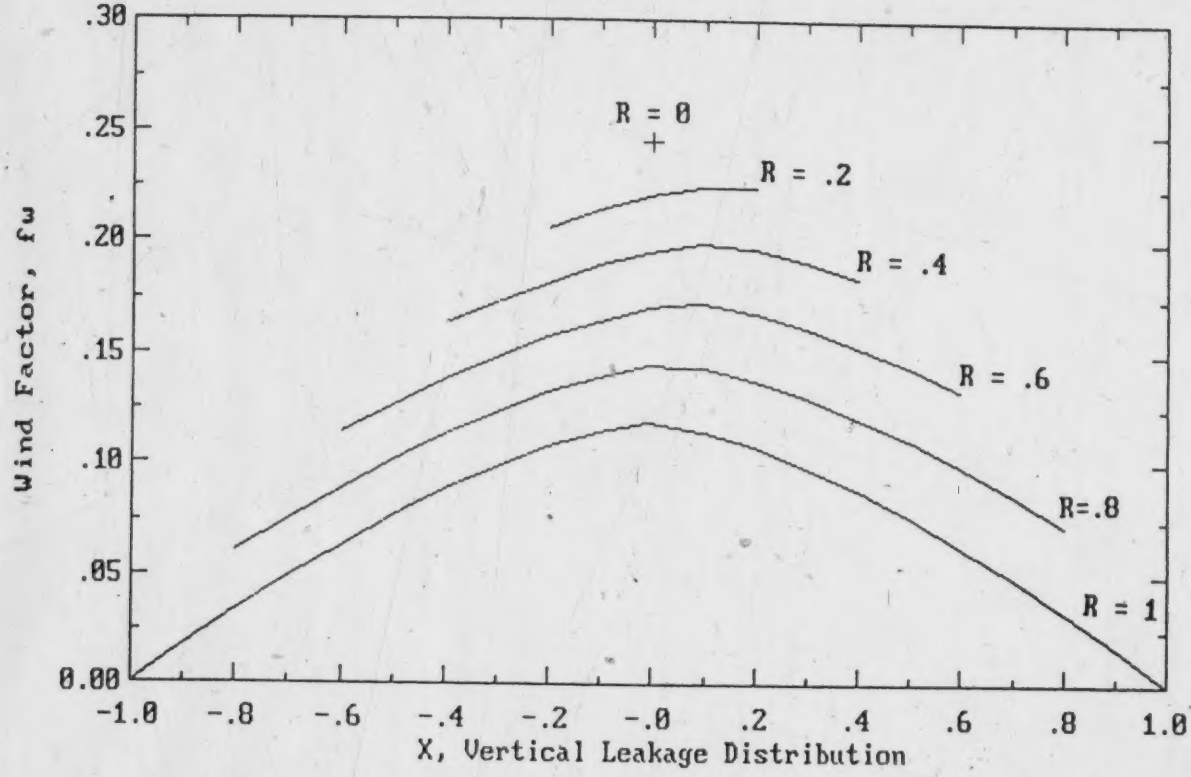

Figure 3.24: Empirical Equation (3.50) for Wind Factor f_w in AIM-2 for a house with a Crawl Space and no Flue Leakage (Y=0), where X is the ceiling-floor difference and R is the ceiling-floor sum

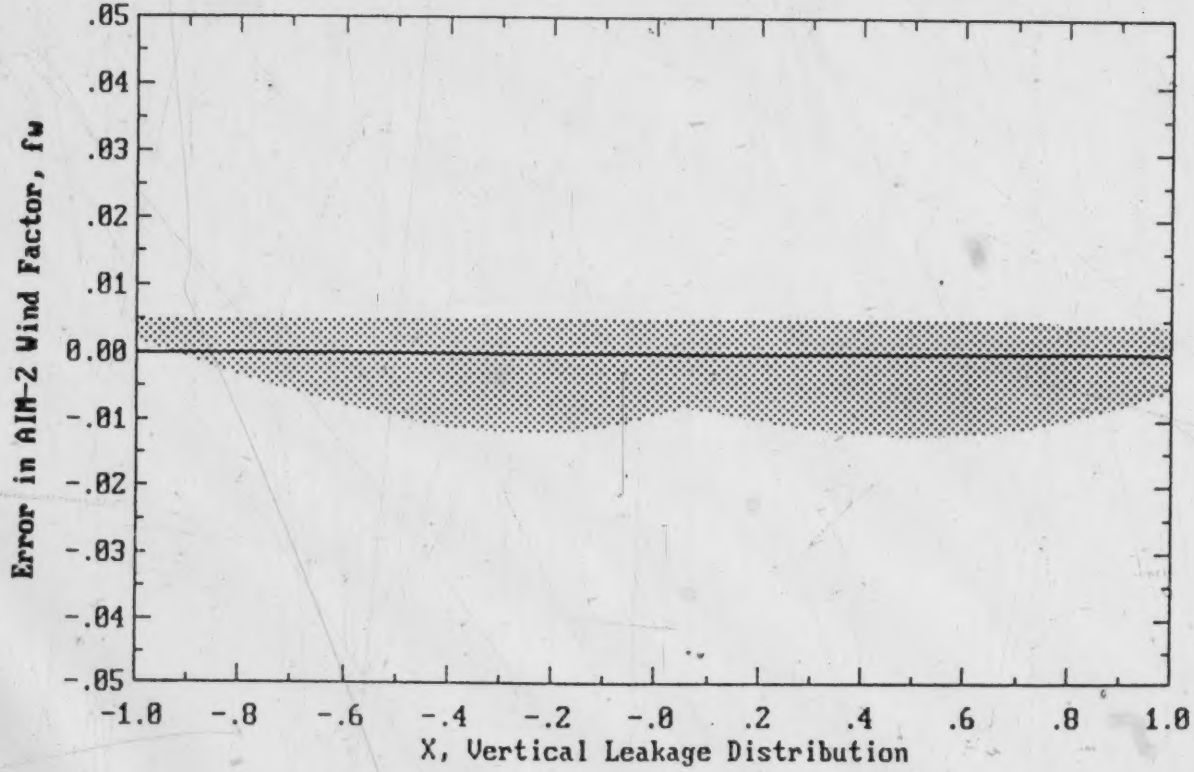

Figure 3.25: Range of Error for the empirical equation (3.50) for f_w in AIM-2 for a house with a Crawl Space and no Flue Leakage (Y=0)

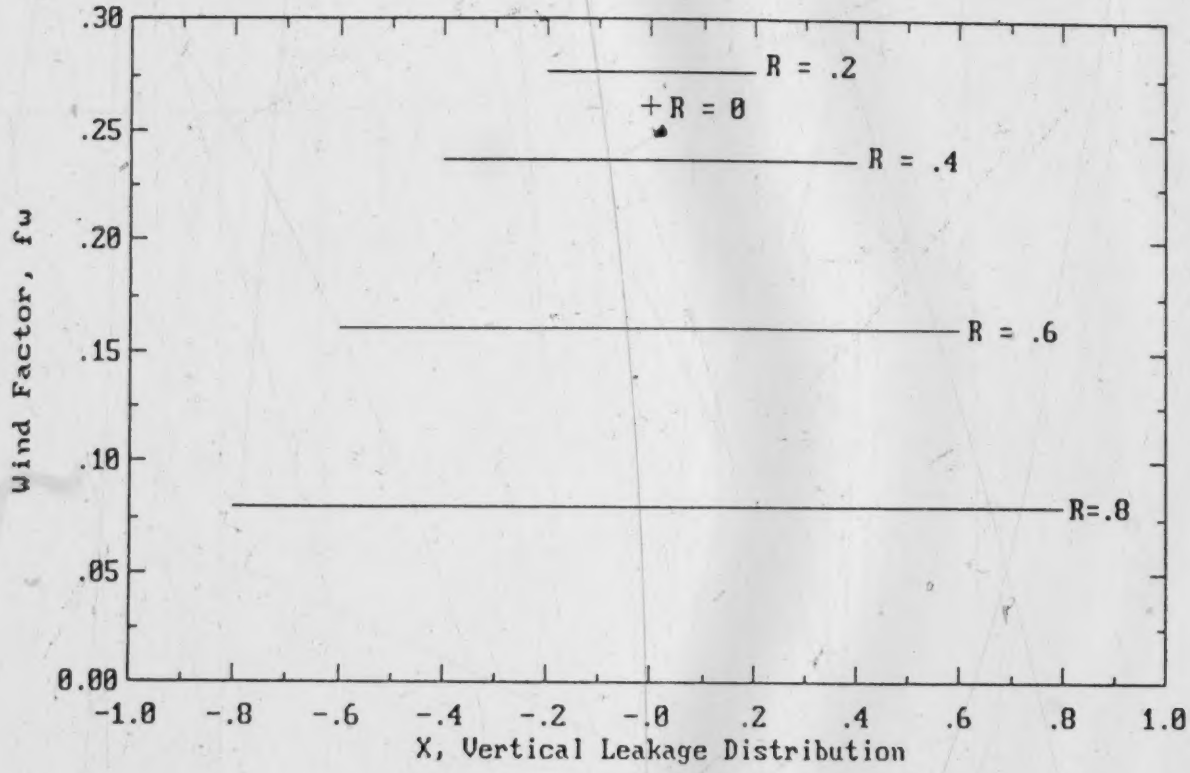

Figure 3.26: Exact Values of f_w calculated by EXACTAIM, using the same assumptions as Sherman: Y=0, n=1/2, Zero external Cp for attic and floor, where the floor is over a crawlspace

and $Cp_{floor} = 0$ (but the pressure difference is not zero). At R = 1 when there is no leakage in the walls and all the leakage is in the floor and ceiling then these assumptions predict zero wind driven ventilation, and there is no dependance on X, the same as equation (3.49). However, the maximum value of f_w occurs when R=0.2 unlike (3.49).

3.11 Superposition of Wind and Stack Effects

Once the separate stack and wind effect flow rates have been calculated they must be superposed in some way to find the total infiltration rate. A popular method used by LBL (Sherman), ASHRAE and Yuill is that of adding the flowrates in quadrature. All these superposition models are for volume flowrates, Q, not mass flowrates , M, because the models assume no density difference between inflowing and outflowing air.

$$Q_{total} = \left(Q_s^2 + Q_w^2\right)^{1/2} \qquad (3.51)$$

where Q_s = Stack driven ventilation rate

Q_w = Wind driven ventilation rate

Another method is that of adding the pressures, used by Shaw (1985), Warren and Webb (1980), and Wilson and Pittman (1983) for a variable n model:

$$Q_{total} = \left(Q_s^{1/n} + Q_w^{1/n}\right)^n \qquad (3.52)$$

Note that (3.51) is a special case of (3.52) if orifice flow, with n = 0.5, is assumed.

Lyberg (1983) looked at several superposition methods:

Simple Addition

$$Q_{total} = Q_s^{\gamma} + Q_w^{\gamma} \tag{3.53a}$$

where γ is some constant

Addition plus a constant

$$Q_{total} = Q_s^{\gamma} + Q_w^{\gamma} + C_1 \tag{3.53b}$$

Replacing the above constant with an "interference" term

$$Q_{total} = Q_s^{\gamma} + Q_w^{\gamma} + C_1 Q_s^{\gamma} Q_w^{\gamma} \tag{3.53c}$$

Note that (3.53c) is dimensionally inconsistent. In addition a hybrid quadrature was examined

$$Q_{total} = \left(Q_s^2 + Q_w^2\right)^{\gamma} \tag{3.53d}$$

Lyberg found that the hybrid quadrature (3.53d) gave the least error with his data measured in Swedish housing, with $\gamma = 1/2$. Yuill (1985) found that quadrature usually overpredicts infiltration, and Modera, Sherman and Levin (1983) found that the overprediction was greatest when stack and wind effect are equal, but when one or the other dominates the error is reduced. This overprediction arises from the interaction between stack and wind effects.

The two effects are not independant since they must both use the same internal pressure to determine the neutral level height β_o and the internal pressure coefficient C_{pin}. To account for this interaction an interference term is used in the present study to act as a simple

first order internal pressure shift correction. In EXACTAIM wind and stack flows are superposed by addition of pressures and an interference term:

$$M_{total} = \left[M_s^{1/n} + M_w^{1/n} + B_1 \left(M_s M_w \right)^{1/2n} \right]^n \qquad (3.54)$$

where B_1 must be determined experimentally. In AIM-2, r = 1.0 and the mass flow rates can be replaced by volume flow rates, Q.

All 3 terms in (3.54) have the same units of mass flowrate, and the proposed interference term becomes insignificant when either stack or wind pressure dominate.

To examine the effectiveness of some of these superposition techniques separate from the other modelling characteristics, equations for estimating Q_s and Q_w have been found by fitting empirically to ΔT and U data. The equations have the following form:

$$Q_w = D_1 U^{2n} \qquad (3.55)$$

$$Q_s = D_2 \Delta T^n \qquad (3.56)$$

where D_1 and D_2 are empirically determined constants.

To find D_1, measured infiltration data was sorted for $\Delta T \leq 10°C$, and for South winds only to remove shelter and leakage distribution effects. For House #4, with an open 15cm diameter flue with a 7.5 cm diameter orifice at the bottom, 2055 hours of infiltration data were reduced, by sorting for low ΔT as above, to 512 hours. D_1 is then found by fitting empirically to this sorted data, and for Q in air changes per hour (ACH), $D_1 = 0.030$. For House #4, with the flue blocked, 2790 hours of infiltration data were reduced to 202 hours,

and D_1 = 0.013. For House #1, with an open 15 cm diameter flue, 4875 hours of infiltration data were reduced to 103 hours, and D_1 = 0.024.

To find D_2, measured infiltration data was sorted for $U \leq 1.5$m/s. For House #4, with an open 15cm diameter flue with a 7.5 cm diameter orifice at the bottom, 2055 hours of infiltration data were reduced, by sorting for low U as above, to 535 hours. D_2 was then found by fitting empirically to this sorted data, and for Q in air changes per hour (ACH), D_2 = 0.013. For House #4, with the flue blocked, 2790 hours of infiltration data were reduced by sorting to 440 hours, and D_2 = 0.006. For House #1, with an open 15 cm diameter flue, 4875 hours of infiltration data were reduced by sorting to 874 hours, and D_2 = 0.023. Table 3.3 gives details of the infiltration data sets from AHHRF used to examine superposition methods. For each house configuration there are two data sets; one for low ΔT (to find D_1), and one for low U (to find D_2). In one case the data set spans four date ranges and in this case the date ranges are presented only once.

Q_w and Q_s are predicted using equations (3.55) and (3.56), and the appropriate fitted values of D_1 and D_2. The same data sets were used to test the superposition methods as were used to find the values of D_1 and D_2. The relative contribution of wind and stack effect is determined by the ratio Q_w/Q_s. To remove the dependance of this ratio on the leakage distributions, expressed as R, X, and Y, a more appropriate non-dimensional ratio is that of the characteristic pressures for wind and stack effect:

$$P_{wind} = \frac{\rho_{out} U^2}{2} \qquad (3.57)$$

$$P_{stack} = \frac{\rho_{out} g H \Delta T}{T_{in}} \qquad (3.58)$$

The four superposition techniques analysed here are:

1. Linear addition of flowrates, equation (3.53a)
2. Pressure addition, equation (3.52)
3. Quadrature addition of flowrate, equation (3.51)
4. Pressure addition with an interaction term, equation (3.54), with B_1 found from data correlation.

The variation of the ratio of ventilation rates predicted by the equations above to measured ventilation rates (Qpred/Qmeas) with the ratio of wind to stack characteristic pressures is shown in Figure 3.27 for House #4 with a 15 cm diameter flue with a 7.5 cm diameter orifice and in Figure 3.28 for House #4 with the flue blocked. The similarity of the two figures shows that the same superposition can be used for a wide range of leakage distributions. The ratio of P_{wind} to P_{stack} for which $Q_w = Q_s$ can be determined analytically by expressing equations (3.55) and (3.56) in terms of P_{wind} and P_{stack} and equating the two flowrates. The pressure ratio for which the stack and wind effect flowrates are equal is also shown in the figures. This is the point at which the subtractive interference term in equation (3.54) is greatest, and when addition by quadrature yields the smallest total ventilation rate for a given Q_w or Q_s. Addition of flowrates overpredicts the ventilation rate, with the greatest overprediction, 45% (.07 ACH), when wind and stack flowrates are close to being equal.

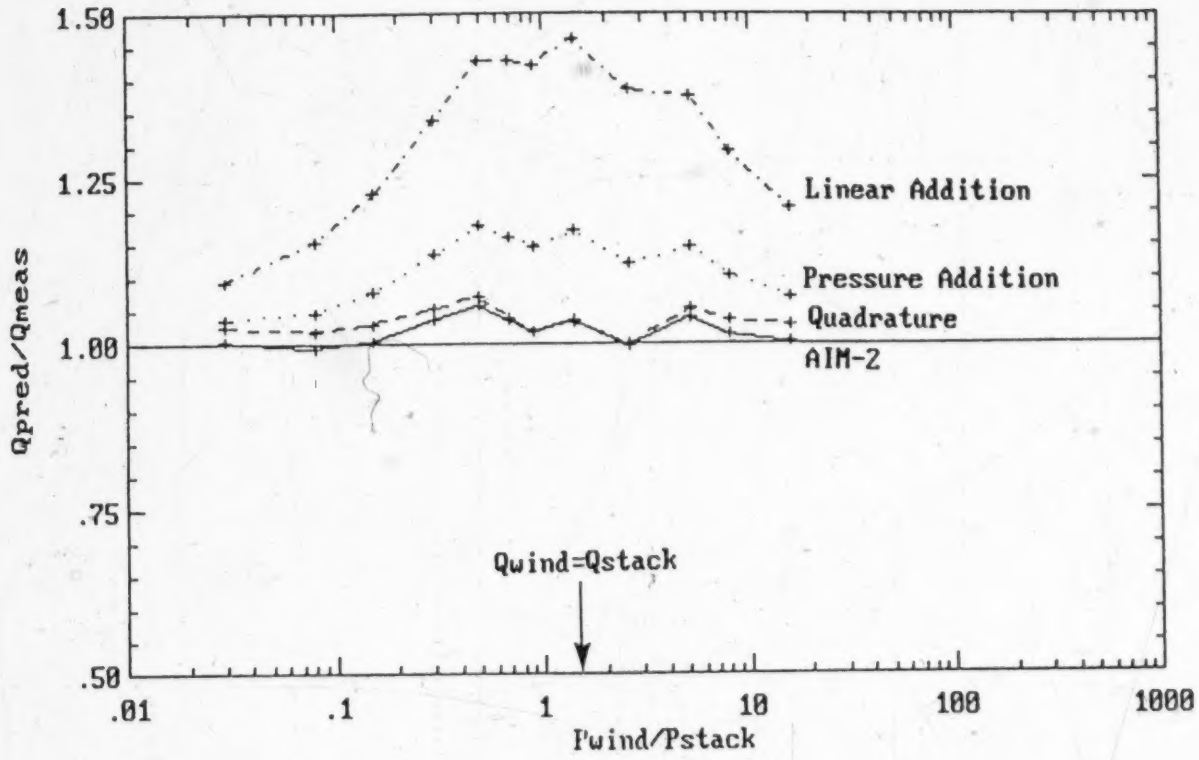

Figure 3.27: Evaluation of Superposition Methods for house#4 with about 40% of Leakage in the Flue (Using 1047 hours)

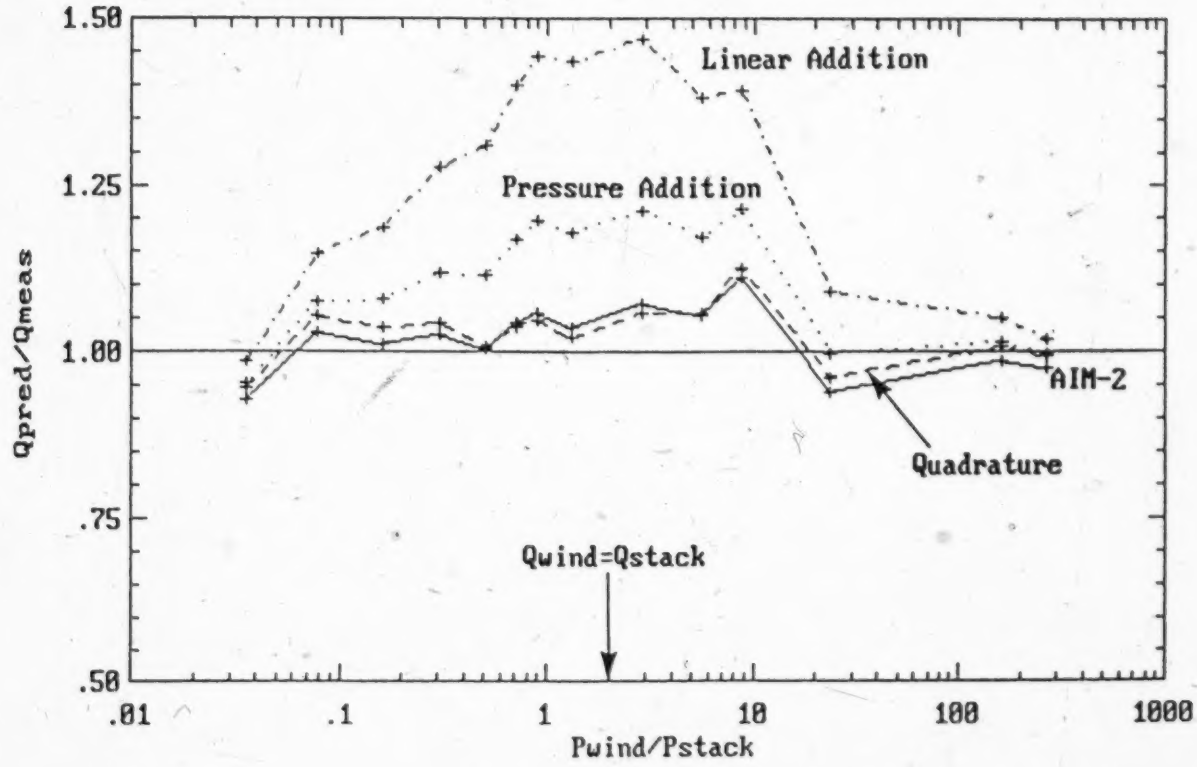

Figure 3.28: Evaluation of Superposition Methods for house#4 with Flue blocked (Using 642 hours)

Pressure addition has the same trend as flowrate addition, but the overprediction is less, 15% (0.02 ACH). Both the quadrature and interaction superposition methods reduce the overprediction to about 5% (.007 ACH), which is close to the measurement limit of the ventilation rate monitoring system (the system resolution is 0.003 ACH). Clearly quadrature and pressure addition with an interaction term (as used in EXACTAIM and AIM2) are suitable methods of superposition. They produce similar results because when $Q_s = Q_w$ equating the total flowrate in equations (3.51) and (3.54) results in $B_1 = (2^{(1/2n)} - 2)$. With $n = 0.71$ for House #4 with the flue blocked then $B_1 = -0.37$, and with $n = 0.68$ for House #4 with the flue open, $B_1 = -0.33$. These values of B_1 are close to the value $B_1 = -1/3$ chosen for AIM-2 and EXACTAIM.

Modera, Sherman and Levin (1983) found that the orifice flow LBL model overpredicted ventilation rates when the stack and wind flowrates were close to being equal. This is not a result of incorrect superposition, rather it stems from the use of orifice flow to predict Q_s and Q_w. The Q_s and Q_w are likely to be relatively low when the two effects are of the same magnitude, because the empirical f_s and f_w used in Sherman's orifice flow equations tend to overpredict low ventilation rates and underpredict high ventilation rates in order to obtain a reasonable average. This overprediction at low ventilation rates will be shown in Chapter 5 and was also noted by Modera, Sherman and Levin. Quadrature superposition is the simplest method of combining Q_s and Q_w that yields satisfactory results; however, this is purely empirical,

and it is more intellectually satisfying to use the AIM-2 method of pressure addition with an interaction term to find flowrates.

Because both Sherman's quadrature, and AIM-2 pressure addition with a correction term are empirical solutions to the problem of adding separate wind and stack effects they are not accurate in all situations. For a house with an atypical leakage distribution no simple superposition method works well. This is shown in Figure 3.29 for house #1 with an open 15 cm diameter flue, where more than three quarters of the total building leakage is in the flue. The use of the four superposition methods outlined above results in overprediction of the total ventilation rate by about a factor of three. This is a large overprediction, but the measured ventilation rate at the point of maximum error is only about 0.03 ACH, so the overprediction in terms of ACH is not as large as an error of 300% might indicate. AIM-2 and Quadrature still produce the least error, and for this reason their use is justified for any leakage distribution.

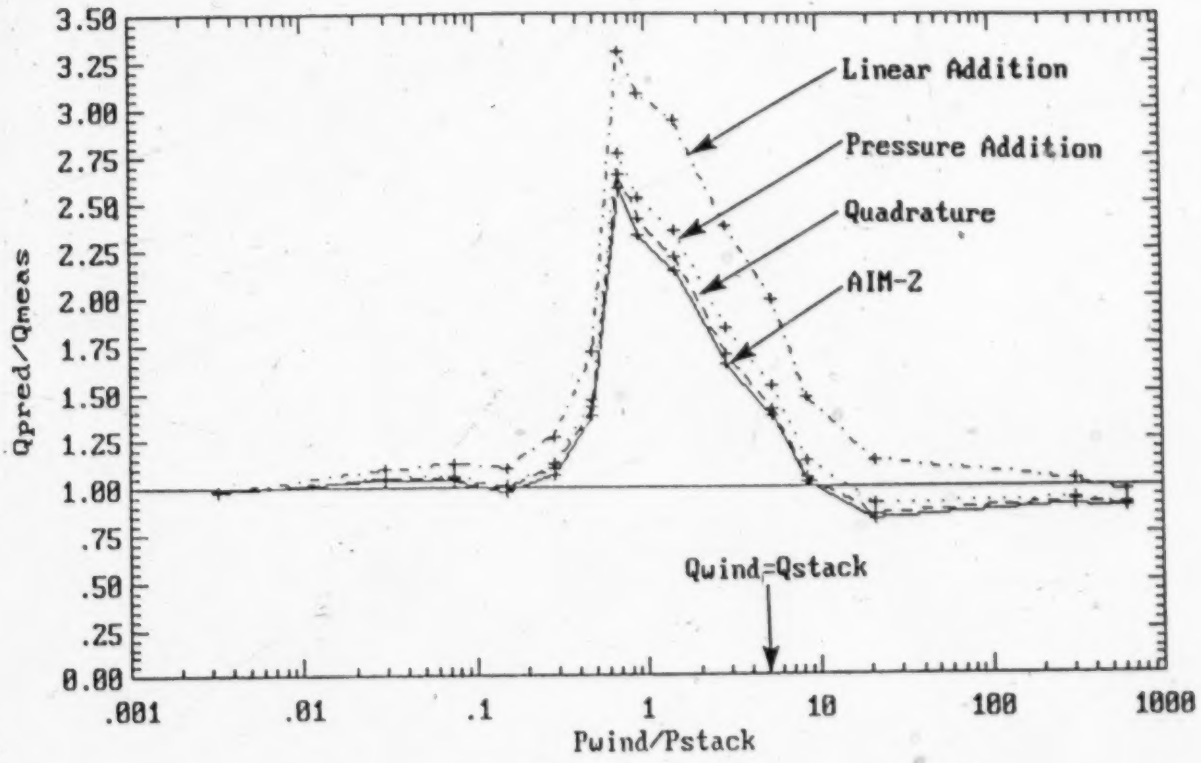

Figure 3.29: Evaluation of Superposition Methods for house#1 with about 75% of Leakage in the Flue (Using 977 hours)

3.12 Superposition of Mechanical Ventilation

In the last 10 to 15 years the trend towards saving energy has produced houses that are more and more airtight. Modern dwellings in northern climates are occasionally too airtight and experience problems of moisture control and increased indoor pollutant levels. To reduce these problems almost all new houses have kitchen and bathroom fans that remove air from these regions of high contamination and exhaust it outside the building. In Canada the trend to more airtight structures has brought about a minimum ventilation standard of 0.3 ACH (CSA Preliminary Standard F326.1-M1989 (1989)), such that new houses are extremely airtight and most of the ventilation is provided by a supply and exhaust mechanical ventilation system. Because mechanical ventilation is being increasingly used in house design, methods of superposing natural and mechanical ventilation are becoming more important.

It is difficult to formulate a simple model to superpose natural and mechanical ventilation due to the non-linear interaction between the pressures that drive the flow. A first step is simple addition of pressures which gives equation (3.59):

$$\Delta P_{total} = \Delta P_{fan} + \Delta P_{natural} \tag{3.59}$$

This results in an equation for total ventilation rate (3.60) as suggested by Shaw (1985):

$$Q_{total} = \left(Q_{fan}^{1/n} + Q_{natural}^{1/n} \right)^{n} + Q_{balanced} \tag{3.60}$$

where Q_{fan} = Flowrate through the fan, either exhaust or intake

$Q_{natural}$ = Flowrate due to stack and wind effects

$Q_{balanced}$ = Flowrate through balanced mechanical ventilation system with equal supply and exhaust rates so that the pressure distribution on the building is unaffected.

If Sherman's simple orifice flow assumption is applied, then (3.60) reduces to equation 12 in Chapter 23 of the ASHRAE handbook (1989).

Kiel and Wilson (1987) developed an equation that allows for the change in the fraction of leaks with flow into the building when unbalanced mechanical ventilation is applied. Their theoretical equation has half of the fan flowrate adding linearly, and half as pressure addition:

$$Q_{total} = \left[Q_{\frac{fan}{2}}^{1/n} + Q_{natural}^{1/n} \right]^{n} + Q_{\frac{fan}{2}} \qquad (3.60)$$

There are other more empirical models like Shaw (1985) where the wind and fan pressures add and the stack pressure is neglected, and Levin (1982) which is purely empirical.

If a model is to be used to provide only estimates of ventilation rate, then it should at least have some physical basis, and be physically realistic. For this reason, AIM-2 uses the superposition method of Kiel and Wilson. The effectiveness of this method will be examined in Chapter 5.

3.13 Summary

· Equations (3.14), (3.15), and (3.16) have been developed to determine the stack driven infiltration rate for EXACTAIM. Equations (3.45), (3.36), and (3.47) have been developed to determine the wind driven infiltration rate for EXACTAIM. These equations require iterative numerical solutions.

· Equations (3.30) and (3.48) have been developed to give estimates of stack and wind factors for AIM-2 for houses with basements or slab-on-grade construction. For a house with a crawl space a wind factor has also been developed and is given by equation (3.50). These empirical relationships approximate the exact theoretical relationships developed for EXACTAIM to within 5%. These stack and wind factors are used in equations (3.15) and (3.47) to determine the stack and wind flowrates.

· An appropriate superposition technique has been found in equation (3.54) to combine the stack and wind flowrates with a term to allow for their interaction. The value of the constant, B_1, in this equation is the only part of AIM-2 or EXACTAIM that has been found by fitting to experimental data from AHHRF. For the AHHRF houses, $B_1 = -1/3$ gives the best fit to the measured ventilation rates.

· A simple equation (3.41) has been developed that allows wind shelter to vary continuously with wind angle, and has been verified by data measured at AHHRF. This is used in conjunction with equation (3.40) which allows the furnace flue to experience different shelter from the rest of the building.

Mechanical ventilation is added to natural ventilation rates in AIM-2 using the method suggested by Kiel and Wilson, where half of the fan flow adds linearly and half is added by pressure addition.

Chapter 4

Comparison of AIM-2 with other Simple Ventilation Models

4.1 Introduction

In this chapter four simple air infiltration models are briefly outlined. They have been chosen for comparison to AIM-2 because they share some major assumptions: The house is a single well mixed zone, there are no vertical temperature gradients, and the wind pressures are spatially averaged over each surface, and are of similar complexity.

These models use theoretical relationships to find the ventilation rate as a function of the total building leakage, leakage distribution, building height, indoor-outdoor temperature difference and windspeed corrected for local shielding and terrain roughness. The separate stack and wind effects are found in terms of these general paramaters so that these models may be applied to many different stuctures. The stack and wind flows are superposed empirically to find the total ventilation rate.

4.2.1 The LBL model of Sherman

The LBL model is described in many publications from Lawrence Berkeley Laboratories (LBL). The derivation outlined here is taken from Sherman and Grimsrud (1980). The main assumptions are:

- The use of orifice flow to describe the pressure-flow relationship for the building envelope. For most buildings $n \neq 0.5$ in $Q = C\Delta P^n$. This effect is dealt with by matching

flowrates at a reference pressure (usually 4 or 10 Pa) and defining an effective leakage area at this reference pressure.

- The air in the building is a single well mixed zone, which implies no vertical temperature gradients.
- The volume of air leaving the building is the same as the volume of air entering the building. This is valid when $\Delta T/T_{in}$ is small ($\rho_{out} - \rho_{in}$). Both the inside volume and mass are conserved because T_{in} is constant.
- The leakage in the walls, at floor or at ceiling level is evenly distributed over that particular section of the building envelope. In addition, each of the 4 walls has the same leakage.
- The wind shielding effects are averaged over each surface.
- The floor is over a crawl space, and both the floor and the ceiling have zero external pressure coefficient for wind effects. This does not imply that there is no pressure differential across the floor or ceiling due to wind effects because the internal pressure required to make the infiltration and exfiltration equal still acts across these leakage sites.
- The pressure generated by the wind is uniform over each surface.
- The leakage of the flue is placed in the ceiling.

The resulting equations for predicting ventilation rates are as follows:

The leakage characteristics, C and n, from a fan pressurization test are used to find the Effective Leakage Area (A_o) at a reference pressure of ΔP_{ref} = 4 Pa, and equations (1.3) and (2.6) are equated at this reference pressure to yield:

$$A_o = KA \frac{4^n C}{\left(\frac{8}{\rho}\right)^{0.5}} \tag{4.1}$$

The wind and stack flowrates are calculated separately. The stack factor, f_s is found using equation I.17.2 in Sherman and Grimsrud (1980):

$$f_s = \frac{\left(1 + \frac{R}{2}\right)}{3} \left[1 - \frac{X^2}{(2-R)^2}\right]^{\frac{3}{2}} \tag{4.2}$$

and from I.15.2 in this reference,

$$Q_{stack} = A_o f_s \left[g \frac{H \Delta T}{T_{in}} \right]^{\frac{1}{2}} \tag{4.3}$$

The equation for f_s is an empirical approximation to the exact relationship between f_s, R and X that is set by the exact equations (3.24) and (3.25). R and X are the same as for AIM-2 except that the flue leakage is not treated separately, and is included in the ceiling leakage instead.

The wind factor, f_w, is an approximation to an exact relationship between R, X, and the external pressure coefficients such that flow in is equal to flow out. Using Akins pressure coefficient data, and introducing a coefficient, C', that accounts for local shelter, Sherman

and Grimsrud used the approximation:

$$f_w = C' (1-R)^{1/3} \qquad (4.4)$$

which they use in:

$$Q_{wind} = A_o f_w U' \qquad (4.5)$$

Where U' is the reduced windspeed accounting for change in height from the meteorological station to the building ceiling and terrain between the weather data measurement site and the building.

To combine Q_{stack} and Q_{wind}, the LBL model assumes that the flows may be added in quadrature. This is pressure addition for orifice flow, where $Q \propto \Delta P^{0.5}$:

$$Q_{total} = (Q_{stack}^2 + Q_{wind}^2)^{1/2} \qquad (4.5)$$

4.2.2 Variable n model

The purpose of this model is to adapt the theory and equations of the LBL model to remove the orifice flow assumption. The pressure-flow relationship is described in more general terms by C and n, from the results of fan pressurisation testing. As with the other models the same n will be applied to all the building leaks. This adaptation was first attempted by Yuill (1985) using the same assumptions (except non-orifice flow) as the LBL model. This work was continued in the Variable Flow Exponent (VFE) models in Reardon (1989). The variable n model outlined here uses some of the ideas developed elsewhere, but was specifically developed for this study.

For wind driven flowrate, Q_{wind} from LBL can be written:

$$Q_{wind} = A_o(1-R)^{1/3}((C'U)^2)^{1/2} \quad (4.6)$$

To remove the orifice flow assumption the 1/2 power is replaced by n, and the following relationship is used to replace A_o:

$$A_o = C\,(\rho_{in}/2)^{1/2}\,\Delta P_{ref}^{(n - 1/2)} \quad (4.7)$$

Substituting (4.7) in (4.6):

$$Q_{wind} = C\,(\rho_{in}/2)^{1/2}\,\Delta P_{ref}^{(n - 1/2)}\,(1 - R)^{1/3}\,C'^{2n}\,U^{2n} \quad (4.8)$$

Note that C' and $(1 - R)^{1/3}$ were found by Sherman for the LBL model and still have hidden assumptions of orifice flow. These assumptions can only be removed by developing these relationships from first principles, the method used in EXACTAIM and AIM-2 in chapter 3. The reference pressure, ΔP_{ref}, for determining leakage area used in the LBL model is 4 Pa, thus (4.8) becomes:

$$Q_{wind} = C\,\rho^{1/2}\,2^{(2n - 3/2)}\,(1 - R)^{1/3}\,C'^{2n}\,U^{2n} \quad (4.9)$$

The major difference between this adaptation and that of Yuill's model and Reardon's Variable Flow Exponent (VFE) models is that density, ρ, appears here in the conversion of leakage area, A_o, to flow coefficient, C. It appears in Yuill's model and the VFE models in the pressure term. In both Yuill's model and Sherman's LBL model it was assumed that in S.I. units ρ = 1 Kg/m^3, and thus the density was neglected. The variable n model developed here and the VFE models include density explicitly, but in the VFE models density has the exponent n rather than an exponent of 1/2 as in (4.9). Assuming ρ=1

makes this variable n model the same as Yuill's model and the VFE models. However, all of these variable n models have incorrect units as a consequence of adapting the existing LBL equations rather than developing relationships from first principles as in EXACTAIM and AIM-2 in chapter 3. This results in errors of small magnitude (less than 5% for typical values of ρ) but vast implications in a scientific sence.

Neglecting density using S.I. units results in small errors, however; in American (ft, lbf, seconds), or other units, the density of air does not have a magnitude close to unity and attempting to use these equations in other systems will generate large errors. In a dimensionally consistent model like EXACTAIM or AIM-2 these problems do not arise if the variables in the model are expressed in any dynamically consistent units, such as ft, lbf, slug, and seconds.

Assuming $\rho_{in} = 1$ Kg/m^3 in equation (4.9) results in a relationship with the same form as the LBL model. The difference is that (4.9) varies with windspeed to the 2n power and the LBL model is linear with windspeed. Equation (4.9) predicts the same value for ventilation rate as the LBL model when $C'U = (C'U)^{2n}$. This occurs when $C'U = 1$. Using the values of C' from Sherman and Grimsrud (1980) it can be shown that the two models predict the same ventilation rates at a windspeed of about 3 m/s for an unsheltered building and about 10 m/s for a heavily sheltered building.

Q_{stack} is found using the same equation as AIM-2:

$$Q_{stack} = C\, f_s\, (\rho\, g\, H\, \Delta T/Tin)^n \qquad (4.10)$$

Where equation (3.22) that relates leakage distribution parameters such that the flow in and out are equal is used to find the neutral level by numerical solution, given R, X, and n (as suggested by Yuill). This value of the neutral level is then used in equation (3.23) to find f_s. Equations (3.22) and (3.23) are found using the same assumptions as the LBL model for leakage distribution. The flowrates, Q_{stack} and Q_{wind}, are combined in quadrature as in the LBL model (See equation (4.5)), to find the total ventilation rate.

4.2.3 Warren and Webb's model

Warren and Webb (1980) give a detailed explanation of their model and its derivation. The main assumptions are:

- The total leakage is distributed uniformly over the building's exterior surface. There are no parameters like R and X governing the distribution of the leakage.
- The building is a single well mixed zone.
- All leaks are similar, and have the same characteristic exponent, n.
- The pressure generated by the wind is uniform over each surface.
- The floor is assumed to be impermeable, except if the underfloor space is ventilated (as a crawlspace) then the surface pressure is assumed to be the mean of the pressures on the 4 walls, as developed independantly in EXACTAIM and

AIM-2. As with the LBL model, floor level leakage is assumed to be evenly distributed over the entire floor area for a crawlspace.

Warren and Webb use the flowrate through the building envelope, Q_T, at a reference pressure, ΔP_T of 50 Pascals to describe the total building leakage, where C and n are found from fan pressurization testing. Such that:

$$Q_T = C\ (\Delta P_T)^n \tag{4.11}$$

where ΔP_T = 50 Pa.

The flowrate due to stack effect is given by Equation 6 in Warren and Webb:

$$Q_{stack} = Q_T \left(\frac{\rho_{out} g\ H\ \Delta T}{\Delta P_T \quad T_{in}} \right)^n F_B \tag{4.12}$$

Where F_B is the same as the stack factor, f_s, in EXACTAIM, with no flue (Y = 0), R = 0.25, X = 0.25, and r = 1. The values of R and X were found using the building dimensions given in Warren and Webb (1980), and using their assumptions about leakage distribution.

The flowrate due to wind effect is given by equation 5 from Warren and Webb:

$$Q_{wind} = Q_T \left(\frac{\rho_{out}\ U^2}{\Delta P_T} \right)^n F_W \tag{4.13}$$

F_W is the same as the wind factor, f_w, in EXACTAIM with no flue and the same leakage distribution as for stack factor. It uses pressure coefficients from the British Standard Code (1972) dealing

with wind loads, and is also funtion of wind direction, θ.

The total ventilation rate is given by equation 3 from Warren and Webb:

$$Q_{total} = Q_T \left(\frac{\rho_{out} U^2}{\Delta P_T} \right)^n F_v \qquad (4.14)$$

where

$$F_v = \left(\left(F_B A_r^n \right)^2 + F_W^2 \right)^{1/2}$$

and

$$A_r = \frac{\Delta T \, g \, H}{T_{in} U^2}$$

A_r is a parameter representing the ratio of the stack to wind driving forces.

It can be shown that the method of combining the stack and wind factors F_B and F_W in equation 4.14 is the same as adding the flows Q_{stack} and Q_{wind} in quadrature. Values of F_B and F_W were calculated by Warren and Webb for three different house types: detached, semi-detached, and terraced (row houses); three values of n: 0.5, 0.6, and 0.7; and with and without a permeable floor. The results are presented as discrete values in tables, unlike AIM-2 and the LBL model, where stack and wind factors are continuous functions of the various parameters.

4.3.1 Shaw's Semi-Empirical NRC model

Shaw's (1985) model developed at the National Research Council of Canada does not use approximations to solutions of theoretical relationships to find Q_{stack} and Q_{wind}. It uses the same $Q = C\Delta P^n$ relationship between flowrate and pressure difference as AIM-2 and the

variable n model, but the total average pressure driving the flow through the building envelope is found by fitting empirical coefficients to measured data, rather than by deriving theoretical equations for f_s and f_w. Some inconsistencies in the derivation were corrected by Reardon (1989).

The stack induced ventilation rate is given by:

$$Q_{stack} = D_{Shaw} \frac{(1000)}{(3600)} C \beta_o (\Delta T)^n \qquad (4.15)$$

where: β_o is the ratio of the neutral level height, h_o, to the ceiling height, H.

D_{Shaw} is a constant of dimensions: $(m^3 s\ Pa^n)/(Litres\ Hours\ \Delta T^n)$

$D_{Shaw} = 0.5$ as found by Shaw by fitting to measured data

(1000)/(3600) converts this equation to have Q_{stack} in m^3/s

A tracer gas decay method was used in a single house in Ontario (Shaw and Brown (1982)), to determine appropriate values of h/H and D_{Shaw} by fitting to the experimental data. For houses with a flue, Shaw recommends using $\beta_o = 0.86$, and with no flue $\beta_o = 0.64$, and for all houses $D_{Shaw} = 0.5$ $(m^3 s\ Pa^n)/(Litres\ Hours\ \Delta T^n)$. Note that D_{Shaw} has dimensions and will have a different value if different units are used.

The wind induced ventilation rate is given for both shielded and exposed sites. From equation 6 in Shaw (1985), where the windspeed, U, is that at a height of 20m:

$$Q_{wind} = 0.4\ C \frac{(1000)}{(3600)} U^{2n} \qquad \text{Unsheltered} \qquad (4.16)$$

$$Q_{wind} = 0.7\ C \frac{(1000)}{(3600)} U^{n} \qquad \text{Sheltered} \qquad (4.17)$$

The constant 0.4 has units of $(Pa^n m^3 s^{2n+1})/(\text{Litres Hours } m^{2n})$, and 0.7 has units of $(Pa^n m^3 s^{n+1})/(\text{Litres Hours } m^n)$. These constants and the power for windspeed, U, are determined by a fit to measured data. The problems arising from the use of these equations are that at low windspeeds a shielded building has more wind induced ventilation than an exposed one. This error is probably the result of fitting an equation for wind effect only to data containing significant stack effect (ΔT up 20°C). Also very few data points were used to determine the above relationships, ten points for the exposed case, and only five for the shielded case. With the great deal of scatter present in ventilation rate measurements, this is an insufficient number of data points. Because all the fitted constants have dimensions Shaw's equations can only be used in S.I. units.

To combine the stack and wind driven flowrates, Shaw uses the method of adding pressures with a multiplicative interaction factor, F',

$$Q_{total} = F' \left[Q_{stack}^{(1/n)} + Q_{wind}^{(1/n)} \right]^n \qquad (4.17)$$

F' accounts for the interaction between stack and wind effects. From equation 10 in Shaw (1985):

$$F' = 1 \qquad \text{for } 0 \leq (Qsml/Qlrg) < 0.1$$

$$F' = 0.8\ (Qsml/Qlrg)^{-0.1} \qquad \text{for } 0.1 \leq (Qsml/Qlrg) \leq 1$$

where: Qsml is the smaller value of Q_{stack} or Q_{wind}

Qlrg is the larger value of Q_{stack} or Q_{wind}

These values for F' were determined empirically using ventilation

rates measured in 3 houses, 2 without flues, and one with a flue, and are for application to all houses.

4.4 Summary

The four ventilation models outlined in this chapter are representative of the current state of the art in simple ventilation models. In the next chapter their predictions will be compared to those of AIM-2, and to measured ventilation rates. The models differ by having coefficients determined from different experimental data sets. The LBL model and the Variable n model use wind tunnel pressure coefficient data measured in the U.S.A. by Akins (1979). Warren and Webb's model uses pressure coefficient data from the British Standard Code (1972) for wind loads on buildings, and was verified by comparison to data measured in British houses. Shaw's coefficients are fitted to field data measured in Canada.

Chapter 5

Model Evaluation

5.1 Introduction

In this chapter AIM-2 and the other four models will be compared to measured data from the Alberta Home Heating Rsearch Facility. EXACTAIM requires numerical iterative solution, and is very close to it's fitted f_s and f_w sister AIM-2, and so was not evaluated. Wind speed and temperature difference dependance will be examined, as well as the models' ability to predict changes in ventilation rate when the leakage distribution changes between the walls ceiling and floor. The change in leakage distribution will be an open or closed furnace flue as well as two houses with different window sizes and locations. The predictions of AIM-2 will be compared to hourly measured ventilation rates over 24 hour periods to examine its ability to track hour by hour ventilation rate changes. This is in contrast to the average ventilation rates over several months that are used to evaluate the windspeed and temperature difference dependancies. In addition, the ability of AIM-2 to superpose natural and mechanical ventilation is examined.

5.2 Outline of Evaluation Procedure

The performance of AIM-2 is evaluated by comparing the ventilation rates predicted by the model to data measured at AHHRF. Four other models will also be compared to the measured data, they are:

- The LBL model (U.S.A.) (Sherman and Grimsrud (1980))
- Variable n extension of the LBL model (Canada) from Yuill (1985))

- The NRC model of Shaw (Canada) (Shaw (1983))
- Warren and Webb's model (England) (Warren and Webb(1980))

These models are described in detail in Chapter 4. There are many other ventilation models, but these were chosen because they are simple single zone models and are of similar complexity to AIM-2. The models are compared by testing their ability to predict wind and stack dominated ventilation rates separately. The effects of different superposition methods are covered in Chapter 3. The effect of additional mechanical ventilation has been studied for AIM-2 only, where quadrature addition and the semi-empirical pressure addition with an interaction term performed best.

There are uncertainties in the ventilation rate measured by the tracer gas system due to roundoff in the number of injections made per hour, the volume of tracer gas released per injection, and in the calculation of the mean hourly concentration. An estimate of typical values of error from Wilson and Dale (1985) is that 95% of the data will fall within ± 5% ± 0.004 ACH, and the system resolution is approximately 0.003 ACH, as can be seen in Figure 5.1.

The ability of the models to predict average hourly ventilation rates for given weather conditions and specified mechanical ventilation flowrate is shown by their bias and scatter compared to the measured data. The measured data is sorted into bins covering 5°C temperature difference and 1 m/s windspeed ranges. The average weather conditions for each bin are used as the input values to the models and the model predictions for a given bin are compared to the average ventilation rate for the measured data in the bin. In the data sorted for high

windspeed the average temperature difference is calculated for each bin and also used in the model predictions, and in the data sorted for high temperature difference the average windspeed is calculated for each bin and used in the model predictions.

The bias and scatter can be expressed as a ratio (%) or in ACH. The %bias is the average ratio of predicted to measured values for all the bins, where:

$$\lambda = \frac{\sum_{i=1}^{j} \frac{Q_{predicted}}{Q_{measured}}}{j} \qquad (5.1)$$

where j is the number of bins, and

$$Bias = 100(1 - \lambda) \qquad (5.2)$$

The ACH bias is the average difference in ACH averaged over all the bins:

$$\text{ACH bias} = \frac{\sum_{i=1}^{j} (Q_{predicted} - Q_{measured})}{j} \qquad (5.3)$$

The bias indicates the average error that would be obtained over a long time period if each bin of windspeed or temperature difference were equally likely to occur. This neglects the probability distribution that describes the likelihood of each windspeed or temperature difference occurring. This probability distribution varies depending on geographical location and terrain, and has been neglected here.

The scatter is the variation in the predicted versus measured averages from bin to bin of ΔT and U, and is an indicator of how well the models follow trends in the data if the bias is removed. This bias can be thought of as the error in proportionality constants, and the scatter is the error in the functional form.

$$\text{scatter} = \frac{100 \sum_{i=1}^{j} \frac{((\text{Qpredicted}/\lambda - \text{Qmeasured})}{\text{Qmeasured}}}{j} \qquad (5.4)$$

$$\text{ACH scatter} = \frac{\sum_{i=1}^{j} (\text{Qpredicted}/\lambda - \text{Qmeasured})}{j} \qquad (5.5)$$

Table 5.1 gives details of the infiltration data sets measured at AHHRF used to validate the simple ventilation models.

5.3 Windspeed Dependence

The models are compared to data taken in House #4 with the flue blocked and in House #5 with an open 15cm diameter flue. All the models use the same C and n derived from blower tests performed in each house, but the leakage distribution must be estimated. For House #4 it is estimated that 50% of the leakage is evenly distributed among the 4 walls, with 25% of the leakage at floor level, and the remaining 25% at ceiling level. For House #5, 60% of the leakage is in the flue, approximately 2/3 of the remaining leakage (30%) is equally distributed

Table 5.1 Details of Infiltration data sets used to Validate Simple Ventilation Models

Data File Name	House	Data Set	Dates YYMMDDHH	# hours in figure	Figure#
NEXT5&12	4	Flue Blocked Sheltered n = 0.7	86042415-86082908	464	5.1 5.2 5.4
NEXT2&7	4	Flue Blocked Unsheltered n = 0.7	86042415-86082908	285	5.3
NEXT4&8	5	15 cm Flue Open Unsheltered n = 0.58	86050101-86082908	279	5.5
NEXT6&13	5	15 cm Flue Open Sheltered n = 0.58	86050101-86082908	461	5.6
TBIN10	4	7.5 cm dia. Orifice in Flue Lo Wind n = 0.66	86092509-87023124	102	5.7
TBIN11	5	Flue Blocked Low Wind n = 0.65	87010101-87023124	74	5.8

among the 4 walls, with 1/6 of the remaining leakage (5%) at ceiling height and the same amount of leakage at floor level. The corresponding values of R, X and Y are shown in Table 5.2, together with the leakage characteristics, C and n, found from fan pressurization tests. The flue height is 5m for all houses at AHHRF. Both houses are typical of modern (post 1970) Canadian wood frame housing. R and X for the LBL and Variable n models include Y in the ceiling and are not the same as R and X for AIM-2. R and X for these models can be found by adding Y to each value of R and X.

The measured data for analysing windspeed dependence was sorted for indoor-outdoor temperature differences of less than 10°C, and binned every 1 m/s. Additionally, the data was sorted by wind direction to reduce the scatter due to differences in shielding. The houses are in the middle of a row of six test houses. The row runs East-West, thus the houses are sheltered from winds from these directions. From the North and South the houses are unsheltered. For unshielded wind driven ventilation rates the data was sorted into bins for winds ± 22.5 degrees from North and ± 22.5 degrees from South. To examine shielded ventilation rates the data was sorted into bins for winds ± 22.5 degrees from East and ± 22.5 degrees from West. For House #4 this sorting procedure reduced a total of 2642 hours of data to 285 hours for North and South winds and 464 hours for East and West winds. Similarly, in House #5 a total of 2554 hours of data was reduced to 279 hours for North and South winds and 461 hours for East and West winds.

As shown in Chapter 3 the leakage distribution can change the ventilation rate by a factor of two. Because all the models assume

Table 5.2 Details of Building Leakage used to evaluate Simple Ventilation Models

House	C	n	R	X	Y	Fig.#
4, Flue Blocked	0.007	0.7	0.5	0	0	5.3 5.4
5, 15cm diameter Flue Open	0.020	0.58	0.1	0	0.6	5.5 5.6
4, 7.5cm diameter Orifice in Flue	0.010	0.66	0.3	0	0.4	5.7
5, Flue Blocked	0.009	0.65	0.33	0	0	5.8
2, 15cm diameter Flue Open, with Mechanical Ventilation	0.020	0.64	0.25	0	0.6	5.12 5.13 5.14
4, 7.5cm diameter Orifice in Flue	0.010	0.66	0	0	0.4	5.9
4, 7.5cm diameter Orifice in Flue	0.010	0.66	0.2	-0.1	0.4	5.10
4, 7.5cm diameter Orifice in Flue	0.010	0.66	0.4	0.2	0.4	5.11

* - The Value of C in this table is from the results of Fan Pressurization Testing and is for Flowrates in m^3/s

that wall leakage is evenly distributed among the 4 walls they tend to underpredict ventilation rates for winds impinging on the leakier walls, and overpredict ventilation rates if the wind impinges on a less leaky wall. To remove this dependance on wall leakage distribution and to remove any bias due to different quantities of data for the different wind directions the data was first sorted in separate North, South, East and West bins. The average ventilation rate and the standard deviation for each bin was calculated separately for North, South, East and West winds. The unsheltered data for a bin was combined by averaging the average ventilation rate and standard deviation from the separate North and South calculations. The sheltered data for a bin is combined by averaging the average ventilation rate and standard deviation from the separate East and West calculations. The error bars in each figure represent ± one standard deviation for all the data in the bin. Even with this data that has been sorted the standard deviation for each bin is still significant, as can be seen in the figures in this chapter. Standard deviations of 20% or more are seen in these data sets despite all of the sorting. This implies that hourly averaged windspeed, wind direction, and temperature cannot be used to predict the ventilation rate for a given hour, but can only be used to predict the average ventilation rate for those meteorological conditions.

Each model uses a different method of introducing shelter effects. For AIM-2, $S_w = 1.0$ was used for unsheltered conditions, and $S_w = 0.5$ was used for the sheltered case, based on examination of the data shown in Chapter 3. In AIM-2 the shelter coefficient S_w appears

directly as a windspeed multiplyer, and is the ratio of an effective sheltered windspeed, $U_{sheltered}$ to the unsheltered windspeed, $U_{unsheltered}$. An equivalent value of S_w may be found for each model using (5.6).

$$S_w = \frac{U_{sheltered}}{U_{unsheltered}} = \left[\frac{Q_{sheltered}}{Q_{unsheltered}} \right]^{\frac{1}{2n}} \qquad (5.6)$$

Substituting the appropriate equations for flowrate, with their different shelter coefficients, and assuming a typical value of n = 2/3, values of effective S_w can be found for each model. These values of effective S_w for each model are summarised in Table 5.3, and range from 0.32 for the LBL model to 1.5 for Shaw's model at U = 1 m/s.

5.3.1 Sheltered Conditions

Figure 5.1 shows data for House #4 for combined East and West winds. The unbinned data illustrates how much data has been averaged in the figures in this chapter (in this case 464 points), and how much scatter is present in the measured data, even for this specifically sorted data set. It is this large variability in ventilation rate for similar weather conditions and wind direction that makes accurate hourly predictions of ventilation rate very difficult. The models examined here are most useful for predicting ventilation rates averaged over a range of wind directions for a given set of U and ΔT conditions, which is why they are compared to binned data as shown in Figure 5.2. With the binned data it is easier to see the trends in the measured data, and how well the models fit the data. The effect of finite injector size on the resolution of the tracer gas measurement system

Table 5.3 Equivalent Shelter Coefficients for simple ventilation models for East and West winds

Model	Wall Shelter Coefficient,Sw	Flue Shelter Coefficient,Swf
AIM-2	0.5	1.0
Variable n	0.32	0.32
LBL	0.32	0.32
Warren and Webb	0.70	0.70
Shaw U=1 m/s	1.5	1.5
Shaw U=5 m/s	0.5	0.5

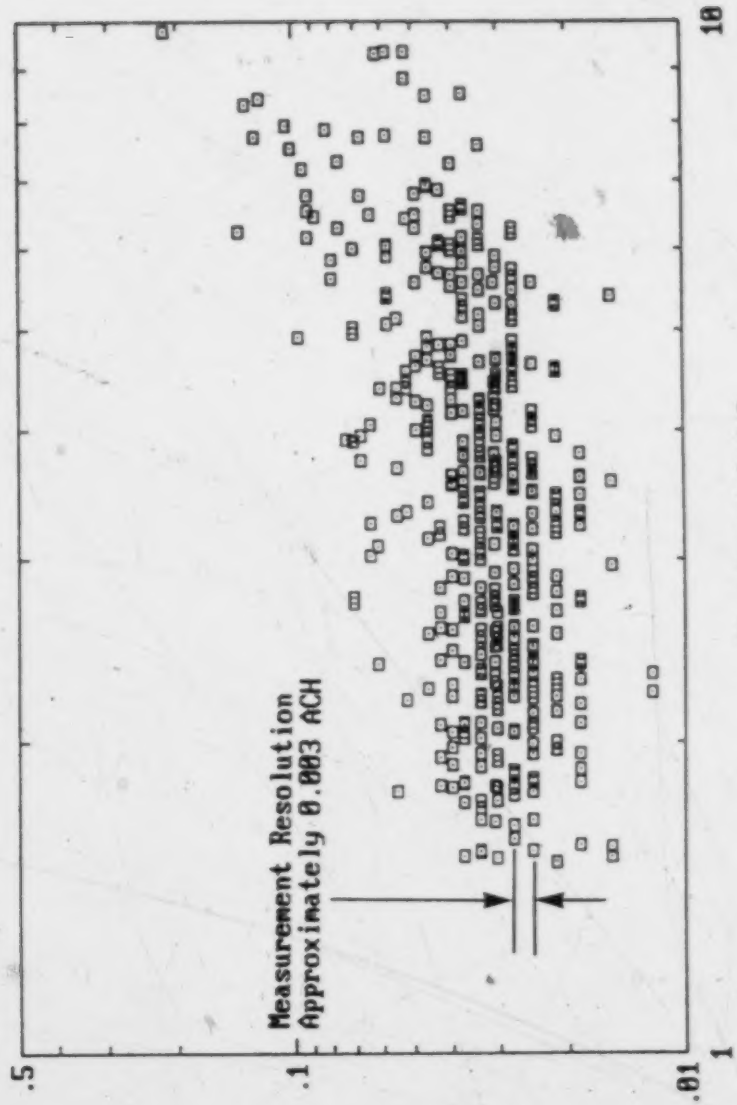

Figure 5.1: Unbinned measured ventilation rates for House #4 with blocked flue, shielded, with $\Delta T \leq 10°C$ and $U \geq 1.5$ m/s (464 hours)

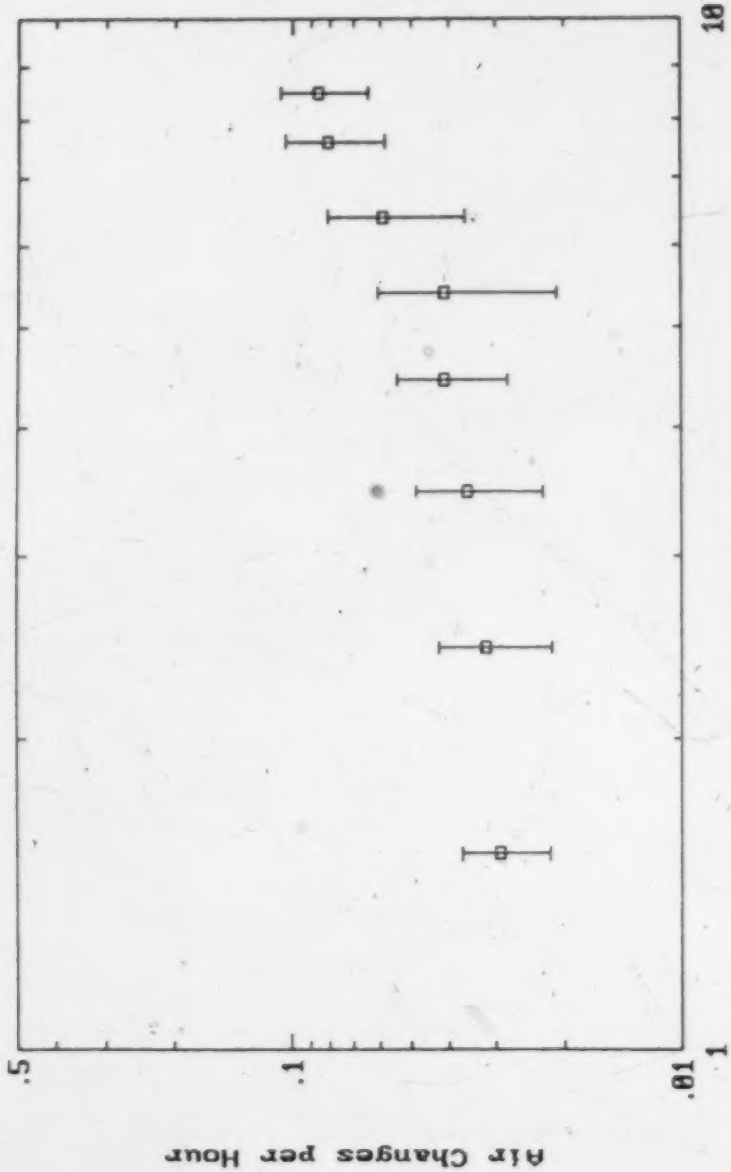

Figure 5.2: Binned measured ventilation rates for House #4 with blocked flue, shielded, with $\Delta T \leq 10°C$ and $U \geq 1.5$ m/s (464 hours)

can be clearly seen in the unbinned data of Figure 5.1, with step changes in Air Changes per Hour at low ventilation rates. The resolution of the ventilation measurement system has been estimated by Wilson and Dale to be approximately 0.003 ACH, and this is the same as the resolution observed in this figure.

Figure 5.3 is for the same House, #4, shielded from the wind (East and West winds). This is the same data as in Figures 5.1 and 5.2, but with the model predictions added. Warren and Webb's and Shaw's models overpredict significantly. This is because the shielded wind factor for these models is based on an empirical fit to data for houses experiencing different shelter from those in this study. In Warren and Webb's model they examined English row houses to determine shelter effects. Although somwhat obscured by the weak windspeed dependance of the measured data, both LBL and Shaw have the wrong slope (as can be seen in a log-log plot), indicating that they do not raise windspeed to the correct power. In Shaw's model this is probably the result of a curve fit to a measured data set contaminated by ΔT effects.

For House #5 with an open unsheltered 15 cm diameter flue, and with the rest of the house shielded from the wind the data (for East and West winds), shown in Figure 5.4, shows that sheltering the house has little effect if there is a large unshielded flue. Once again all of the models underpredict, but AIM-2 is clearly better because its shielding coefficient allows the flue to remain unshielded

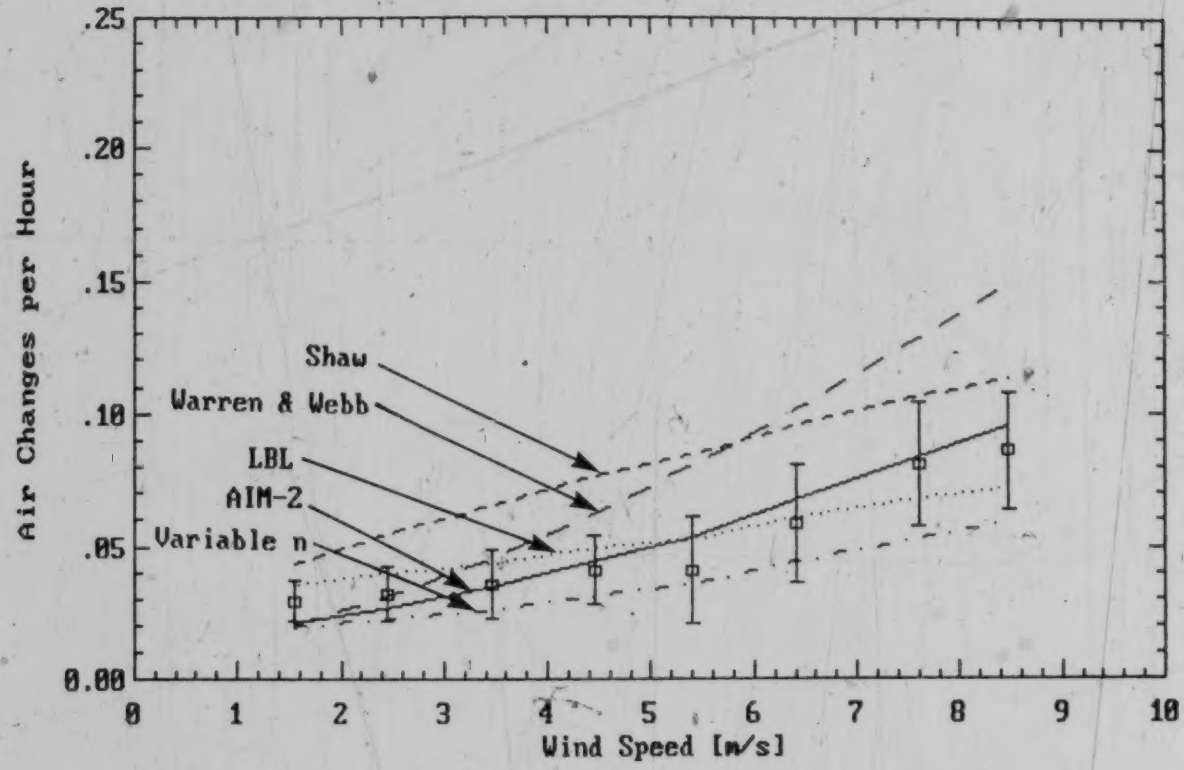

Figure 5.3: Comparison of Ventilation Models with measured data for Shielded Windspeed dependance (East and West Winds) in house #4 with blocked flue and $\Delta T \leq 10°C$ and $U \geq 1.5$ m/s (464 hours)

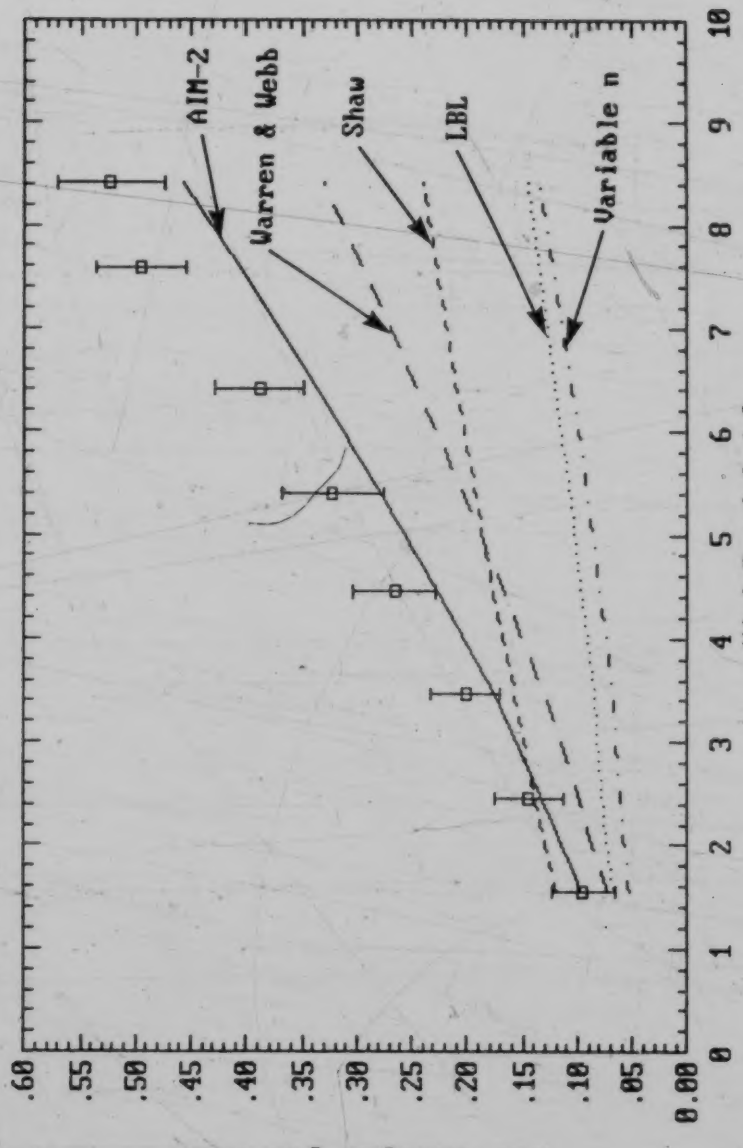

Figure 5.4: Comparison of Ventilation Models with measured data for Shielded Windspeed dependance (East and West Winds) in House #5 with an open 15cm diameter flue with $\Delta T \leq 10^{\circ}C$ and $U \geq 1.5$ m/s (461 hours)

5.3.2 Unsheltered Conditions

For House #4 with no flue and unshielded (North and South winds), Figure 5.5 shows that the LBL model has an incorrect dependance on varying windspeed (the wrong slope) when compared to the other models. This is due to the orifice flow assumption forcing n = 1/2. Here the ventilation rates are clearly much greater than in Figure 5.3, because there is no sheltering effect from the adjacent houses. Shaw's model overpredicts the most because its constants are fitted to data measured in different houses. The variable n model overpredicts consistently, possibly because the wind factor for this model is the same as that for the LBL model and contains the hidden assumption of orifice flow.

For House #5 with an open unsheltered 15 cm diameter flue, and with the rest of the house unshielded from the wind, the model predictions are compared to the measured data in Figure 5.6 (for North and South winds). All of the models underpredict for the case of this unusual leakage distribution, where 60% of the total leakage is in the flue. Even though Shaw's model overpredicts the most for House #4 with the flue blocked, it underpredicts here more than AIM-2, showing that allowing the flue to be treated as a separate leak in AIM-2 is very significant.

The scatter and bias for each model for shielded and unshielded buildings are presented in Tables 5.4 and 5.5 respectively, which show that AIM-2 is the best of the models, for the variations in ventilation rate studied here. In these tables, the % errors are the average of the % errors in each bin and the ACH errors are the average ACH error for each bin so that models with the same % error may not have the same

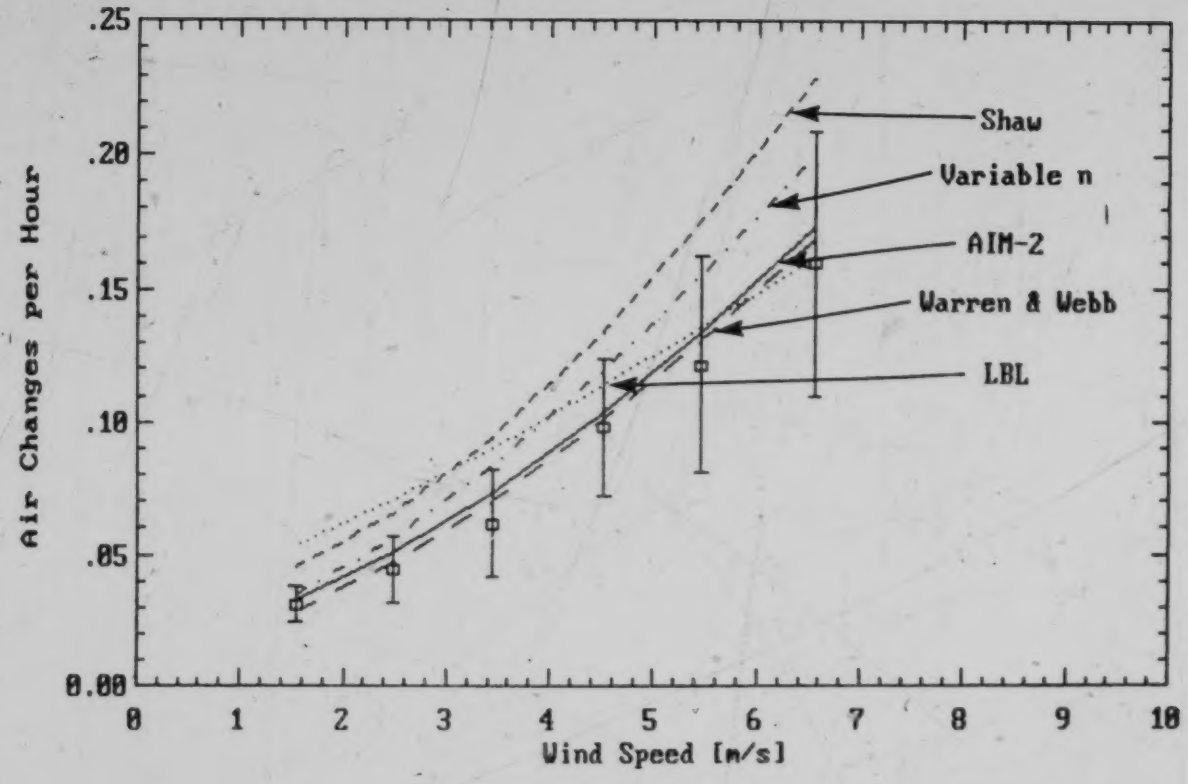

Figure 5.5: Comparison of Ventilation Models with measured data for Unshielded Windspeed dependance (North and South Winds) in House #4 with blocked flue, and $\Delta T \leq 10°C$ and $U \geq 1.5$ m/s (285 hours)

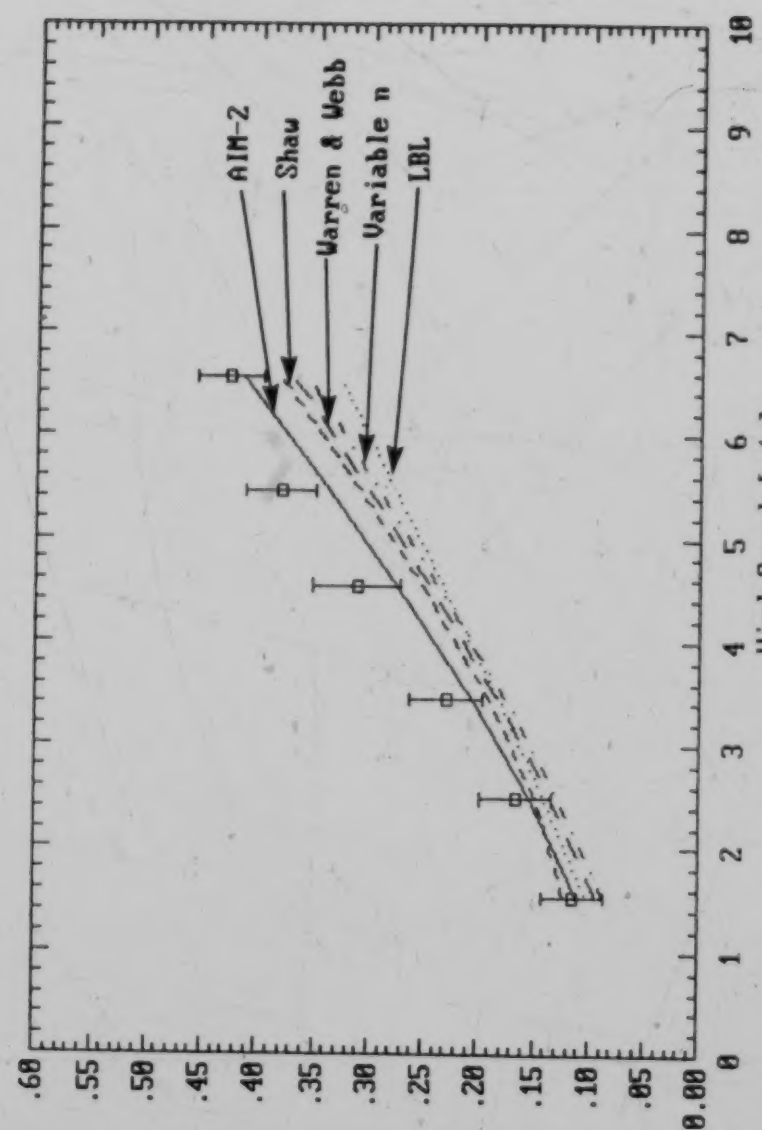

Figure 5.6: Comparison of Ventilation Models with measured data for Unshielded Windspeed dependance (North and South Winds) in House #5 with an open 15cm diameter flue with $\Delta T \leq 10^{\circ}C$ and $U \geq 1.5$ m/s (279 hours)

Table 5.4 Model Errors for Binned Averages of Wind Dominated Ventilation for Sheltered Buildings at AHHRF

	House #4 Flue Closed		House #5 15 cm Flue Open	
Model	Bias	Scatter	Bias	Scatter
AIM-2	2% (0.003)	14% (0.006)	-12% (-0.041)	4% (0.011)
LBL (Sherman)	11% (0.002)	14% (0.008)	-60% (-0.199)	28% (0.078)
Variable n (Yuill)	-27% (-0.014)	7% (0.004)	-66% (-0.215)	23% (0.063)
Shaw	65% (0.030)	13% (0.007)	-29% (-0.122)	30% (0.084)
Warren and Webb\	43% (0.027)	24% (0.011)	-35% (-0.112)	6% (0.014)

* - Values in brackets are in Air Changes per Hour, ACH.

Table 5.5 Model Errors for Binned Averages of Wind Dominated Ventilation for Unsheltered Buildings at AHHRF

	House #4 Flue Closed		House #5 15 cm Flue Open	
Model	Bias	Scatter	Bias	Scatter
AIM-2	10% (0.008)	3% (0.002)	-8% (-0.022)	4% (0.011)
LBL (Sherman)	34% (0.018)	18% (0.016)	-20% (-0.061)	6% (0.016)
Variable n (Yuill)	25% (0.022)	4% (0.003)	-22% (-0.059)	3% (0.009)
Shaw	45% (0.038)	2% (0.002)	-12% (-0.038)	8% (0.017)
Warren and Webb	4% (0.005)	5% (0.003)	-19% (-0.051)	2% (0.009)

* - Values in brackets are in Air Changes per Hour, ACH.

ACH error.

5.4 Model Accuracy for Stack Effect

The models were compared to data taken in House #4 with an open 15 cm diameter flue with a 7.5 cm diameter orifice at the bottom, and in House #5 with no flue. The data was sorted for windspeeds less than 1.5 m/s and averaged in bins every 5 °C temperature difference, ΔT. A windspeed of 1.5 m/s is not low enough to remove all significant wind effects, but a lower windspeed results in too little data for analysis. To remove scatter due to changes in shelter for the wind only winds from ± 22.5° from North and South were included when sorting the data. Sorting for East and West winds would reduce the wind effect but results in insufficient data for analysis. The North and South data was combined in the same way as when examining windspeed effects. For House #4, 2201 hours of data were reduced to 102 hours by sorting, and for House #5, 1254 hours of data were reduced to 74 hours by sorting. The error bars in each figure represent ± one standard deviation for the data in that bin. For House #5 the same leakage distribution was assumed as for wind effect, with 67% of the leakage in the 4 walls, 16.5% at ceiling level and 16.5% at floor level. For House #4, 30% of the leakage was in the 4 walls and 15% of the leakage at ceiling level and 15% of the leakage at floor level. The corresponding values of R, X, and Y are shown in Table 5.2, together with the leakage characteristics, C and n, found from fan pressurization tests.

The models are compared to data measured in House #4 (flue open) and House #5 (no flue) in Figures 5.7 and 5.8 respectively. The bias

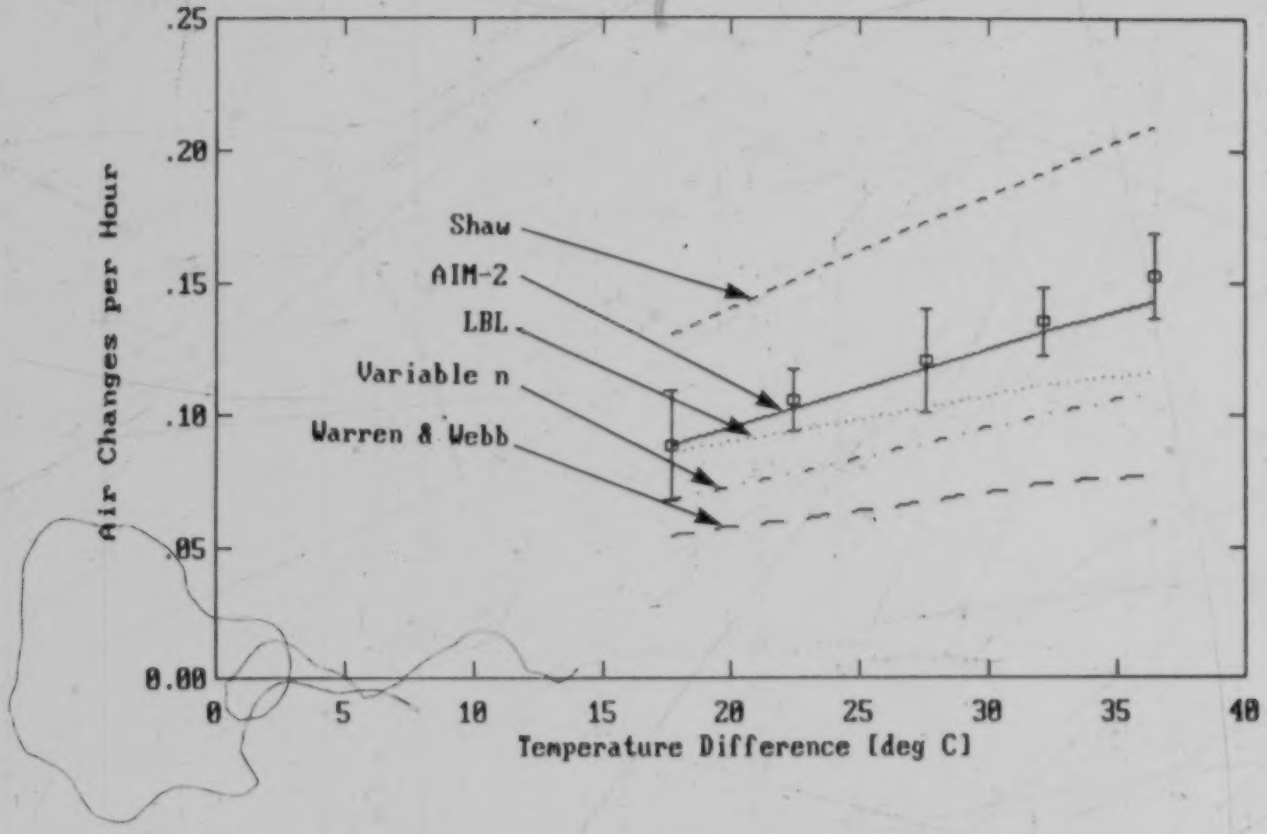

Figure 5.7: Comparison of Ventilation Models to measured data for ΔT dependance in House #4 with an open 7.5cm diameter orifice in the flue, with $\Delta T \geq 10°C$ and $U \leq 1.5$ m/s. R=0.3, X=0, Y=0.4, and $\beta_f = 1.5$ (102 hours)

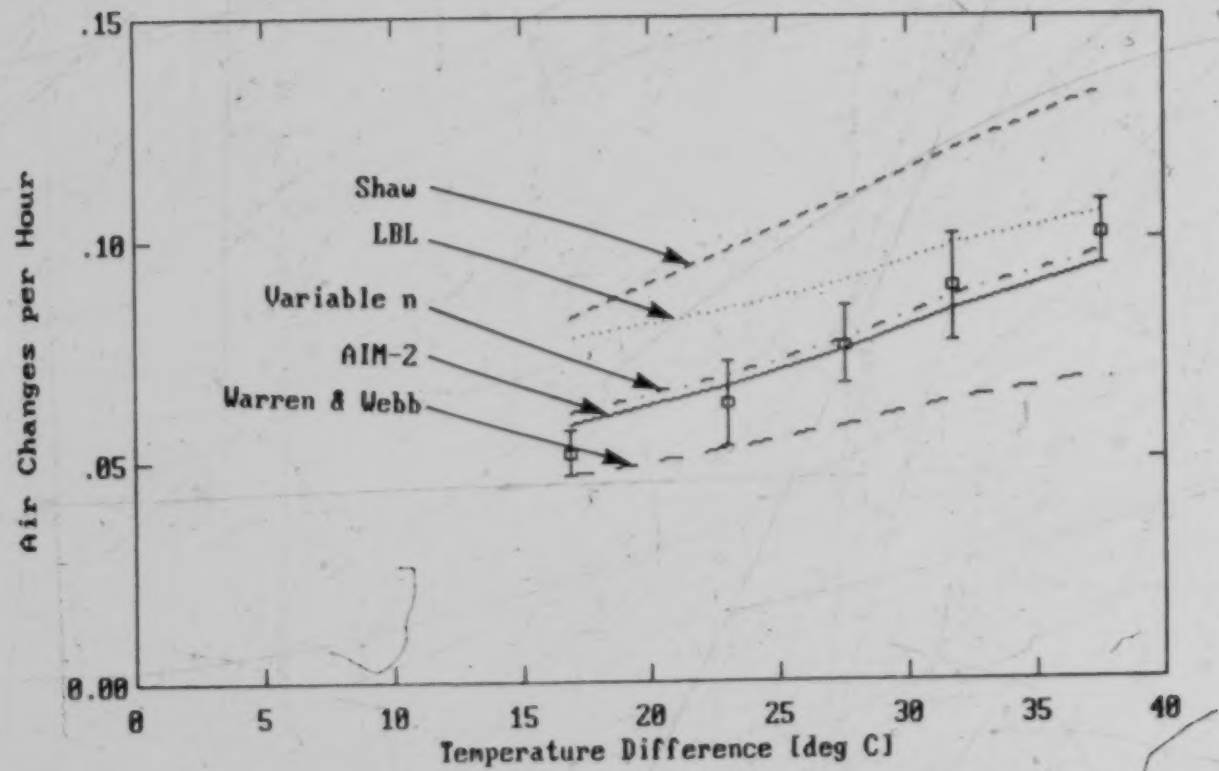

Figure 5.8: Comparison of Ventilation Models to measured data for ΔT dependance in House #5 with flue blocked with $\Delta T \geq 10°C$ and $U \leq 1.5$ m/s (74 hours)

in the models is due to leakage distribution effects generating different values of f_s based on the different model assumptions. The large bias of Warren and Webb's and Shaw's models is probably because their stack effect constants were found by fitting to data measured in houses of different construction type and leakage distribution compared to the houses used in this study. Ignoring the bias errors, all the models have the correct temperature difference dependance, except for the LBL model whose orifice flow assumption gives a slope of $n = 1/2$ rather than $n = 0.66$ for House #4 with a flue, and $n = 0.65$ for House #5 with no flue (as can be seen in a log-log plot). The change in leakage distribution is handled well by AIM-2 since it has the ability to treat the flue as a separate leak with the parameters Y and β_f. Shaw's model uses a value for dimensionless neutral level, β_o, resulting from a fit to measured data that increases f_s for houses with flues, and thus Shaw's model overpredicts by a similar amount with and without a flue. All the other models underpredict open flue ventilation, even the LBL model which overpredicts closed flue ventilation by 24%. Table 5.6 gives a complete listing of the bias and scatter errors associated with each model for stack dominated ventilation, which show that AIM-2 has the best overall performance.

Table 5.6 Model Errors for Binned Averages of Stack Dominated Ventilation at AHHRF

	House #4 7.5 cm Flue Open		House #5 Flue Closed	
Model	Bias	Scatter	Bias	Scatter
AIM-2	-3.4% (-0.005)	1.5% (0.002)	0.7% (0.001)	6.6% (0.005)
LBL (Sherman)	-14.1% (-0.019)	6.9% (0.008)	23.8% (0.015)	12.0% (0.009)
Variable n (Yuill)	-26.1% (-0.032)	1.7% (0.002)	4.4% (0.002)	7.0% (0.005)
Shaw	42.6% (0.051)	1.9% (0.002)	44.7% (0.032)	6.8% (0.005)
Warren and Webb	-44.2% (-0.054)	5.1% (0.006)	-22.3% (-0.018)	9.4% (0.007)

* - Values in brackets are in Air Changes per Hour, ACH.

5.5 Effect of Changing Leakage Distribution on Model Predictions

To test the effect of leakage distribution, four different values for the parameters R and X were chosen with Y (the fraction of leakage in the flue) and β_f (the nondimensional flue height) unchanged. The resulting model predictions were compared to data where stack effect dominates taken at AHHRF in House #4 with a 7.5 cm diameter orifice in the flue. This is the same data set as used in the previous section. R (the sum of ceiling and floor leakage) was varied from zero to 0.4, and X (the difference between ceiling and floor leakage) was varied from -0.1 to 0.2. The fraction of flue leakage, Y, was constant at 0.4, and the nondimensional flue height, β_f , was 1.5. The combinations tested are listed in Table 5.2. The results of changing these parameters are shown in Table 5.7, and the model predictions are compared to the measured values in Figures 5.7, 5.9, 5.10, and 5.11.

Shaw's and Warren and Webb's models do not have leakage distribution parameters, and their predictions do not change for these different cases. Their predictions for House #4 with a 7.5 cm diameter orifice in the flue are shown in Table 5.6. Their predictions are shown in Figures 5.9, 5.10, and 5.11 for comparison.

The models compared in this section are AIM-2, LBL and the Variable n model. The case of R=0.3 and X=0 is the baseline case used in the previous section comparing the model predictions, and will be the basis for comparison for this section. The results show that the scatter of the models are not significantly changed by the leakage distribution parameters, as one would expect because R, X, Y, and β_f do not change the functional forms of the equations predicting the

Table 5.7 The Effect of Leakage Distribution Estimates on Model Predictions of Stack Dominated Ventilation for House #4 with an open 7.5 cm² diameter orifice in a 15 cm diameter flue

Leakage Configuration		AIM-2	LBL (Sherman)	Variable n (Yuill)
R = 0.3 X = 0 Y = 0.4	Bias	-3.4% (-0.005)	-14.1% (-0.019)	-26.1% (-0.032)
	Scatter	1.5% (0.002)	6.9% (0.008)	1.7% (0.002)
R = 0 X = 0 Y = 0.4	Bias	-1.2% (-0.002)	-16.2% (-0.021)	-31.6% (-0.039)
	Scatter	1.8% (0.002)	8.0% (0.010)	3.0% (0.004)
R = 0.2 X = -0.1 Y = 0.4	Bias	5.1% (0.006)	-9.9% (-0.014)	-23.2% (-0.030)
	Scatter	1.6% (0.002)	7.0% (0.008)	1.9% (0.002)
R = 0.4 X = 0.2 Y = 0.4	Bias	-24.2% (-0.030)	-32.0% (-0.040)	-41.3% (-0.050)
	Scatter	1.5% (0.002)	7.2% (0.009)	2.0% (0.002)

* - Values in brackets are in Air Changes per Hour, ACH.

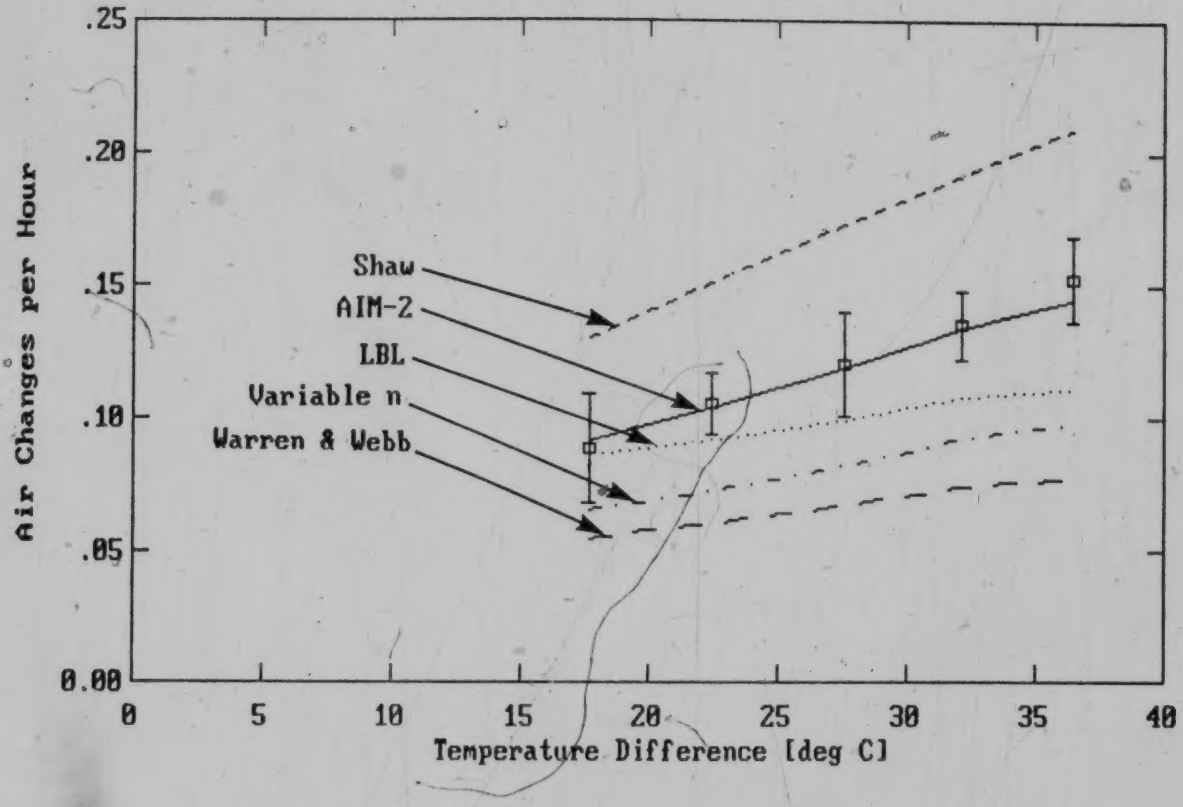

Figure 5.9: Comparison of Ventilation Models to measured data for ΔT dependance in House #4 with an open 7.5cm diameter orifice in the flue, with $\Delta T \geq 10°C$ and $U \leq 1.5$ m/s. R=0, X=0, Y=0.4, and β_f=1.5 (102 hours)

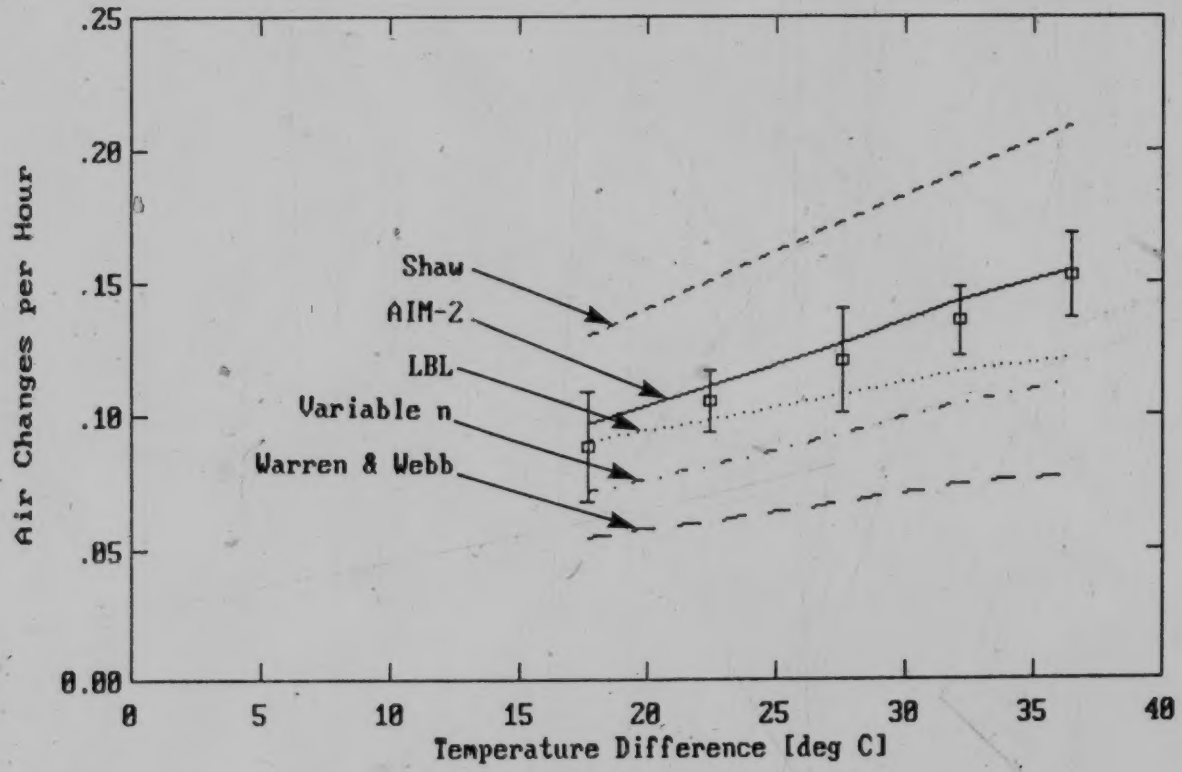

Figure 5.10: Comparison of Ventilation Models to measured data for ΔT dependance in House #4 with an open 7.5cm diameter orifice in the flue, with $\Delta T \geq 10°C$ and $U \leq 1.5$ m/s. R=0.2, X=-0.1, Y=0.4, and β_f=1.5 (102 hours)

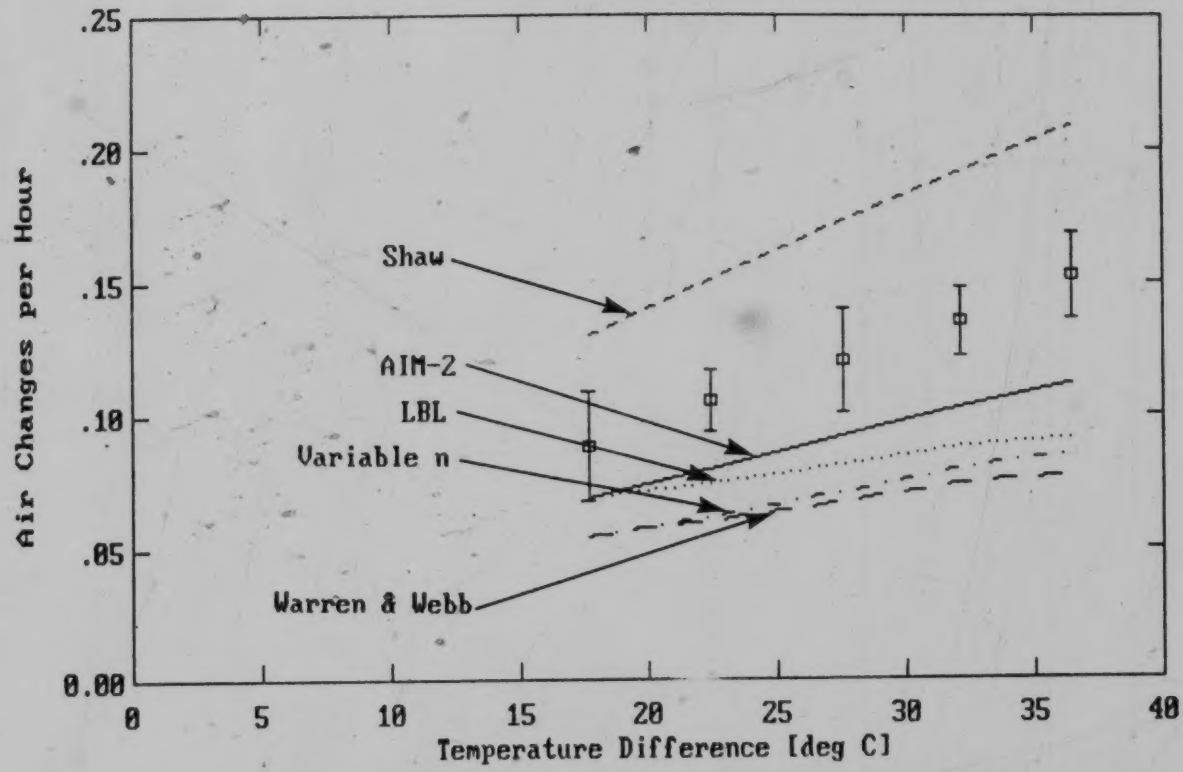

Figure 5.11: Comparison of Ventilation Models to measured data for ΔT dependance in House #4 with an open 7.5cm diameter orifice in the flue, with $\Delta T \geq 10°C$ and $U \leq 1.5$ m/s. R=0.4, X=0.2, Y=0.4, and β_f=1.5 (102 hours)

flowrates. Instead, these parameters change the lead constants, the stack and wind factors, f_s, and f_w.

For R=0 and X=0, with all the non-flue leakage in the walls (which is not a typical leakage distribution), the model predictions are changed by less than 6%, a relatively small amount (see Figure 5.9), with AIM-2 underpredicting less, and LBL and the Variable n model underpredicting more. For R=0.2 and X=-0.1, the models increase their predicted values by less than 8%, such that AIM-2 now overpredicts by 5.1% rather than underpredicting by 3.4%, and the underpredictions of the LBL and Variable n models are less by a similar amount (see Figure 5.10). The final distribution is R=0.4 and X=0.2. Unlike putting all the leakage in the walls this does not seem like an unlikely leakage distribution, yet it yields predictions reduced by about 20% for all three models (see Figure 5.11).

These tests show that correctly estimating leakage distribution can be an important factor in predicting ventilation rates. However, it also shows that it is possible for an atypical leakage distribution to produce reasonable results.

5.6 Accounting for Mechanical Ventilation with AIM-2

In AIM-2 mechanical ventilation is superposed on the total natural ventilation rate using the superposition theory developed by Kiel and Wilson (1987), where half of the flowrate adds linearly, and half is included as pressure addition:

$$Q_{total} = \left[Q_{\frac{fan}{2}}^{1/n} + Q_{natural}^{1/n} \right]^n + Q_{\frac{fan}{2}} \qquad (5.7)$$

This relationship is described in more detail in Chapter 3.

The measured data used to test the ability of AIM-2 to predict ventilation rates with added mechanical ventilation was taken in House #2 at AHHRF, with an open 15 cm diameter flue. The leakage distribution parameters are summarised in Table 5.2, with R=0.25, X=0, and Y=0.6. An exhaust fan provided 0.213 ACH in addition to the natural building ventilation. A total of 374 hours were taken over three weeks; 195 hours with the fan on and 179 hours with the fan off. Over the test period the average ventilation rate with the fan off was 0.32 ACH and with the fan on this was raised to 0.51 ACH. Thus the fan provided about 40% of the total building ventilation. The fan was cycled to be four hours on, then four hours off. This was done so that it was possible to determine if the model was predicting the correct natural ventilation rate for the house. During the test period the average windspeed was about 4 m/s and the average temperature difference was about 12°C. This implies that the natural ventilation for this data set has equal contributions of stack and wind effects.

Comparing the predicted to the measured values of ventilation rate shows that AIM-2 underpredicts both the natural ventilation rate and the the ventilation rate with the fan on. The natural ventilation rates are underpredicted on the average by 0.06 ACH (19%) bias and the corresponding scatter (with the bias removed) is 0.04 ACH (12%). The scatter is reduced by allowing S_w to vary with wind angle. With the fan on the average underprediction is 0.09 ACH (17%) and the scatter is 0.05 ACH (10%). This indicates that much of the error with the fan

on is attributable to estimating the natural ventilation rate incorrectly. Thus this method of superposing natural and mechanical ventilation is adequate for a simple model like AIM-2.

The method yielding the best results for combining natural and mechanical ventilation for this data set was simple linear addition. This linear solution to a non-linear problem is not well understood, and requires further research. This is the same result found by Kiel and Wilson (1987) who used fitted data, rather than a ventilation model, to predict the natural ventilation rates. This apparently strange result may be due to the leakage distribution of the house, where 60% of the leakage is located in a single site: the furnace flue.

Figures 5.12, 5.13 and 5.14 contain timelines showing both the measured and predicted ventilation rates for 24 hour periods. The natural ventilation rates are wind dominated in Figure 5.12 (Qwind/Qstack = 1.66), temperature difference dominated in Figure 5.13 (Qwind/Qstack = 0.44), and in Figure 5.14 neither dominates (Qwind/Qstack = 0.88). The figures show that over a wide range of ambient weather conditions and ventilation rates AIM-2 always underpredicts the ventilation rate with the fan on even when it makes good predictions when the fan is off. Also, the timeline plots show that the model tracks the changes in ventilation rate well, and that the error is one of bias.

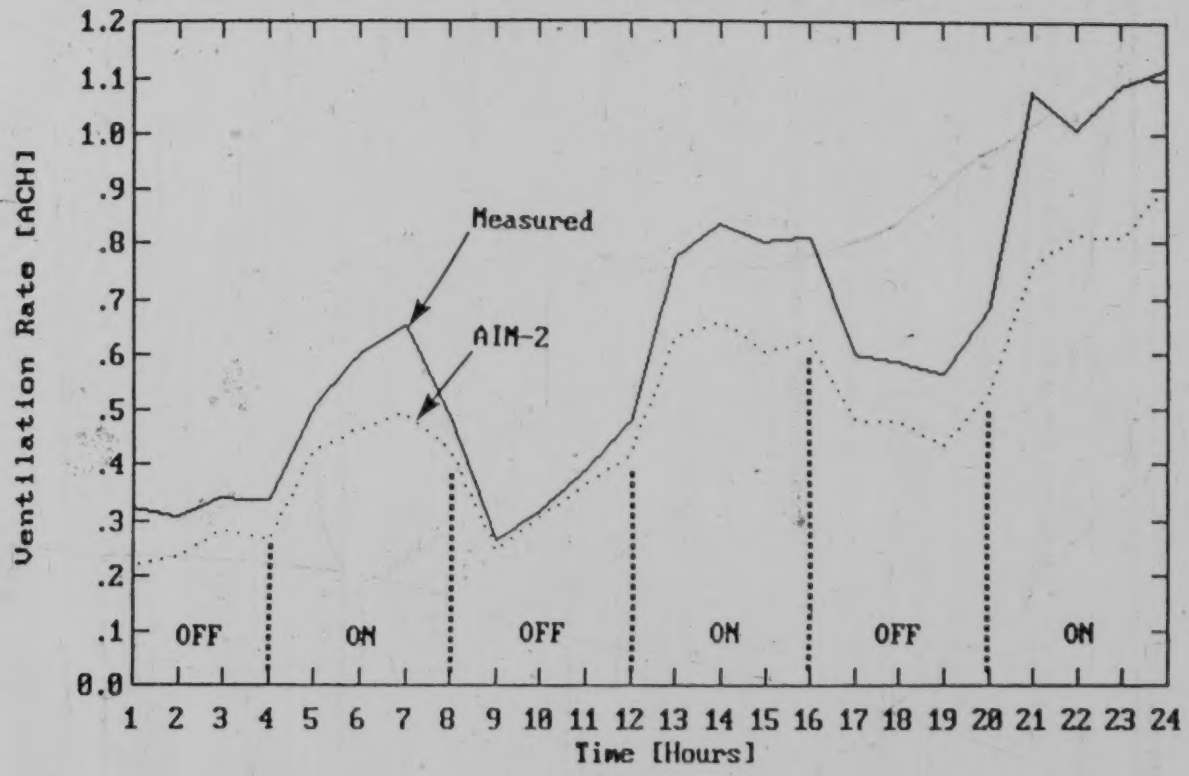

Figure 5.12: Predicted and measured ventilation rates in House #2 with an open 15 cm diameter flue with mechanical ventilation cycling every 4 hours for wind dominated natural ventilation: U=7.0m/s, ΔT=15.8°C, Qwind/Qstack=1.66

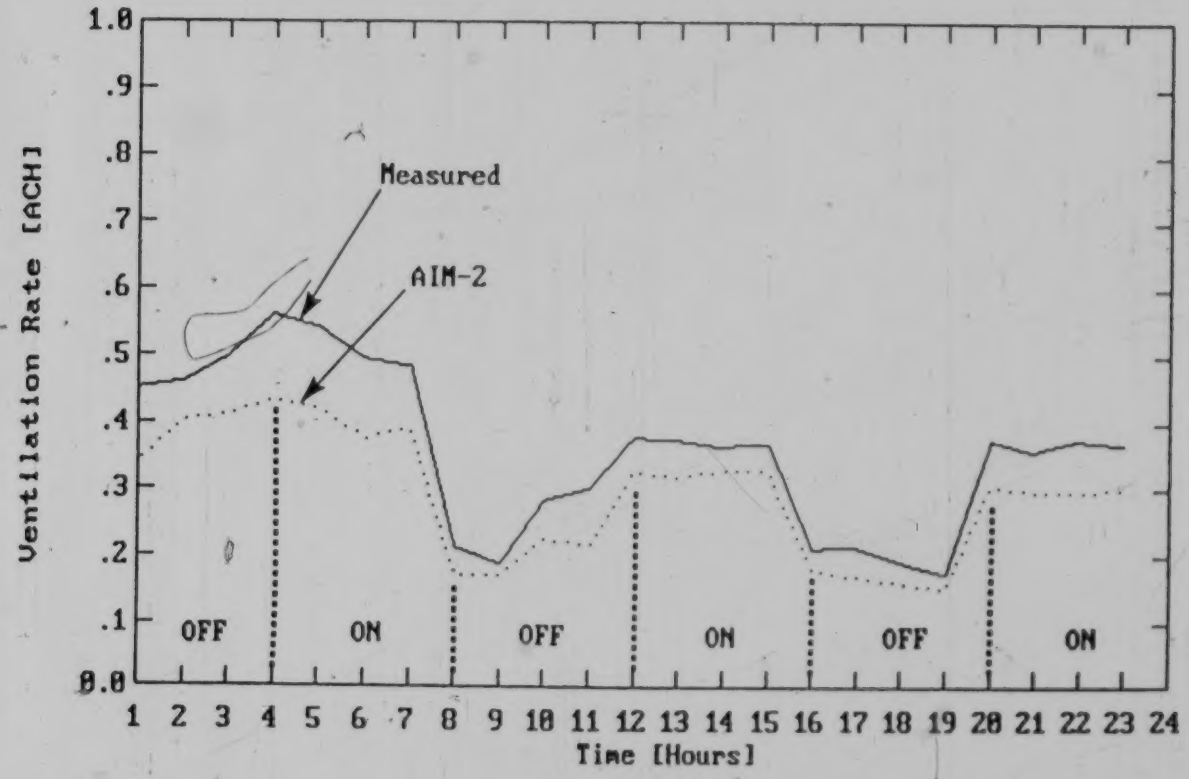

Figure 5.13: Predicted and measured ventilation rates in House #2 with an open 15 cm diameter flue with mechanical ventilation cycling every 4 hours for stack dominated natural ventilation: U=2.6m/s, ΔT=13.3°C, Qwind/Qstack=0.44

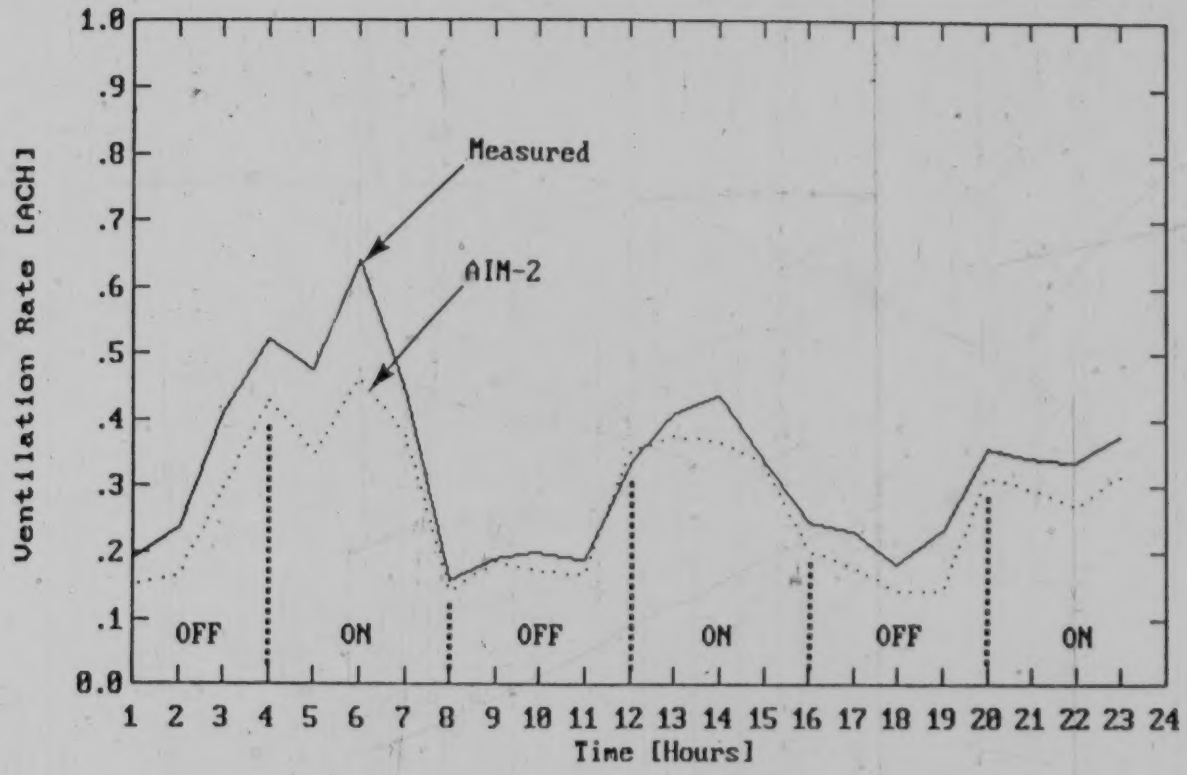

Figure 5.14: Predicted and measured ventilation rates in House #2 with an open 15 cm diameter flue with mechanical ventilation cycling every 4 hours for similar stack and wind effects: U=2.9m/s, ΔT=9.3°C, Qwind/Qstack=0.88

5.7 Predicting Hourly Ventilation Rates

In previous sections the windspeed and temperature difference dependance of model predictions has been studied based on carefully sorted data averaged over several months. Whilst this is of interest scientifically in determining the physics of ventilation modelling and in long term energy loads, the application of a ventilation model to indoor air quality may depend on its ability to predict hourly ventilation rates. It has been shown that AIM-2 is able to predict the average ventilation rate for given weather conditions with a bias less than 10% and scatter less than 5%. Looking at single hourly ventilation rates will show how well AIM-2 can predict the ventilation rate for a single hour.

Table 5.8 lists the bias and scatter for AIM-2 compared to measured data for short term ventilation rates. The measured data was from 24 hour periods of wind dominated ventilation, stack dominated ventilation, and where both wind and stack effects are significant, in House #4 with an open 7.5 cm diameter orifice in a 15 cm diameter flue that is about 40% of the total building leakage. The same values of R, X, and Y were used as in the analysis of binned data, where R=0.3, X=0, Y=0.4, and a flue height of 5m were used. As with studying mechanical ventilation S_w was allowed to vary with wind angle. The bias error is due to errors in estimating the total leakage (C and n), leakage distribution (R,X and Y), and other model inputs, such as wind shelter factor S_w, or to general failure of model assumptions such as averaging pressure coefficients over a wall and assumed C_p values etc. The bias is typically an underprediction of 0.015 ACH (11%). The

Table 5.8 Summary of AIM-2 Errors in Predicting Hourly Ventilation rates in House #4 at AHHRF with a 7.5 cm diameter orifice in the Flue

	Bias	Scatter
Wind Dominated Ventilation (Qwind/Qstack = 1.85)	-18% (-0.026)	11% (0.016)
Stack Dominated Ventilation (Qwind/Qstack = 0.32)	-4% (-0.006)	7% (0.009)
Both Wind and Stack Significant (Qwind/Qstack = 1.0)	-10% (-0.013)	10% (0.012)

* - Values in brackets are in Air Changes per Hour, ACH.

scatter is typically 0.012 ACH (10%). The scatter error is due to changes in the measured ventilation rate that AIM-2 is unable to predict. An estimate of typical values of error from Wilson and Dale (1985) is that 95% of the data will fall within ± 5% ± 0.004 ACH, and the system resolution is approximately 0.003 ACH. This indicates that at least a quarter of the scatter may be due to the infiltration measurment system. The scatter error can be attributed to a large extent to the use of hourly averaged windspeed, temperature difference and wind direction. Because the ventilation rate is not linearly dependant on windspeed or temperature difference the use of hourly averages for these parameters must introduce some error. Also, the use of an average wind angle can create significant errors in estimating wind shelter, as shown in Chapter 3. This can be seen in the larger errors associated with wind dominated ventilation compared with the stack dominated results. There is about four times as much error when calculating the wind dominated ventilation rates as for the stack dominated ventilation rates. There is no way to remove these errors from a simple ventilation model, and these errors place a limit on how well any model can predict short term ventilation rates.

Figures 5.15, 5.16 and 5.17 show the variation in measured ventilation rate and the ventilation rate predicted by AIM-2 on an hourly basis over a 24 hour period. The data in Figure 5.15 is wind dominated (Qwind/Qstack = 1.85), Figure 5.16 is stack dominated (Qwind/Qstack = 0.32), and in Figure 5.17 both effects are significant (Qwind/Qstack = 1.0). These figures show that AIM-2 always underpredicts but is able to track the changes in hourly ventilation

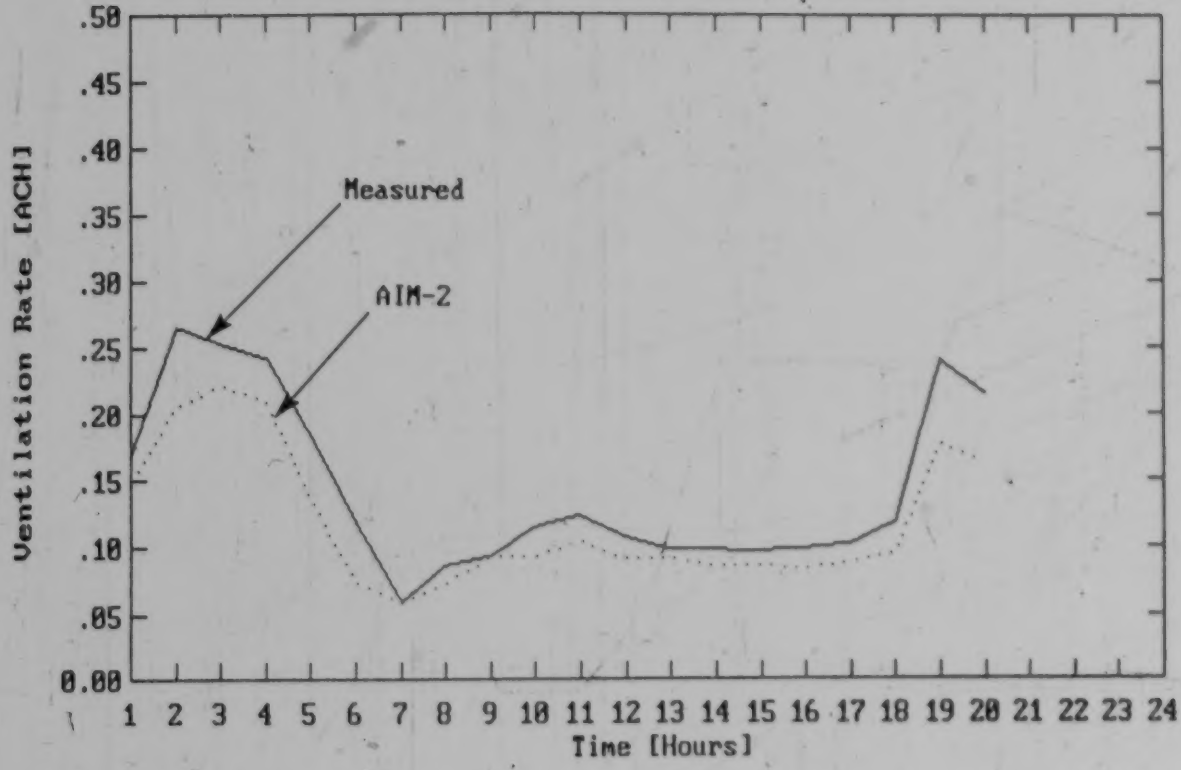

Figure 5.15: Predicted and measured natural ventilation rates for wind dominated natural ventilation in House #4 with a 7.5cm diameter orifice in the flue. U=4.1m/s, ΔT=9.4°C, Qwind/Qstack=1.85

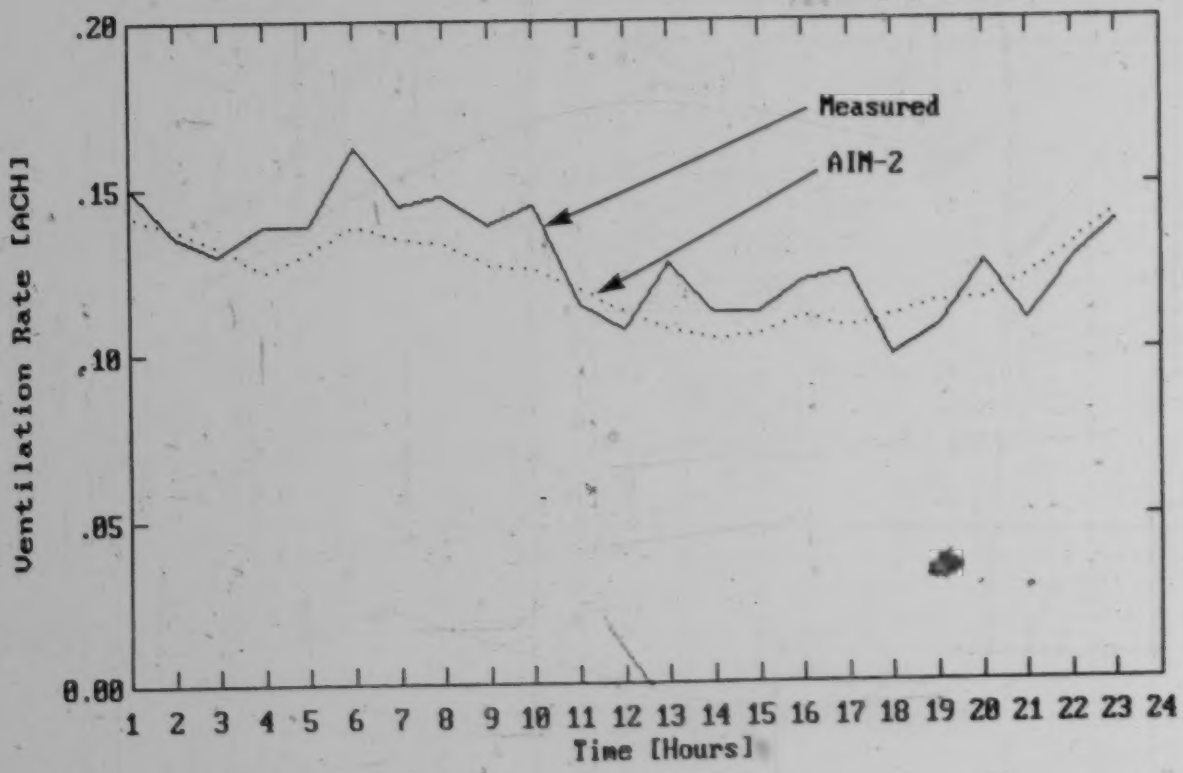

Figure 5.16: Predicted and measured natural ventilation rates for stack dominated natural ventilation in House #4 with a 7.5cm diameter orifice in the flue. U=1.7m/s, ΔT=27.9°C, Qwind/Qstack=0.32

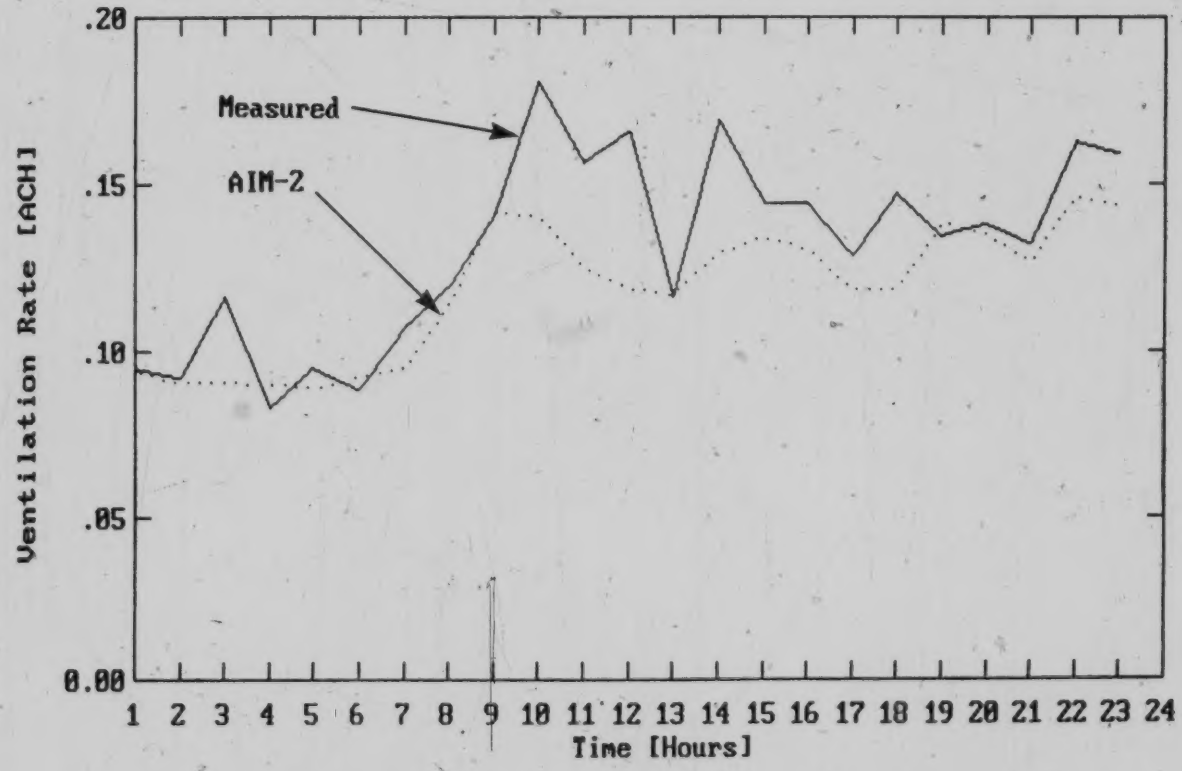

Figure 5.17: Predicted and measured ventilation rates, both wind and stack effects significant in House #4 with a 7.5cm diameter orifice in the flue. U=3.7m/s, ΔT=16.7°C, Qwind/Qstack=1.0

rates for a range of weather conditions. The bias is the same for ΔT dominated conditions as for the binned data at the same ΔT and U in Figure 5.7, and is only twice the measurement system resolution. The bias is much more significant for U dominated conditions, and is probably due to underestimating f_w for a house with a flue. The same trend is seen for the predictions for House #5 with an open 15 cm diameter flue in Tables 5.4 and 5.5.

5.7 Summary

· Tables 5.4 to 5.6 summarize numerically the errors associated with each model under various conditions, showing that AIM-2 performs the best for the different houses and leakage distributions tested.

· The large amount of scatter seen in hourly measured ventilation rates means that at best a ventilation model can only predict what the average ventilation rate would be under given conditions, and exact prediction of an hourly ventilation rate is not possible for simple models. From Table 5.8 typical values for bias and scatter are about 10%. For the sorted binned data in this chapter it can be seen that the standard deviation of the data in each bin can be greater than 20%, thus the bias and scatter found for AIM-2 are acceptable values.

· The orifice flow assumption of the LBL model means that it does not have the correct slope with U and ΔT. Because the leakage exponent, n, is greater than 0.5 for a typical house, this model tends to overpredict at low ventilation rates and underpredict at high ventilation rates such that for average conditions of ΔT and U, if the appropriate stack and wind factors are used, it can predict correct

values.

· AIM-2, Variable n, Warren and Webb and Shaw have the correct slope with U and ΔT, but the predicted ventilation rates differ by the constants determined by leakage distribution and wind shelter estimates.

· All the models underpredict ventilation rates for a house with an open flue. AIM-2 follows the change in ventilation rate when a flue is opened better than the other models because of its inherent ability to treat the flue as a separate leak.

· The prediction of ventilation rates for a sheltered building is highly dependant on how well one can estimate the sheltering effect. Because ventilation rates for a sheltered building can be much lower than for an unsheltered building (by factors of 3 or more) the estimation of degree of shelter can be a major source of error when using any model to predict ventilation rates.

· For AIM-2, Kiel and Wilson's method of superposing natural and mechanical ventilation always underpredicts the total ventilation rate. About half of this underprediction is due to the bias in AIM-2 underpredicting the natural ventilation rate. This method for combining natural and mechanical ventilation is quite acceptable for the level of complexity allowed in AIM-2.

· The results of varying leakage distribution in Table 5.7 show that the model predictions can vary by about 30%, and it is possible for unlikely leakage distributions to produce good estimates of ventilation rates. For small changes in leakage distribution involving less than 15% of the total building leakage the model predictions do

not vary substantially (less than 10%), thus this is as good as the leakage distribution estimates need to be.

Chapter 6

Conclusions and Recommendations

Laboratory testing of furnace flues and fan pressurization tests performed at the Alberta Home Heating Research Facility (AHHRF) have been performed to find the characteristic flow coefficient, C, and exponent, n, describing building leakage. Tracer gas infiltration measurements at AHHRF have been used to validate infiltration models developed for this study (EXACTAIM and AIM-2) and compare their predictions to those of other simple models (Variable n model developed from Yuill (1985), LBL model developed in the U.S.A. from Sherman (1980), Shaw's Variable Flow Exponent model from Shaw (1985), and Warren and Webb's model developed in England from Warren and Webb (1980)).

Furnace Flue Testing

A single value of C and n can be applied over a wide pressure difference and flow rate range. In the tests performed for this study pressure differences ranging fom 0.1 Pa to 100 Pa were applied to the furnace flues. This range encompasses the range of pressure differences a furnace flue experiences in a building due to wind, stack and mechanical ventilation effects. There is no observable trend from laminar flow (where $n = 1.0$) at low flowrates to turbulent flow at high flowrates (where $n = 1/2$) because the flow is not fully developed for a significant length of the flue and the flow characteristics are dominated by entry and exit losses and an accelerating flow regime.

Fan Pressurization Testing

The results of fan pressurization tests over a range of 1 Pa to 100 Pa performed for this study have shown that the building leakage coefficient, C, and exponent, n, do not vary over this range. As with furnace flues this is because the flow in the cracks in a building envelope is dominated by entry and exit losses and an accelerating flow regime. It has been found by examination of pressurization tests performed over a wide range of windspeeds that for reliable results at pressures less than 10 Pa the windspeed must be less than 1.5 m/s. At pressures greater than 10 Pa windspeeds may be up to 4 m/s before the test is unreliable. These results indicate that the current CGSB and ASTM fan pressurization standards using pressure differences greater than 10 Pa are adequate to determine the characteristic C and n for a building even though these pressures are greater than those ocurring on a building due to wind and stack effects (typically 4 Pa).

Model Development and Verification

EXACTAIM has been developed to find building ventilation rates by numerical solution of non-linear equations derived from crack flow theory, wind tunnel pressure coefficients, from Akins (1979), and simplifying assumptions about leakage distribution. AIM-2, a simpler model not requiring numerical solution techniques, has been developed from EXACTAIM. AIM-2 has empirical equations that have been formulated to give the same results as EXACTAIM to within 5%, with smaller differences over typical ranges of leakage distribution estimates. These equations were designed to have the correct

asymptotic behaviour for the limiting cases

The weaknesses of AIM-2 and EXACTAIM are the need to estimate leakage distributions and wind shelter effects. Choosing an incorrect leakage distribution can cause infiltration errors of up to 25%. Selecting an appropriate value for wind shelter is difficult due to the vast number of possible goemetries due to neighbouring buildings, trees, and terrain effects. For AIM-2 and EXACTAIM five categories of building shelter have been defined as a rough guide. Selecting the wrong value for building shelter can create errors of a factor of two or more in predicting ventilation rates.

The equations for AIM-2 and EXACTAIM have been developed to be dimensionally consistent so that they are applicable in any dimensionally consistent set of units. AIM-2 and EXACTAIM differ from other simple models by having separate equations for houses with basements or slab-on-grade construction and crawl spaces. EXACTAIM was not included in the model verification because it predicts virtually the same ventilation rates as AIM-2.

Other differences that have been found to be significant are:

- Flowrates due to stack and wind effects are combined using pressure addition with a non-linear empirical interaction term to account for the interaction between stack and wind pressures. The interaction term is negligable when either stack or wind effects are dominant and has a maximum effect when the stack and wind flowrates are equal. Quadrature addition used in other models (LBL and Variable n in this study) has a similar effect. A constant, B_1, in the interaction term is the only parameter in AIM-2 and EXACTAIM that is

found empirically by fitting to measured data from AHHRF. All other constants are found from theory or from independant wind tunnel data sets.

• The flue is treated as a separate leakage site by introducing two leakage distribution parameters describing the flue: Y and β_f. Y is the fraction of total building leakage in the flue and β_f is the height of the top of the flue non-dimensionalised with the ceiling height of the building. Model verification using infiltration data measured at AHHRF has shown that AIM-2 is the best of the models tested here for predicting the changes in ventilation rate between houses with and without flues.

• A simple equation for finding effective building shelter, S_w, gives building shelter for any wind direction given estimates of shelter for winds perpendicular to the four faces of a building. This has been shown to be effective for predictions of the average ventilation rate for winds from a given direction, but the process of using hourly averaged wind direction means that the ventilation rate for winds from a single direction can vary by up to 20% and this variability cannot be accounted for. S_w allows the flue to remain unsheltered when the building is sheltered. This has been shown to be effective when predicting ventilation rates for heavily sheltered buildings.

• Including mechanical ventilation using the method of Kiel and Wilson (1987) has been found to underpredict the total ventilation rate consistently by about 17%. However, most of this underprediction is due to underpredicting the natural ventilation rate for a house with

about 60% of the total leakage in the flue (optimum results for AIM-2 are for less than 40% of the leakage in the flue). For the mechanical exhaust ventilation system tested at AHHRF linear addition of natural and mechanical ventilation rate appears to yield better results. This perplexing result merits further investigation.

• AIM-2 was found to have the best overall performance of the models tested here. Bias and scatter are typically 10% when compared to data measured at AHHRF. These are adequate values for a simple model considering the variability of measured ventilation rates with wind direction.

Recommendations

Further research is needed in the following areas to improve estimates of building ventilation rates.

• Finding pressure coefficients for more complex building shapes that are common in modern housing (pressure coefficients for a square, flat roofed building were used in the development of AIM-2). In addition, measurements of the local pressure coefficients on eaves and their influence on attic pressures are needed.

• Accounting for the variability in wind direction during an averaging period. The standard deviation of wind direction could be used to predict upper and lower bounds on the estimated ventilation rate.

• Predicting shelter effects. Although much work has been performed in wind tunnel tests in this area, the complexity and variability of the shelter for an individual building is only a rough

estimate.

• Addition of mechanical ventilation. The results of measurements at AHHRF show that the process by which mechanical ventilation and natural ventilation are combined is not well defined. More work on finding a theoretically based method for combining natural and mechanical ventilation is needed.

REFERENCES

References

Akins, R.E., Peterka, J.A., and Cermak, J.E., (1979), "Averaged Pressure Coefficients for Rectangular Buildings", Wind Engineering Vol.1, Proc. Fifth International Conf., Fort Collins, U.S.A., July 1979, Pergamon Press, pp. 369-380.

ASHRAE Fundamentals Handbook, (1989), Chapter 14 and Chapter 23, ASHRAE, Atlanta, Georgia.

ASHRAE Standard (Draft), (1986), "Ventilation for Acceptable Indoor Air Quality", ANSI/ASHRAE 62-1981R, ASHRAE, Atlanta, Georgia.

ASTM Standard, (1982), "Measuring Air Leakage by the Fan Pressurization Method", Annual book of ASTM Standards, part 18, pp.1484-1493.

Beach, R.K., (1979), "Relative Tightness of New Housing in the Ottawa Area", Building Research Note No.149, Division of Building Research, National Research Council of Canada.

British Standard CP3 : Code of Basic Data for the design of buildings, (1971), Chapter V. Loading Part 2. Wind Loads.

CGSB Standard 149.10-M86, (1986), "Determination of Airtightness of Building Envelopes by the Fan Depressurization Method", Canadian General Standards Board.

Counihan, J., (1975), "Adiabatic Atmospheric Boundary Layers: A Review and Analysis of Data from the Period 1880-1972", Atmospheric Environment, Vol. 9, pp. 871-905.

CSA Preliminary Standard F326.1-M1989, (1989), "Residential Mechanical Ventilation Requirements", Canadian Standards Association.

Dick, J.B., (1950), "The Fundamentals of Natural Ventilation of Houses", Journal of Inst. Heat. and Vent. Eng., Vol.18.

Dumont, R.S., Orr, R.W., and Figley, D.A., (1981), "Air Tightness Measurements of Detached Houses in Saskatoon Area", Building Research Note No.178, Division of Building Research, National Research Council of Canada.

Gustén, J., (1984), "Full-Scale Wind Pressure Measurements on Low-Rise Buildings", Proc. Air Infiltration Centre Wind Pressure Workshop, Brussels, Belguim, March 1984.

Handa, K., and Gustén, J., (1982), "Estimation of rate of Air Infiltration based on Full-Scale Wind Pressure Measurements", Proc. Third Air Infiltration Centre Conf., London, England, September 1982, pp. 21.1-21.14

Haysom, J.C., and Swinton, M.C., (1987), "The Influence of Termination Configuration on the Flow Performance of Flues", Canada Mortgage and Housing Research Report.

Holmes, J.D., (1976), Capter 12. In "Wind Loads on Low Rise Buildings: The structural and environmental effects of wind in buildings and structures", Faculty of Engineering, Monash University, Melbourne, Autralia.

Holmes, J.D., (1979), "Mean and Fluctuating Internal Pressures Induced by Wind", Wind Engineering Vol.1, Proc. Fifth International Conf., Fort Collins, U.S.A., July 1979, Pergamon Press, pp. 435-450.

Honma, H., (1975), "Ventilation Of Dwellings and its Disturbances", Tekniska Meddelanden No.63 1975:2 (Vol.3) of Institutionen För Uppvärmings-och Ventilation Steknik, Teknika Högskolan.

Hopkins, L.P., and Hansford, B., (1974), "Air Flow Through Cracks", Building Services Engineer, Vol.42, September 1974, pp. 123-131.

Irwin, J.S., (1978), "A Theoretical Variation of the Wind Profile Power-Law Exponent as a Function of Surface Roughness and Stability", Atmospheric Environment, Vol.13, Pergamon Press, pp. 191-194.

Jones, W.R., (1987), private correspondance with D.J. Wilson (U. of A.), M. Modera and W.J. Fisk (L.B.L.).

Kiel, D.E., and Wilson, D.J., (1987), "Influence of Natural Ventilation on Total Building Ventilation Dominated by Strong Fan Exhaust", ASHRAE Trans. 1987, Vol.93, Part 2.

Kiel, D.E., Wilson, D.J., and Sherman, M.H., (1985), "Air Leakage Flow Correlations for Varying House Construction Types", ASHRAE Trans. 1985, Vol.91, Part 2.

Kostuik, L.W., and Dale, J.D., (1985), "Final Report on the Thermal Performance of an Insulated Masonry Structure", Department Report Number 52, Department of Mechanical Engineering, University of Alberta, Edmonton, Alberta.

Kreith, F., and Eisenstadt, R., (1957), "Pressure Drop and Flow Characteristics of Short Capillary Tubes at Low Reynolds Numbers", ASME Trans., July 1957, pp. 1070-1078.

Kronvall, J., (1980), "Air Flows in Building Components", Report TVBH-1002, Division of Building Technology, Lund Institute of Technology, Lund, Sweden.

Lee, B.E., Hussian, M., and Soliman, B., (1979), "A Method for the Assessment of the Wind Induced Natural Ventilation Forces acting on Low Rise Building Arrays", Report Number BS 50, Department of Building Science, University of Sheffield.

Levin, P.E., (1982), "Measured Effect of Forced Ventilation on House Infiltration Rate", Proc. of D.O.E. Conf. on Thermal Performance of Exterior Envelopes of Buildings, Las Vegas, December 1982.

Liddament, M.W., (1986), "Air Infiltration Calculation Techniques - An Applications Guide", Air Infiltration and Ventilation Centre

Lipschutz, R.D., Girman, J.R., Dickinson, J.B., Allen, J.R., and Traynor, G.W., (1981), "Infiltration and Indoor Air Quality in Energy Efficient Houses in Eugene, Oregon" Report No. LBL-12924, Lawrence Berkeley Laboratories, University of California.

Lyberg, M.D., (1983), "Models of Infiltration and Natural Ventilation", Bulletin M83:23, National Swedish Institute for Building Research.

Modera, M., Sherman, M.H., and Levin, P.A., (1983), "A Detailed Examination of the LBL Infiltration Model using the Mobile Infiltration Test Unit",Report No. LBL-15636, Lawrence Berkeley Laboratories, University of California.

Miller, I., and Freund, J.E., (1985), "Probability and Statistics for Engineers - Third Edition", Prentice Hall, p.297.

Offerman, F.J., Dickinson, J.B., Fisk, W.L., Grimsrud, D.T., Hollowell, C.D., Krinkel, D.L., Roseme, G.D., Desmond, R.M., DeFrees, J.A., and Lints, M.C., (1982), "Residential Air Leakage and Indoor Air Quality in Rochester, New York", Report No. LBL-13100, Lawrence Berkeley Laboratories, University of California.

Pasquill, F., and Smith, F.B., (1983), "Atmospheric Diffusion, Third Edition", John Wiley and Sons. p.336.

Peterson, F., (1982), "On Flow in Narrow Slots Applied to Infiltration", Proc. 3rd AIC conf., London, U.K., pp. 23.1-23.8.

Reardon, J.T., (1989), "Air Infiltration Modelling Study", Report #CR5446.3, Energy, Mines and Resources Canada, National Research Council Canada.

Reid, D.B., (1844), "Illustrations of the Theory and Practise of Ventilation", Longman, Brown, Green and Longmans.

Schlicting, H., (1979), "Boundary-Layer Theory, Seventh Edition", McGraw-Hill, p. 597.

Shapiro, A.H., Siegel, R., and Klein, S.J., (1954), "Friction Factor in the Laminar Entry Region of a Small Tube", Proc. Second U.S. National Congress of Applied Mechanics, Michigan, 1954, ASME, pp. 733-741.

Shaw, C.Y., and Brown, W.C., (1982), "Effect of a Gas Furnace Chimney on the Air Leakage Characteristic of a Two-Storey Detached House", Proc. Third Air Infiltration Centre Conf., London, England, September 1982, pp. 12.1-12.13.

Shaw, C.Y., (1985), "Methods for Estimating Air Change Rates and Sizing Mechanical Ventilation Systems for Houses", Building Research Note 237, Division of Building Research, National Research Council of Canada.

Shaw, Sir W.N., (1907), "Air Currents and Laws of Ventilation", Cambridge University Press.

Sherman, M.H., (1980), "Air Infiltration in Buildings", Ph.D. Thesis, Energy and Environment Division, Lawrence Bekeley Laboratory, University of California

Sherman, M.H., and Grimsrud, D.T., (1980), "The measurement of Infiltration using fan pressurization and weather data", Report No. LBL-10852, Lawrence Berkeley Laboratories, University of California.

Sherman, M.H., Wilson, D.J., and Kiel, D.E., (1984), "Variability in Residential Air Leakage", Proc. ASTM Symposium on Measured air Leakage Performance of Buildings, Philadelphia, PA.

Stathopoulus, T., Surrey, D., and Davenport, A.G., (1979), "Internal Pressure Characteristics of Low-Rise Buildings due to Wind Action", Wind Engineering Vol.1, Proc. Fifth International Conf., Fort Collins, U.S.A., July 1979, Pergamon Press, pp. 451-463.

Sulatisky, M., (1984), "Airtightness Tests on 200 New Houses Across Canada : Summary of Results", Buildings Energy Technology Transfer Program, Publication No.84.01, Energy, Mines and Resources Canada.

Swami, M.V., and Candra, S., (1987), "Procedure for Calculating Natural Ventilation Airflow Rates in Buildings", Final Report, ASHRAE Reasearch Project 448-RP.

Turner, W.A., Treitman, R.D., Bearg, D., Sexton, K., and Sengler, J.D., (1982), "Home Energy Efficiency and Indoor/Outdoor Air Pollution in a Predominantly Wood Burning Community", Harvard School of Public Health, Department of Environmental Science and Physiology.

Vickery, B.J., Baddour, R.E., and Karakatsanis, C.A, (1983), "A study of the External Wind Pressure Distributions and Induced Ventilation Flows in Low-Rise and Domestic Structures", Research Report BLWT-SS2-1983, Boundary Layer Wind Tunnel Laboratory, University of Western Ontario.

Warren, P.R., and Webb, B.C., (1980), "The relationship Between Tracer Gas and Pressurization Techniques in Dwellings", Proc. First Air Infiltration Centre Conference, pp.245-276.

Wiren, B.G., (1984), "Wind Pressure Distributions and Ventilation losses for a Single-Family house as Influenced by Surrounding Buildings - A Wind Tunnel Study", Proc. Air Infiltration Centre Wind Pressure Workshop, Brussels, Belguim, March 1984.

Wilson, D.J., and Dale, J.D., (1985), "Measurment of Wind Shelter Effects on Air Infiltration", Proc. Thermal Performance of the Exterior Envelopes of Buildings, Florida 1985.

Wilson, D.J., and Pittman, W., (1983), "Correlating Measured Infiltration for Wind from a Single Direction", ASHRAE trans., Vol.89, Part 2.

Yuill, G.K., (1985), "Investigation of Sources of Error and their effects on the accuracy of the Minimum Ventilation Procedure", Report for Saskatchewan Research Council.

APPENDIX A

Appendix A

Derivation of Equations for AIM2 and EXACTAIM

A.1 Finding the pressure difference across the building envelope as a function of height.

The pressure gradient is given by:

$$\frac{d\Delta P_{env}}{dz} = -g\,\rho_{out}\,\frac{\Delta T}{T_{in}} \qquad (A.1)$$

where: ΔP_{env} = Pressure difference across the building envelope

g = acceleration due to gravity

ρ_{out} = density of outside air

T_{in} = indoor temperature

ΔT = indoor - outdoor temperature difference

z = height above reference (outside ground level)

Equation (A.1) is integrated to find the pressure difference as a function of height, z

$$d\Delta P_{env} = -g\,\rho_{out}\,\frac{\Delta T}{T_{in}}\,dz$$

$$\int_o^z d\Delta P_{env} = \int_o^z -g\,\rho_{out}\,\frac{\Delta T}{T_{in}}\,dz$$

$$\Delta P_{env}(z) - \Delta P(o) = -g\,\rho_{out}\,\frac{\Delta T}{T_{in}}\,z$$

Let ΔP at $z = 0$ be ΔP_o; this is an offset pressure from equating inflow and outflow that results in the location of the neutral pressure level, β_o, where there is no pressure difference across the building envelope.

$$\Delta P_{env} = \Delta P_o - g\,\rho_{out}\,z\,\frac{\Delta T}{T_{in}} \qquad (A.2)$$

A.2 Derivation of Exact Solution for Stack Effect

Let:

$\beta = \frac{h}{H}$ Dimensionless height, where h is some height above the outside ground reference level and H is height of the ceiling of the conditioned space.

$\beta_f = \frac{H_f}{H}$ Dimensionless flue height, where H_f is the height of the flue.

$\beta_o = \frac{h_o}{H}$ Dimensionless neutral level height, where h_o is the height on the building envelope where there is no indoor-outdoor pressure difference.

$\frac{C_c}{C}$ - fraction of leaks at ceiling height where $\beta = 1$

$\frac{C_f}{C}$ - fraction of leaks at floor height where $\beta = 0$

$\frac{C_{flue}}{C} = Y$ - fraction of leakage in the flue where $\beta = \beta_f$

$\frac{C_w}{C}$ - fraction of leakage in the walls where $0 \leq \beta \leq 1$

Note that the fraction of the total leakage, C, is not the same as the fraction of total leakage flow areas.

ΔP_s is the driving pressure difference due to stack effect:

$$\Delta P_s = \rho_{out}\,g\,H\,\frac{\Delta T}{T_{in}} \qquad (A.3)$$

where ρ_{out} = density of outdoor air

g - acceleration due to gravity

H - building ceiling height

$\Delta T = T_{in} - T_{out}$, indoor-outdoor temperature difference

T_{in} - indoor temperature

T_{out} - outdoor temperature

The pressure across a leak at height h is:

$$\Delta P_i = \Delta P_s(\beta_o - \beta) \qquad (A.4)$$

The flow rate through the i^{th} leak is given by

$$Q_i = C_i \ (\Delta P_i)^n \qquad (A.5)$$

Infiltration and exfiltration must be kept separate as the total of each will be equated later. Assuming $T_{in} > T_{out}$ and with the neutral pressure level somewhere below the ceiling ($\beta_o \leq 1$, Equations (A.5) and (A.4) can be used to write the flow rate through four different sections of the building envelope. The case where the neutral pressure level is above the ceiling, $\beta_o > 1$ will be dealt with later.

1. The ceiling where h = H:

$$Q_{ceiling} = C_c \ \Delta P_s^n \ (1 - \beta_o)^n \qquad \text{outflow}$$

2. The floor where h = 0

$$Q_{floor} = C_f \ \Delta P_s^n \ (\beta_o)^n \qquad \text{inflow}$$

3. The flue where $h = H_f$

$$Q_{flue} = C_{flue} \Delta P_s^n \ (\beta_f - \beta_o)^n \qquad \text{outflow}$$

4. The walls. To find the flow through the walls the pressure must be integrated as the pressure changes with height.

Using $dC_w = \frac{C_w\, dz}{H}$ and $d\beta = \frac{dz}{H}$

and assuming that the leaks are evenly distributed over the wall:

$$dQ_{wall} = C_w\, (\Delta P_s(\beta_o - \beta))^n\, d\beta$$

Below the neutral level, β_o, the infiltration flow is:

$$Q_{wallin} = C_w \Delta P_s^n \int_0^{\beta_o} (\beta_o - \beta)^n\, d\beta$$

$$= C_w\, \Delta P_s^n \left[\frac{-1}{n+1}\ (\beta_o - \beta)^{n+1} \right]_0^{\beta_o}$$

$$Q_{wallin} = C_w\, \Delta P_s^n\ \frac{\beta_o^{n+1}}{n+1}$$

Above the neutral level the exfiltration flow is:

$$Q_{wallout} = C_w \Delta P_s^n \int_{\beta_o}^{1} (\beta - \beta_o)^n\ d\beta$$

$$= C_w \Delta P_s^n \left[\frac{-1}{n+1}\ (\beta - \beta_o)^{n+1} \right]_{\beta_o}^{1}$$

$$Q_{wallout} = C_w \Delta P_s^n\ \frac{(1 - \beta_o)^{n+1}}{n+1}$$

Note that for the outflows equation (A.4) was taken to be:

$$\Delta P_i = P_s\, (\beta - \beta_o)$$

to ensure that the flows have a positive sign.

The building leakage distribution may be described by non-dimensional leakage distribution parameters defined as follows:

$$R = \frac{C_c + C_f}{C} \quad \text{The ceiling floor leakage sum}$$

$$X = \frac{C_c - C_f}{C} \quad \text{The ceiling floor leakage difference}$$

$$Y = \frac{C_{flue}}{C}$$

The ceiling, floor, flue and wall leakage can be written in terms of R, X and Y:

$$C_c = C\,\frac{(R+X)}{2}$$

$$C_f = C\,\frac{(R-X)}{2}$$

$$C_{flue} = CY$$

$$C_w = C(1-R-Y)$$

Grouping the inflow terms (floor and walls below neutral level) together and the outflow terms (ceiling, flue and walls above neutral level) together, and substituting non-dimensional leakage distribution parameters in place of the C's for each leak, as outlined above, yields the following pair of equations:

$$Q_{stackin} = C\Delta P_s^n \left[\frac{(R-X)}{2}\ \beta_o^n + \frac{(1-R-Y)}{n+1}\ \beta_o^{n+1} \right] \qquad (A.6)$$

$$Q_{stackout} = C\Delta P_s^n \left[\frac{(R+X)}{2} (1-\beta_o)^n + \frac{(1-R-Y)}{n+1} (1-\beta_o)^{n+1} + Y(\beta_f - \beta_o)^n \right] \quad (A.7)$$

The neutral level, β_o, is found by applying conservation of mass within the building envelope.

$$\dot{M}_{stackin} = \rho_{out} Q_{stackin} \quad (A.8)$$

$$\dot{M}_{stackout} = \rho_{in} Q_{stackout} \quad (A.9)$$

The density ratio is defined by r, which for an ideal gas is:

$$r = \frac{\rho_{in}}{\rho_{out}} = \frac{T_{out}}{T_{in}}$$

For conservation of mass:

$$\dot{M}_{stackin} - \dot{M}_{stackout} = 0 \quad (A.10)$$

Substituting equations (A.6) and (A.7) in (A.8) and (A.9), then equating (A.8) and (A.9) as in (A.10) yields,

$$\rho_{out} \frac{(R-X)}{2} \beta_o^n + \rho_{out} \frac{(1-R-Y)}{n+1} \beta_o^{n+1} - \rho_{in} \frac{(R+X)}{2} (1-\beta_o)^n$$

$$-\rho_{in} \frac{(1-R-Y)}{n+1} (1-\beta_o)^{n+1} - \rho_{in} Y(\beta_f - \beta_o)^n = 0$$

Rearranging to isolate the ceiling-floor difference and ceiling-floor sum factors:

$$\frac{X}{2}\left[\rho_{out}\,\beta_o^n + \rho_{in}(1-\beta_o)^n\right] - \frac{R}{2}\left[\rho_{out}\,\beta_o^n - \rho_{in}(1-\beta_o)^n\right]$$

$$+\frac{(1-R-Y)}{n+1}\left[\rho_{out}\,\beta_o^{n+1} - \rho_{in}(1-\beta_o)^{n+1}\right] - Y\rho_{in}\,(\beta_f^n - \beta_o)$$

Then solving for the difference factor X:

$$X = \frac{R\left[\beta_o^n - r(1-\beta_o)^n\right] + \frac{2(1-R-Y)}{n+1}\left[\beta_o^{n+1} - r(1-\beta_o)^{n+1}\right] - 2rY(\beta_f-\beta_o)^n}{\left[\beta_o^n + r\,(1-\beta_o)^n\right]} \qquad (A.11)$$

Equation (A.11) is not meant to define X but is used to determine β_o uniquely as a function of R,X,Y,β_f, r and n. The value of β_o found from equation (A.11) can be used in equations (A.8) and (A.9) to find the infiltration and exfiltration rates, which will be equal.

To find the infiltration for EXACTAIM and AIM-2 , $\dot{M}_{stackin}$ and $\dot{M}_{stackout}$ are averaged in equation (A.12), where $\dot{M}_{stack}$ is the average of the infiltration and the exfiltration. Averaging the two values will reduce any errors arising from errors in the calculation of β_o. Note that finding β_o by equating $\dot{M}_{stackin}$ and $\dot{M}_{stackout}$ ensures that either $\dot{M}_{stackin}$ or $\dot{M}_{stackout}$ will be the air exchange rate.

$$\dot{M}_{stack} = \frac{\dot{M}_{stackin} + \dot{M}_{stackout}}{2}$$

$$\dot{M}_{stack} = \rho_{out} \frac{C\Delta P_s^n}{2} \left[\frac{R}{2} \beta_o^n - \frac{X}{2} \beta_o^n + \frac{\beta_o^{n+1}}{n+1} - \frac{R\beta_o^{n+1}}{n+1} \right.$$

$$- \frac{Y\beta_o^{n+1}}{n+1} + r \frac{R}{2} (1-\beta_o)^n + r \frac{X}{2} (1-\beta_o)^n + r \frac{(1-\beta_o)^{n+1}}{n+1}$$

$$\left. - \frac{rR(1-\beta_o)^{n+1}}{n+1} - \frac{rY(1-\beta_o)^{n+1}}{n+1} + rY(\beta_f-\beta_o)^n \right] \quad (A.12)$$

Substitute (A.11) in (A.12)

$$\dot{M}_{stack} = \rho_{out} \frac{C\Delta P_s^n}{2} \left[\frac{R}{2} \beta_o^n - \frac{R\left[\beta_o^n - r(1-\beta_o)^n\right]\beta_o^n}{2(\beta_o^n + r(1-\beta_o)^n} \right.$$

$$- \frac{\beta_o^n (1-R-Y)(\beta_o^{n+1} - r(1-\beta_o)^{n+1}}{n+1\left[(\beta_o^n + r(1-\beta_o)^n\right]} + \frac{rY(\beta_f-\beta_o)^n \beta_o^n}{\left[\beta_o^n + r(1-\beta_o)^n\right]}$$

$$+ \frac{\beta_o^{n+1}}{n+1} - \frac{R\beta_o^{n+1}}{n+1} - \frac{Y\beta_o^{n+1}}{n+1} + r \frac{R}{2} (1-\beta_o)^n$$

$$+ \frac{rR(1-\beta_o)^n(\beta_o^n - r(1-\beta_o)^n}{2\left[\beta_o^n + r(1-\beta_o)^n\right]} + \frac{r(1-\beta_o)^n(1-R-Y)\left[\beta_o^{n+1} - r(1-\beta_o)^{n+1}\right]}{n+1\left[\beta_o^n + r(1-\beta_o)^n\right]}$$

$$- \frac{r^2Y(\beta_f - \beta_o)^n(1-\beta_o)^n}{\beta_o^n + r(1-\beta_o)^n} + \frac{r(1-\beta_o)^{n+1}}{n+1} - \frac{rR(1-\beta_o)^{n+1}}{n+1}$$

$$\left. - \frac{rY(1-\beta_o)^{n+1}}{n+1} + rY(\beta_f - \beta_o)^n \right] \quad (A.13)$$

Equation (A.13) can be expanded to 36 terms, each with the same denominator. Half of these terms form pairs that add, and half form pairs that cancel. After considerable algebraic manipulation equation (A.14) results.

$$\dot{M}_{stack} = \frac{\rho_{out}\, r\, C\Delta P_s^{\,n}}{(\beta_o^n + r(1-\beta_o))}\left[\beta_o^n(1-\beta_o)^n\left[\frac{1+nR-Y}{n+1}\right] + Y(\beta_f-\beta_o)^n\beta_o^n\right] \tag{A.14}$$

Now define the stack factor f_s:

$$f_s = \frac{\left[\beta_o^n(1-\beta_o)^n\left[\frac{1+nR-Y}{n+1}\right] + Y(\beta_f-\beta_o)^n\beta_o^n\right]}{\left[\beta_o^n + r(1-\beta_o)^n\right]} \tag{A.15}$$

And now (A.14) can be written as:

$$\dot{M}_{stack} = \rho_{out}\, r\, C\, f_s P_s^n \tag{A.16}$$

For AIM-2 it is assumed that r = 1 in equation (A.15). Other ventilation models do not have the flue as a separate leak, and the equations for AIM-2 and EXACTAIM can be adapted for this case. Ignoring the density differences between air flowing in and out of the building and putting the leakage of the flue in the ceiling means that:

$r = 1$

$Y = 0$ and $\beta_f = 1$

Equation (A.11) which determines β_o becomes

$$X = \frac{R\left[\beta_o^n - (1-\beta_o)^n\right] + \frac{2(1-R)}{n+1}\left[\beta_o^{n+1} - (1-\beta_o)^{n+1}\right]}{\beta_o^n + (1-\beta_o)^n} \qquad (A.17)$$

Equation (A.15) for the stack factor becomes

$$f_s = \frac{\beta_o^n (1-\beta_o)^n \left[\frac{1+nR}{n+1}\right]}{\beta_o^n + (1-\beta_o)^n} \qquad (A.18)$$

Equations (A.17) and (A.18) are identical to those derived by Yuill (1985).

If it is further assumed that orifice flow equations describe the airflow through the building envelope then n is always equal to 1/2. Equations (A.17) and (A.18) may be further reduced to the following form:

$$X = \frac{R\left[\beta_o^{1/2} - (1-\beta_o)^{1/2}\right] + \frac{4(1-R)}{3}\left[\beta_o^{3/2} - (1-\beta_o)^{3/2}\right]}{\beta_o^{1/2} + (1-\beta_o)^{1/2}} \qquad (A.19)$$

$$f_s = \frac{\beta_o^{1/2}(1-\beta_o)^{1/2}\left[\frac{2+R}{3}\right]}{\beta_o^{1/2} + (1-\beta_o)^{1/2}} \qquad (A.20)$$

Equations (A.19) and (A.20) are the same as those derived by Sherman (1980) for the assumption of orifice flow.

2.2 Solution for Stack Effect When $\beta_o > 1$

Though unlikely, it is possible that the neutral level may lie above the ceiling. The air exchange will then be outflow through the flue and inflow everywhere else. The flows through the building envelope will be as follows:

$$Q_{ceiling} = C_c \Delta P_s^n (\beta_o - 1)^n \qquad \text{inflow}$$

$$Q_{floor} = C_f \Delta P_s^n \beta_o^n \qquad \text{inflow}$$

$$Q_{flue} = C_{flue} \Delta P_s^n (\beta_f - \beta_o)^n \qquad \text{outflow}$$

The flowrate through the walls is found by integration.

$$Q_{wallin} = C_w \Delta P_s^n \int_0^1 (\beta_o - \beta)^n \, d\beta$$

$$Q_{wallin} = C_w \Delta P_s^n \left[\frac{-1}{n+1} \, [\beta_o - \beta]^{n+1} \right]_{\beta=0}^{\beta=1}$$

$$Q_{wallin} = \frac{C_w \Delta P_s^n}{n+1} \left[\beta_o^{n+1} - (\beta_o - 1)^{n+1} \right]$$

Grouping the inflow terms (floor, ceiling and walls) together and the outflow terms (flue) together, and substituting non-dimensional leakage distribution parameters in place of the C's for each leak, as outlined above, yields the following pair of equations:

$$Q_{stackin} = C\Delta P_s^n \left[\left[\left(\frac{R-X}{2}\right)\beta_o^n + \left(\frac{R+X}{2}\right)(\beta_o-1)^n + \frac{(1-R-Y)}{n+1}\left[\beta_o^{n+1} - (\beta_o-1)^{n+1}\right]\right]\right]$$

Because the flue is the only outflow site,

$$Q_{stackout} = C\Delta P_s^n \, Y(\beta_f-\beta_o)^n$$

Applying conservation of mass to the building volume:

$$\rho_{out}\left(\frac{R-X}{2}\right)\beta_o^n + \rho_{out}\frac{(R+X)}{2}(\beta_o-1)^n + \rho_{out}\frac{(1-R-Y)}{n+1}\left[\beta_o^{n+1} - (\beta_o-1)^{n+1}\right] - \rho_{in}\,Y(\beta_f-\beta_o)^n = 0$$

Rearranging

$$\frac{X}{2}\rho_{out}\left[\beta_o^n - (\beta_o-1)^n\right] = \frac{R}{2}\rho_{out}\left[\beta_o^n + (\beta_o-1)^n\right] + \rho_{out}\frac{(1-R-Y)}{n+1}\left[\beta_o^{n+1} - (\beta_o-1)^{n+1}\right] - \rho_{in}Y(\beta_f-\beta_o)^n$$

results in,

$$X = \frac{R\left[\beta_o^n+(\beta_o-1)^n\right]+2\frac{(1-R-Y)}{n+1}\left[\beta_o^{n+1}-(\beta_o-1)^{n+1}\right]-2rY(\beta_f-\beta_o)^n}{\left[\beta_o^n - (\beta_o-1)^n\right]} \qquad (A.21)$$

Averaging the inward and outward mass flows to find the net infiltration rate,

$$\dot{M}_{stack} = \frac{\rho_{out}C\Delta P_s^n}{2}\left[\frac{R}{2}\beta_o^n - \frac{X}{2}\beta_o^n + \frac{\beta_o^{n+1}}{n+1} - \frac{R\beta_o^{n+1}}{n+1}\right.$$

$$- \frac{Y\beta_o^{n+1}}{n+1} + \frac{R}{2}(\beta_o-1)^n + \frac{X}{2}(\beta_o-1)^n - \frac{(\beta_o-1)^{n+1}}{n+1}$$

$$+ \frac{R(\beta_o-1)^{n+1}}{n+1} + \frac{Y(\beta_o-1)^{n+1}}{n+1} + rY(\beta_f-\beta_o)^n\Big] \quad (A.22)$$

Substituting (A.21) in (A.22)

$$\dot{M}_{stack} = \frac{\rho_{out} C \Delta P_s^n}{2}\left[\frac{R}{2}\beta_o^n - \frac{R\left[\beta_o^n+(\beta_o-1)^n\right]\beta_o^n}{2\left[\beta_o^n - (\beta_o-1)^n\right]}\right.$$

$$- \frac{\beta_o^n(1-R-Y)\left[\beta_o^{n+1} - (\beta_o-1)^{n+1}\right]}{(n+1)\left[\beta_o^n - (\beta_o-1)^n\right]} + \frac{\beta_o^n\, rY(\beta_f-\beta_o)^n}{\left[\beta_o^n - (\beta_o-1)^n\right]}$$

$$+ \frac{\beta_o^{n+1}}{n+1} - \frac{R\beta_o^{n+1}}{n+1} - \frac{Y\beta_o^{n+1}}{n+1} + \frac{R}{2}(\beta_o-1)^n$$

$$+ \frac{R(\beta_o-1)^n\left[\beta_o^n+(\beta_o-1)^n\right]}{2\left[\beta_o^n - (\beta_o-1)^n\right]}$$

$$+ \frac{(\beta_o-1)(1-R-Y)\left[\beta_o-1^{n+1} - (\beta_o-1)^{n+1}\right]}{(n+1)\left[\beta_o^n - (\beta_o-1)^n\right]}$$

$$- \frac{(\beta_o-1)^n rY(\beta_f-\beta_o)^n}{\left[\beta_o^n - (\beta_o-1)^n\right]} - \frac{(\beta_o-1)^{n+1}}{n+1} + \frac{R(\beta_o-1)^{n+1}}{n+1}$$

$$\left. + \frac{Y(\beta_o-1)^{n+1}}{n+1} + rY(\beta_f-\beta_o)^n\right] \quad (A.23)$$

As with equation (A.13), equation (A.23) may be expanded to 36 terms, each with the same denominator. In this case 32 of the terms form pairs that cancel, only 4 form pairs that add. This simplifies the equation to the form:

$$\dot{M}_{stack} = \rho_{out} r C \Delta P_s^n Y (\beta_f - \beta_o)^n \qquad (A.24)$$

It is interesting that the average of inflows and outflows reduces to a single term, the outflow through the flue in equation (A.24).

A.3 Exact Solution for Wind Effect

The flow rate through each leak for wind effect is governed by equation (A.3). Writing (A.3) in terms of mass flowrate for leak i:

$$\dot{M}_i = \rho_i C_i (\Delta P_i)^n \qquad (A.25)$$

where ρ_i = density of air in the leak

ΔP_i = pressure differential across leak i

C_i = flow coefficient for leak i .

n = flow exponent of leak i. It is assumed that all the leaks have the same flow exponent.

Now, ΔP_i can be written in terms of the external pressure coefficients at each leak and the internal pressure coefficient which is the same for each leak.

$$\Delta P_i = \left[\frac{1}{2} \rho_{out} U^2 \right] \left[Cp_i - Cp_{in} \right] \qquad (A.26)$$

where Cp_i = external pressure coefficient for leak i

Cp_{in} - internal pressure coefficient, same for all leaks

The internal pressure coefficient is analogous to the neutral pressure level for stack effect and it changes to equalise the inflows and outflows.

The inflow is for leaks where $Cp_i > Cp_{in}$

$$\dot{M}_{in} = \sum_i \rho_i C_i (\Delta P_i)^n$$

and, for outflow where $Cp_{in} > Cp_i$

$$\dot{M}_{out} = \sum_i \rho_i C_i (\Delta P_i)^n$$

For mass conservation

$$\dot{M}_{in} - \dot{M}_{out} = 0 \qquad (A.27)$$

Equation (A.27) determines Cp_{in}, which may be found by using the above equations for inflow and outflow in (A.27)

$$\dot{M}_{in} - \dot{M}_{out} = \sum_i \rho_i C_i \left(\frac{1}{2} \rho_{out} U^2 \right) (Cp_i - Cp_{in}) (|Cp_i - Cp_{in}|)^{n-1} = 0 \qquad (A.28)$$

Equation (A.28) must be solved iteratively to find the indoor pressure coefficient, Cp_{in}. Once Cp_{in} is known, the infiltration rate due to wind effect may be found by averaging inflow and outflow to minimize errors.

$$\dot{M}_{wind} = \frac{\dot{M}_{in} + \dot{M}_{out}}{2} \qquad (A.29)$$

The iterative solution to equation (A.28) may be tedious and is also unsuitable for repetitive design estimates of infiltration rate. An

alternative is to write the equation for $\dot{M}_{wind}$ in the form

$$\dot{M}_{wind} = \rho_{out} C f_w \left[\frac{1}{2} \rho_{out} (S_w U)^2 \right]^n \quad (A.30)$$

where S_w - Shielding Factor

f_w - Wind Factor

f_w contains all the information about pressure coefficients and leakage distribution. If some assumptions are made about pressure coefficients and leakage distribution, the exact solutions for f_w may be derived, and approximating equations found. As with the stack effect the total leakage is divided into four parts: walls, floor, ceiling and flue. The external pressure coefficients are determined as follows:

Walls: Cp_{wall} taken from published wind tunnel data.

Ceiling: $Cp_{ceiling}$ depends on the pressure in the attic. This pressure is determined by the pressure on the ventilation holes in the roof, that have the pressure coefficient for the roof, and by the pressure on the holes in the soffit vents under the eaves. It is assumed that the soffit vents have the same Cp as the wall below them. For simplicity C_{proof} is taken to be the average of the windward and leeward Cp's taken from wind tunnel data, and the pressure coefficient for the soffit vents is the average of the Cp's on the walls weighted by wall area.

$$\overline{Cp_{walls}} = \frac{\Sigma A_i Cp_i}{\Sigma A_i}$$

where the overbar indicates a spatial average and

A_i = area of each wall

Cp_i = Cp for each wall

Further assuming that the roof and soffit vents have about the same total leakage areas, they are equally weighted to find the pressure coefficient for the attic space above the ceiling as,

$$Cp_{ceiling} = \frac{\overline{Cp_{walls}} + Cp_{roof}}{2}$$

Floor: For a house with a basement or slab on grade the leaks at floor level in each side of the building are given the same Cp as the wall above them. This combines the floor leakage with the walls. It is assumed that the floor leaks are evenly distributed around the perimeter of the house so that their distribution will be proportional to wall area.

Flue: The external pressure coefficient for the flue is the Cp at the flue top, inside the raincap. Because the flue is at or above the roof ridge then it is assumed that there are no wind angle effects and for a round flue with a raincap, Cp_{flue} = - 0.5 (Haysom (1987)). A correction must be made for the increased windspeed at the flue top, compared to the reference windspeed at ceiling height used to find the Cp's for the walls. Assuming a power law velocity profile:

$$\frac{U_{flue}}{U} = A_1 \left(\frac{H_{flue}}{H} \right)^p = A_1 \beta_{flue}^p$$

A_1 is a factor due to the acceleration of the wind flow over the building. This correction term depends on wind direction, roof slope, and wall width to height ratio. Because of this it is too complex to be included explicitly in EXACTAIM or AIM-2, so A_1 is assumed to be equal to unity. With $A_1 = 1.0$, and $C_p = -0.5$,

$$Cp_{flue} = -0.5\, \beta_f^{2p}$$

The flow rates through each leak may now be expressed in terms of R, X, Y, C, n, β_f, ρ_{in} U, Cp's and the only unknown Cp_{in}. With the floor level leaks combined in the walls:

$$\dot{M}_{wallj} = \rho_j C \left(1 - \frac{R}{2} + \frac{X}{2} - Y\right) \frac{A_j}{\Sigma A_j} \left(\frac{1}{2} \rho_{out} U^2 \right)^n \left(Cp_{wallj} - Cp_{in} \right)^n \qquad (A.31)$$

$$\dot{M}_{ceiling} = \rho_j C \left(\frac{R+X}{2} \right) \left(\frac{1}{2} \rho_{out} U^2 \right)^n \left(\frac{\overline{Cp_{walls}} + C_{proof}}{2} - Cp_{in} \right)^n \qquad (A.32)$$

$$\dot{M}_{flue} = \rho_j CY \left(\frac{1}{2} \rho_{out} U^2 \right)^n \left(-0.5\beta_f^{2p} - Cp_{in} \right)^n \qquad (A.33)$$

where ρ_j is the density of flow, depending on sign of $(Cp_{wallj} - Cp_{in})$.

$\rho_j = \rho_{out}$ for inflow

$\rho_j = \rho_{in}$ for outflow

C, R, X, Y, ρ_{out}, U are as before.

$Cp_{wall\,j}$ - Cp for wall j

$\frac{A_j}{\Sigma A_j}$ - fraction of total wall area in wall j, 1/4 for a square building

EXACTAIM allows the fraction of total wall area in wall j to be specified by building geometry, but for simplicity AIM-2 uses 1/4. Cp_{in} is found by substituting equations (A.31), (A.32) and (A.33) into (A.28). Once Cp_{in} is found then the direction of flow through each leak is determined by the sign of $(Cp_j - Cp_{in})$, and M_{wind} found using equation (A.29). The local shielding coefficient from Table 3.2 may then be applied to U to find the wind driven infiltration rate.

The tedious and sometimes unstable iterative solution to equation (A.28) can be avoided by determining an appropriate empirical relationship for wind factor, f_w, in equation (A.30). In order to find a simple algebraic expression for f_w the following assumptions and simplifications were made.

1. The pressure coefficients were taken from a single data set by Akins (1979) for a single wind angle perpendicular to the upwind wall and for a square flat roofed building. The same pressure coefficients as used Sherman (1980) in the LBL model.
2. The difference in densities between air flowing in and air flowing out was ignored.

Equation (A.34) generates values of f_w within 10% of the exact solution. The funtional form was chosen to have the correct asymptotic

limits for extremes of leakage distribution.

$$f_w = 0.19(2-n)\left[1 - \left(\frac{X+R}{2}\right)^{1.5-Y}\right] - \frac{Y}{4}\left[Z - 2YZ^4\right] \quad (A.34)$$

where $Z = \frac{X+R+2Y}{2}$

A.3.1 Wind Factor for a house with a Crawl Space

For a house with a crawl space the assumptions about floor level leakage must change. Rather than allowing the floor leakage to become part of the wall leakage, the floor level leaks experience the pressure within the crawl space. The crawl space pressure coefficient is assumed to be the average of the wall pressure coefficients. Then, equation (A.31) must be divided into separate wall and floor flow rates.

$$\dot{M}_{wallj} = \rho_j C\,(1-R-Y)\,\frac{A_j}{\Sigma A_j}\left(\frac{1}{2}\rho_{out}\,U^2\right)^n\left(C_{pwallj} - Cp_{in}\right)^n \quad (A.35)$$

$$\dot{M}_{floor} = \rho_j C\,\frac{(R-X)}{2}\left(\frac{1}{2}\rho_{out}\,U^2\right)^n\left(\overline{Cp_{walls}} - Cp_{in}\right)^n \quad (A.36)$$

An empirical equation for f_w has also been found for this case, in the form,

$$f_w = 0.19(2-n)\,X^*R^*Y^* \quad (A.37)$$

$$R^* = 1 - R\left(\frac{n}{2} + 0.2\right)$$

$$Y^* = \left(1 - \frac{Y}{4}\right)$$

$$X^* = 1 - \left[\left(\frac{X-X_s}{2-R}\right)^2\right]^{0.75}$$

where $$X_s = \left[\frac{(1-R)}{5}\right] + 1.5Y$$

By iteratively solving the exact equations (as for EXACTAIM) it has been observed that above a critical value of X the wind factor does not vary with X, and the value of X used in the equations above should not change if X is greater than X_{crit}. An empirical estimate for X_{crit} is given by:

$$X_{crit} = 1-2Y$$

If $X > X_{crit}$ then $X = X_{crit}$

A.4 Effect of Wind Speed Fluctuations on Wind Driven Infiltration Rate

Using equation A.3,

$$Q = C(\Delta P)^n \qquad (A.38)$$

and looking at wind pressure only,

$$\Delta P = \frac{1}{2} \rho \, Cp \, U^2 \qquad (A.39)$$

where ΔP and U are instantaneous values. Separating ΔP and U into average ($\overline{\Delta P}$ and $\bar{U}$) and fluctuating ($\Delta P'$ and U") components:

$$\overline{\Delta P} + \Delta P' = \frac{1}{2} \rho \, Cp \, (\bar{U} + U")^2 \qquad (A.40)$$

Similarly the flowrate, Q, can be separated into average ($\bar{Q}$) and fluctuating (Q') components, and using (A.40):

$$\bar{Q} + Q' = C \left[\frac{1}{2} \rho Cp (\bar{U} + U'')^2 \right]^n \qquad (A.41)$$

Assuming 20% atmospheric turbulence intensity, as typical of rough terrain,

$$\frac{(U''^2)^{1/2}}{\bar{U}} = 20\% \qquad (A.42)$$

squaring and rearranging equation (A.42)

$$U''^2 = 0.04\ \bar{U}^2 \qquad (A.43)$$

rearranging equation (A.41)

$$\bar{Q} + Q' = C \left[\frac{1}{2} \rho\ Cp \right]^n \left[\bar{U}^2 + U''^2 \right]^n \qquad (A.44)$$

substitute (A.43) into (A.44)

$$\bar{Q} + Q' = C \left[\frac{1}{2} \rho Cp \right]^n \left[\bar{U}^2 + 0.04\ \bar{U}^2 \right]^n$$

$$\bar{Q} + Q' \simeq C \left[\frac{1}{2} \rho Cp \right]^n (1.02)\ \bar{U}^{2n} \qquad (A.45)$$

Let the average flowrate occur for the average windspeed,

$$\bar{Q} = C \left[\frac{1}{2} \rho Cp \right]^n \bar{U}^{2n}$$

Then the flutuation in flowrate is

$$Q' = 0.02\ C \left[\frac{1}{2} \rho\ Cp \right]^n \bar{U}^{2n}$$

Thus for 20% turbulence intensity the fluctuation in flowrate is only about 2%.